

5-31-1991

Automated determination of air content in hardened concrete

Anita R. Navalurkar
New Jersey Institute of Technology

Follow this and additional works at: <https://digitalcommons.njit.edu/theses>



Part of the [Civil Engineering Commons](#)

Recommended Citation

Navalurkar, Anita R., "Automated determination of air content in hardened concrete" (1991). *Theses*. 2569.
<https://digitalcommons.njit.edu/theses/2569>

This Thesis is brought to you for free and open access by the Electronic Theses and Dissertations at Digital Commons @ NJIT. It has been accepted for inclusion in Theses by an authorized administrator of Digital Commons @ NJIT. For more information, please contact digitalcommons@njit.edu.

Copyright Warning & Restrictions

The copyright law of the United States (Title 17, United States Code) governs the making of photocopies or other reproductions of copyrighted material.

Under certain conditions specified in the law, libraries and archives are authorized to furnish a photocopy or other reproduction. One of these specified conditions is that the photocopy or reproduction is not to be “used for any purpose other than private study, scholarship, or research.” If a user makes a request for, or later uses, a photocopy or reproduction for purposes in excess of “fair use” that user may be liable for copyright infringement,

This institution reserves the right to refuse to accept a copying order if, in its judgment, fulfillment of the order would involve violation of copyright law.

Please Note: The author retains the copyright while the New Jersey Institute of Technology reserves the right to distribute this thesis or dissertation

Printing note: If you do not wish to print this page, then select “Pages from: first page # to: last page #” on the print dialog screen

The Van Houten library has removed some of the personal information and all signatures from the approval page and biographical sketches of theses and dissertations in order to protect the identity of NJIT graduates and faculty.

ABSTRACT

Title of Thesis : Automated Determination of Air Content
 in Hardened Concrete.

Name : Anita Navalurkar,
 Master of Science in Civil Engineering, 1991

Thesis directed by : Dr. Farhad Ansari

An automated system was developed for the microscopic determination of air content and the related parameters in hardened concrete using the principles of Image Analysis and Computer Technology. Slices taken from the concrete specimen were viewed through a microscope with 40X magnification. The magnified image of the concrete slice is digitized by an Image Analyzing Software. Methodologies were developed for analysis of the digitized image and determination of air content and the required parameters. The automated system included a motorized positioner which translated microscope stage in a frame by frame sequence so that the whole image is digitized. Several tests were conducted on mortar and concrete to observe the behavior of entrained air with varying amounts of air entraining agents.

**AUTOMATED DETERMINATION OF AIR CONTENT
IN HARDENED CONCRETE**

by

Anita R. Navalurkar

Thesis submitted to the faculty of the Graduate School of
the New Jersey Institute of Technology in partial fulfillment of
the requirements for the degree of
Master of Science in Civil Engineering

1991

APPROVAL SHEET

Title of thesis : Automated Determination of Air Content
in Hardened Concrete.

Name of Candidate : Anita R. Navalurkar
Master of Science
Civil Engineering (Structures)
May 1991

Thesis and Abstract approved by :

Dr. Farhad Ansari
Associate Professor
Civil & Environmental
Engineering

Date

Dr. William Spillers
Professor, and Chairman of
Civil & Environmental
Engineering

Date

VITA

Name : Anita R. Navalurkar

Permanent Address :

Degree to be conferred : Master of Science, 1991
Civil Engineering (Structures)

Date of Birth :

Place of Birth :

Collegiate Institutes Attended	Dates	Degree
New Jersey Institute Of Technology Newark, NJ 07102	01-90 to 05-91	MSCE
College of Engineering Pune, INDIA	7-84 to 06-88	BSCE

Positions Held	Date
Teaching Assistant Civil Engineering Dept. NJIT	01-90 to 05-91
Civil Engineer Grafikon Constructions Pune, INDIA	07-88 to 12-89

Acknowledgement

I would like to thank my advisor, Dr. Ansari, without whose invaluable guidance and encouragement this thesis would not have been possible. His sincerity and enthusiasm made working with him a pleasure.

I would also like to thank Mr. Qiyu Chen and Mr. Zhaowu Zhang who helped me with any electrical problems that came up during the course of this thesis.

And last but not the least I would like to thank my husband for his patience and understanding at all times.

Contents

1	Introduction	1
1.1	Purpose of entrained air	1
1.2	Theoretical Background	2
1.2.1	Terms commonly used	3
1.3	Existing Methods	6
1.3.1	Linear Traverse Method	6
1.3.2	Point Count Method	6
1.3.3	Need for a New Method:	7
2	Image Processing and Computer Automation	8
2.1	Methodology	8
2.2	Applications of Image Analysis	9
2.2.1	Application in Medicine	9
2.2.2	Application in Robotics	10
2.2.3	Manufacturing	10
2.2.4	Remote sensing	10
2.3	Image Analysis and Air Content Determination	10
2.4	System Configuration	11
2.5	Image Processing on P.C.s	11
2.6	Methodology	13

2.6.1	Methodolgy in Linear Traverse method	13
2.6.2	Point Count Method	14
2.6.3	Automated Microscopical Determination of Air Content . . .	15
2.7	Image Analysis for Determination of Air Content	15
2.8	Motor operating Software	16
2.9	Explanation of Programs used	19
3	Experiments	24
3.1	Testing Program	24
3.2	Air Content Measurements in Fresh Concrete	24
3.3	Measurement Technique in Hardened Concrete	25
3.3.1	Description of Testing Apparatus	25
3.4	Calibration of pixel length and motor	29
3.4.1	Determination of Spatial Resolution of a Pixel	29
3.4.2	Calibration of the motor	30
3.5	Experimental Progam	30
3.5.1	Preparation of Sample	30
3.6	Experimental Procedure	33
3.6.1	Determination of Paste Content	33
3.6.2	Determination of Air Content	37
4	Results and Discussion	41
4.1	Results for Air Content	41
4.2	Results for other Parameters	42
4.3	Size Distribution	42
4.4	Comparison between Air Entrainment in Concrete and Mortar . . .	44

5 Concluding Remarks	114
5.1 Conclusions	114
5.2 Future Research	115
Bibliography	116
Appendix A	119
Appendix B	120
Appendix C	121

List of Figures

1.1	Schematic Diagram showing Spacing Factor of Air Voids	5
2.1	Configuration of Setup	12
2.2	Diagram showing white air voids against the black concrete matrix .	17
2.3	Graph of pixel points versus pixel values when the line of traverse crosses an air void	18
2.4	Diagram showing lengths of traverse on a single slice	21
2.5	Flow Chart of the batch program IMAGE	23
3.1	Schematic Diagram of the experimental Setup	27
3.2	Photograph of the experimental Setup	28
3.3	Diagram showing specimen with slices marking	32
3.4	Diagram showing traverse lengths on each slice	34
3.5	Diagram showing prepared Concrete surface for determination of paste content	36
3.6	Photograph of prepared slice seen through the microscope with 40X magnification for the determination of air content	39
4.1	Graph showing results of mortar in the hardened state and in the fresh state (Fiber Optic and Pressure Meter results)	51
4.2	Graph showing results of concrete in the fresh and hardened state .	52

4.3	Graph showing air contents of concrete and mortar with different amounts of AEA	53
4.4	Graph showing the Bubble Size Distribution for mortar with no AEA (traverse length = 103 inches)	54
4.5	Graph showing the Bubble Size Distribution for Slice # 1 of the mortar specimen with no AEA (traverse length = 20.57 inches) . . .	55
4.6	Graph showing the Bubble Size Distribution for Slice # 2 of the mortar specimen with no AEA (traverse length = 20.57 inches) . . .	56
4.7	Graph showing the Bubble Size Distribution for Slice # 3 of the mortar specimen with no AEA (traverse length = 20.57 inches) . . .	57
4.8	Graph showing the Bubble Size Distribution for Slice # 4 of the mortar specimen with no AEA (traverse length = 20.57 inches) . . .	58
4.9	Graph showing the Bubble Size Distribution for Slice # 5 of the mortar specimen with no AEA (traverse length = 20.57 inches) . . .	59
4.10	Graph showing the Bubble Size Distribution for mortar with 2 ml AEA (traverse length = 103 inches)	60
4.11	Graph showing the Bubble Size Distribution for Slice # 1 of the mortar specimen with 2 ml AEA (traverse length = 20.57 inches) . .	61
4.12	Graph showing the Bubble Size Distribution for Slice # 2 of the mortar specimen with 2 ml AEA (traverse length = 20.57 inches) . .	62
4.13	Graph showing the Bubble Size Distribution for Slice # 3 of the mortar specimen with 2 ml AEA (traverse length = 20.57 inches) . .	63
4.14	Graph showing the Bubble Size Distribution for Slice # 4 of the mortar specimen with 2 ml AEA (traverse length = 20.57 inches) . .	64
4.15	Graph showing the Bubble Size Distribution for Slice # 5 of the mortar specimen with 2 ml AEA (traverse length = 20.57 inches) . .	65

4.16	Graph showing Bubble Size Distribution for mortar with 5.5 ml AEA (traverse length = 103 inches)	66
4.17	Graph showing Bubble Size Distribution for Slice # 1 of mortar with 5.5 ml AEA (traverse length = 20.57 inches)	67
4.18	Graph showing Bubble Size Distribution for Slice # 2 of mortar with 5.5 ml AEA (traverse length = 20.57 inches)	68
4.19	Graph showing Bubble Size Distribution for Slice # 3 of mortar with 5.5 ml AEA (traverse length = 20.57 inches)	69
4.20	Graph showing Bubble Size Distribution for Slice # 4 of mortar with 5.5 ml AEA (traverse length = 20.57 inches)	70
4.21	Graph showing Bubble Size Distribution for Slice # 5 of mortar with 5.5 ml AEA (traverse length = 20.57 inches)	71
4.22	Graph showing Bubble Size Distribution for mortar with 10 ml AEA (traverse length = 103 inches)	72
4.23	Graph showing Bubble Size Distribution for Slice # 1 of mortar with 10 ml AEA (traverse length = 20.57 inches)	73
4.24	Graph showing Bubble Size Distribution for Slice # 2 of mortar with 10 ml AEA (traverse length = 20.57 inches)	74
4.25	Graph showing Bubble Size Distribution for Slice # 3 of mortar with 10 ml AEA (traverse length = 20.57 inches)	75
4.26	Graph showing Bubble Size Distribution for Slice # 4 of mortar with 10 ml AEA (traverse length = 20.57 inches)	76
4.27	Graph showing Bubble Size Distribution for Slice # 5 of mortar with 10 ml AEA (traverse length = 20.57 inches)	77
4.28	Graph showing Bubble Size Distribution for mortar with 15 ml AEA (traverse length = 103 inches)	78

4.29	Graph showing Bubble Size Distribution for Slice # 1 of mortar with 15 ml AEA (traverse length = 20.57 inches)	79
4.30	Graph showing Bubble Size Distribution for Slice # 2 of mortar with 15 ml AEA (traverse length = 20.57 inches)	80
4.31	Graph showing Bubble Size Distribution for Slice # 3 of mortar with 15 ml AEA (traverse length = 20.57 inches)	81
4.32	Graph showing Bubble Size Distribution for Slice # 4 of mortar with 15 ml AEA (traverse length = 20.57 inches)	82
4.33	Graph showing Bubble Size Distribution for Slice # 5 of mortar with 15 ml AEA (traverse length = 20.57 inches)	83
4.34	Graph showing Bubble Size Distribution for concrete with no AEA (traverse length = 100.5 inches)	84
4.35	Graph showing Bubble Size Distribution for Slice # 1 of concrete with no AEA (traverse length = 13.96 inches)	85
4.36	Graph showing Bubble Size Distribution for Slice # 2 of concrete with no AEA (traverse length = 13.96 inches)	86
4.37	Graph showing Bubble Size Distribution for Slice # 3 of concrete with no AEA (traverse length = 13.96 inches)	87
4.38	Graph showing Bubble Size Distribution for Slice # 4 of concrete with no AEA (traverse length = 13.96 inches)	88
4.39	Graph showing Bubble Size Distribution for Slice # 5 of concrete with no AEA (traverse length = 13.96 inches)	89
4.40	Graph showing Bubble Size Distribution for Slice # 6 of concrete with no AEA (traverse length = 13.96 inches)	90
4.41	Graph showing Bubble Size Distribution for Slice # 7 of concrete with no AEA (traverse length = 13.96 inches)	91

4.42	Graph showing Bubble Size Distribution for Slice # 8 of concrete with no AEA (traverse length = 13.96 inches)	92
4.43	Graph showing Bubble Size Distribution for concrete with 2 ml AEA (traverse length = 100.5 inches)	93
4.44	Graph showing Bubble Size Distribution for Slice # 1 of concrete with 2 ml AEA (traverse length = 13.96 inches)	94
4.45	Graph showing Bubble Size Distribution for Slice # 2 of concrete with 2 ml AEA (traverse length = 13.96 inches)	95
4.46	Graph showing Bubble Size Distribution for Slice # 3 of concrete with 2 ml AEA (traverse length = 13.96 inches)	96
4.47	Graph showing Bubble Size Distribution for Slice # 4 of concrete with 2 ml AEA (traverse length = 13.96 inches)	97
4.48	Graph showing Bubble Size Distribution for Slice # 5 of concrete with 2 ml AEA (traverse length = 13.96 inches)	98
4.49	Graph showing Bubble Size Distribution for Slice # 6 of concrete with 2 ml AEA (traverse length = 13.96 inches)	99
4.50	Graph showing Bubble Size Distribution for Slice # 7 of concrete with 2 ml AEA (traverse length = 13.96 inches)	100
4.51	Graph showing Bubble Size Distribution for Slice # 8 of concrete with 2 ml AEA (traverse length = 13.96 inches)	101
4.52	Graph showing Bubble Size Distribution for concrete with 5.5 AEA (traverse length = 103 inches)	102
4.53	Graph showing Bubble Size Distribution for Slice # 1 of concrete with 5.5 AEA (traverse length = 20.57 inches)	103
4.54	Graph showing Bubble Size Distribution for Slice # 2 of concrete with 5.5 AEA (traverse length = 20.57 inches)	104

4.55	Graph showing Bubble Size Distribution for Slice # 3 of concrete with 5.5 AEA (traverse length = 20.57 inches)	105
4.56	Graph showing Bubble Size Distribution for Slice # 4 of concrete with 5.5 ml AEA (traverse length = 20.57 inches)	106
4.57	Graph showing Bubble Size Distribution for Slice # 5 of concrete with 5.5 AEA (traverse length = 20.57 inches)	107
4.58	Graph showing Bubble Size Distribution for concrete with 10 AEA (traverse length = 103 inches)	108
4.59	Graph showing Bubble Size Distribution for Slice # 1 of concrete with 10 AEA (traverse length = 20.57 inches)	109
4.60	Graph showing Bubble Size Distribution for Slice # 2 of concrete with 10 AEA (traverse length = 20.57 inches)	110
4.61	Graph showing Bubble Size Distribution for Slice # 3 of concrete with 10 AEA (traverse length = 20.57 inches)	111
4.62	Graph showing Bubble Size Distribution for Slice # 4 of concrete with 10 AEA (traverse length = 20.57 inches)	112
4.63	Graph showing Bubble Size Distribution for Slice # 5 of concrete with 10 AEA (traverse length = 20.57 inches)	113

Chapter 1

Introduction

1.1 Purpose of entrained air

Deterioration of concrete structures due to freezing and thawing is one of the major problems of concrete industries in northern climates. Deterioration is caused by the expansion of freezing water in the void system of the cement paste in concrete exposed to freezing and thawing [1].

When water freezes, it expands; if restrained this expansion can cause a high internal pressure sufficient to disrupt even the strongest concrete. Air voids entrained in concrete act as empty reservoirs for the water and relieve this pressure. Thus air voids entrained in concrete increase its ability to withstand freeze-thaw cycling [2].

The main purpose of introducing air is usually to protect hardened concrete from frost action. Sometimes it is also done because of the beneficial effect on the workability of plastic concrete having a relatively low cement content. Air Entrainment improves the workability and is accompanied by less segregation and bleeding and results in a more homogenous mix [1-3].

Air content of normal concrete after full compaction is usually about 2 to 3 percent whereas the optimum air content to give maximum resistance to freezing and thawing is about 5 to 7 percent. This additional entrainment of air is accomplished by means of a suitable air entraining agent which forms stable air bubbles. Air content in concrete should be carefully controlled, since the resistance to freezing and thawing would be impaired if the concrete contains an insufficient amount of air, and the strength would be critically reduced if the percentage of air is excessive [3].

1.2 Theoretical Background

Air content in concrete can be categorised by entrained and entrapped air. Entrapped air is that which is found in a given mixture when an air-entraining agent(AEA) is not used, and accordingly, entrained air is said to be that in excess of entrapped air present because of the air-entraining agent [5].

Entrapped air is the result of insufficient compaction, and air voids present in the form of entrapped air are unstable and large in size (generally greater than 1 mm). These voids do not contribute towards increasing the resistance of concrete to the freeze-thaw action. Entrained air consists of small, evenly distributed air voids that are produced by the stabilizing action of a suitable AEA on the air bubbles.

In terms of quality control of concrete we are generally concerned with the air content of fresh concrete [4], but it has been found that, it is not only the total amount of entrained air but also the size and distribution of the air voids that are important factors contributing to the increased resistance of concrete to freezing and thawing. At present the study of such characteristics of entrained air such as void size, void concentration, and uniformity of distribution is only possible by the

study of hardened concrete [5].

In addition it is known that field performance is sometimes inconsistent with general expectations. This fact has been documented by several authors [6-9]. Thus the microscopical determination of the air void content and its parameters in hardened concrete is carried out both for estimating the potential durability of concrete that may be exposed to a freeze-thaw environment, and in examining concrete that has failed service.

1.2.1 Terms commonly used

- (1) Air Void : is a small space enclosed by the cement paste in concrete and occupied by air. This term includes both “entrapped” and “entrained ” air voids [10].
- (2) Air Void Content : is the percentage of the ratio of the volume of air to the volume of concrete. Over here it is approximated as the percentage of the ratio of the total length of air voids to the length of traverse [5,10].

$$A = \frac{\Delta v}{V} = \frac{\Delta l}{L} \quad (1.1)$$

- (3) Total length of Traverse : is the total length of the line of traverse [5].
- (4) Total Length of air bubble : is the sum total of all the lengths which were crossed in the line of traverse [5].
- (5) Mean Chord Length : is the average length of the air bubble. (or it is also defined as the total length of air bubbles divided by the total number of air bubbles). Mean Chord Length is also called the Mean Chord Intercept [10].

$$\text{Mean Chord Length (MCL)} = \frac{\Delta l}{n} \quad (1.2)$$

- (6) Specific Surface (α) : is the boundary area of the bubbles divided by the total volume of bubbles [5].

$$\alpha = \frac{4n}{A} = \frac{4}{MCL} \quad (1.3)$$

where n is the total number of bubbles encountered. Thus smaller the voids, bigger is the Specific Surface (α).

- (7) Paste Content (p) : is the ratio of the weight of cement and water to the combined weight of cement, sand, aggregate and water [5].

$$p = \frac{C + W}{C + S + A + W} \quad (1.4)$$

- (8) Spacing Factor (\bar{L}) : is an index relating to the maximum distance of any point in the cement paste from the periphery of an air void [10] or as shown in figure 2.1, it is also defined as a number relating to the distance between air bubbles [5].

$$\bar{L} = \frac{p}{\alpha A} \quad (1.5)$$

or

$$\bar{L} = \frac{3}{\alpha} [1.4(\frac{p}{A} - 1)^{\frac{1}{3}} - 1] \quad (1.6)$$

where α is the specific surface area as given above, A is the air content, and p is the paste content.

The Spacing Factor is calculated by one of the above two formulae, i.e. Eq (1.5) or Eq (1.6) whichever gives a smaller value. From the above equations, it is evident that for a given percent of air, greater the surface area (α), smaller is the average distance between bubbles.

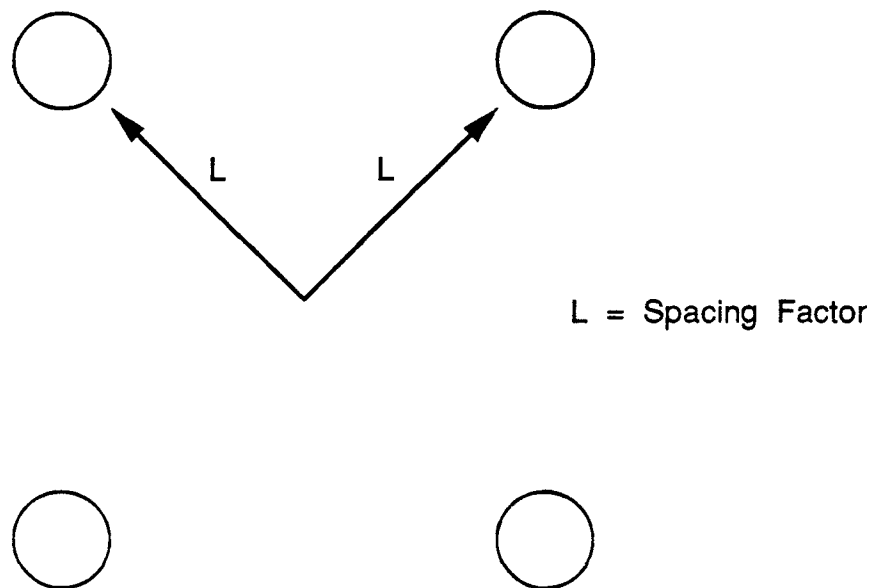


Figure 1.1: Schematic Diagram showing Spacing Factor of Air Voids

1.3 Existing Methods

Microscopical Determination of air void content and the parameters relating to it, is generally accomplished by one of the two following methods [5,10,11] :

- (1) The Linear Traverse Method (Rosiwal Method)
- (2) The Modified Point Count Method

1.3.1 Linear Traverse Method

This method involves cutting the specimen, polishing the cut surface, and measuring the fraction of total area occupied by sections of air bubbles [5,10-12].

This method is based on the principle that, provided the bubbles are randomly arranged, a straight line passed through a sufficiently large specimen, or a sufficient number of lines through any given specimen, will encounter a representative sample of the air bubbles, and, of the total length of the lines that fraction which lies within the voids is the same as the volume fraction of air in the sample.

Thus the air content of a sample can be calculated by means of Equation (1.7):

$$A = \frac{\Delta v}{V} = \frac{\Delta l}{L} \quad (1.7)$$

where A is the volume of air; V is the volume of the sample; Δl is the length of an individual air bubble in the line of traverse; and L is the total length of traverse.

1.3.2 Point Count Method

This method involves examination of the finely ground surface or a thin section under a microscope at regularly spaced points. This method consists of placing a

rectangular grid on the plane surface and counting each grid intersection that falls within a void section. The air content of the sample is then equal to the number of such coincidences with voids divided by the number of grid intersections as given by equation (1.8):

$$A = \frac{S_v}{S_t} \quad (1.8)$$

where A is the volume of air expressed as a fraction of the volume of concrete; S_v is the number of points falling within the section of an air void; S_t is the total number of points observed. In practice a grid is created optically, point by point, by means of a mechanical stage capable of bilateral stepwise movements, mounted under a fixed binocular microscope [10,11].

1.3.3 Need for a New Method:

Inspite of the fact that the existing methods are very commonly used, these methods have two major drawbacks :

- (1) The accuracy of results depends on the efficiency of the operator in recognizing the edge of the air bubble. Different operators have been known to produce results varying quite vastly from each other [13].
- (2) The existing methods are cumbersome and time consuming, since the observations of the entire length of traverse are taken manually.

Thus an attempt has been made to develop an automated system using Image Analysis and Computer Technology to overcome these drawbacks retaining the principle behind ‘The Linear Traverse Method’. The method developed is faster, accurate, and does not require manual supervision.

Chapter 2

Image Processing and Computer Automation

2.1 Methodology

An image is a picture, photograph or a display giving a visual representation of any object or a scene. However, in Image Analysis, an image is considered to consist of 512×512 pixels arranged in a rectangular array to form a complete image. Thus a pixel is a small element of the image used to represent that portion of the image. Pixel Value is the average brightness intensity of a pixel which can range from 0 to 255. Ideally a pixel value of 255 corresponds to white and a pixel value of 0 corresponds to black. Any value in between corresponds to various shades of grey with the pixel value decreasing as the darkness increases [14,15]. Thus in Image Analysis, any picture is converted to 512×512 points or pixels each having a certain pixel value. This is referred to as Image Digitization. An Image Analyzing software performs this digitization and gives the pixel numbers along with the pixel values as output. This output can then be used by the user and fed into the computer to be used as input for some programs to obtain the desired results. This

principle of Image Analysis has been used in determining the air void content and its associated parameters.

2.2 Applications of Image Analysis

Image Analysis has a variety of scientific, industrial, business, and graphic applications. Some of the fields in which Image Analysis is widely used are :

- (1) Medicine
- (2) Robotics
- (3) Manufacture
- (4) Remote Sensing

2.2.1 Application in Medicine

Image Analysis has been adapted to suit many purposes of the medical field. Spatial Filtering, Contrast Enhancement, and edge detection techniques[15] are applied to images of X-rays to aid the diagnosis of diseased organs or to detect the presence of any abnormality. This can be done by storing one image of a healthy organ for comparison with an X-ray image of the organ to be analyzed and reporting any unusual patterns or dark spots. Image Measurement functions of Image Analysis can be used to aid the documentation of any abnormal growth [16,20].

2.2.2 Application in Robotics

Robots are an integral part of any manufacturing. Robot vision systems can be built to incorporate an Image Analysis software to aid in the analysis of images captured by robots. Images captured by robots can be also stored for manual analysis [16,19].

2.2.3 Manufacturing

During the manufacturing process, image processing workstations can be used to inspect parts coming off an assembly line. Parts with critical sizing requirements can be digitized and compared to a standard image for any deformations or imperfections. Critical locations in parts can be measured and compared against product specifications [16,17].

2.2.4 Remote sensing

Satellite images can be processed in many ways by Image Analysis. To enhance special areas of interest the contrast enhancement can be used to improve clarity of images. Image areas can be magnified or reduced in scope [16,18].

2.3 Image Analysis and Air Content Determination

The main purpose behind the research reported here was to develop an automated method for determining the air content in Hardened Concrete which had the following advantages :

- (1) Its accuracy would not depend on the operator's efficiency.

- (2) To produce rapid and accurate results.

2.4 System Configuration

Microscopical Determination of air content of concrete was done using Image Analysis. The setup in this system consisted of :

- (1) Computer PC/AT
- (2) Microscope
- (3) TV Camera along with the monitor and amplifier
- (4) Two-Phase Motor

Details pertaining to the above mentioned components are given in Chapter 3. The concrete slice to be analyzed is placed under the microscope. The Image Analyzing software captures and digitizes the magnified image of the slice through the camera which is attached to the microscope assembly. The digitized image is then sent to the computer as input. FORTRAN programs MAIN.FOR, COMPACT.FOR, COMBIN.FOR, and FINAL.FOR take this input and perform the required operations to give the required parameters of air content of the sample to be analyzed. A two phase motor system moves the slice according to the depth of the microscope objective lens frame. In this way, the entire slice is analyzed frame by frame. The configuration of this setup is shown in Fig 2.1

2.5 Image Processing on P.C.s

For Image Processing on a P.C., a software “DT-IRIS” version 1.04 was used. This software was installed into the PC/AT to be used in conjunction with the

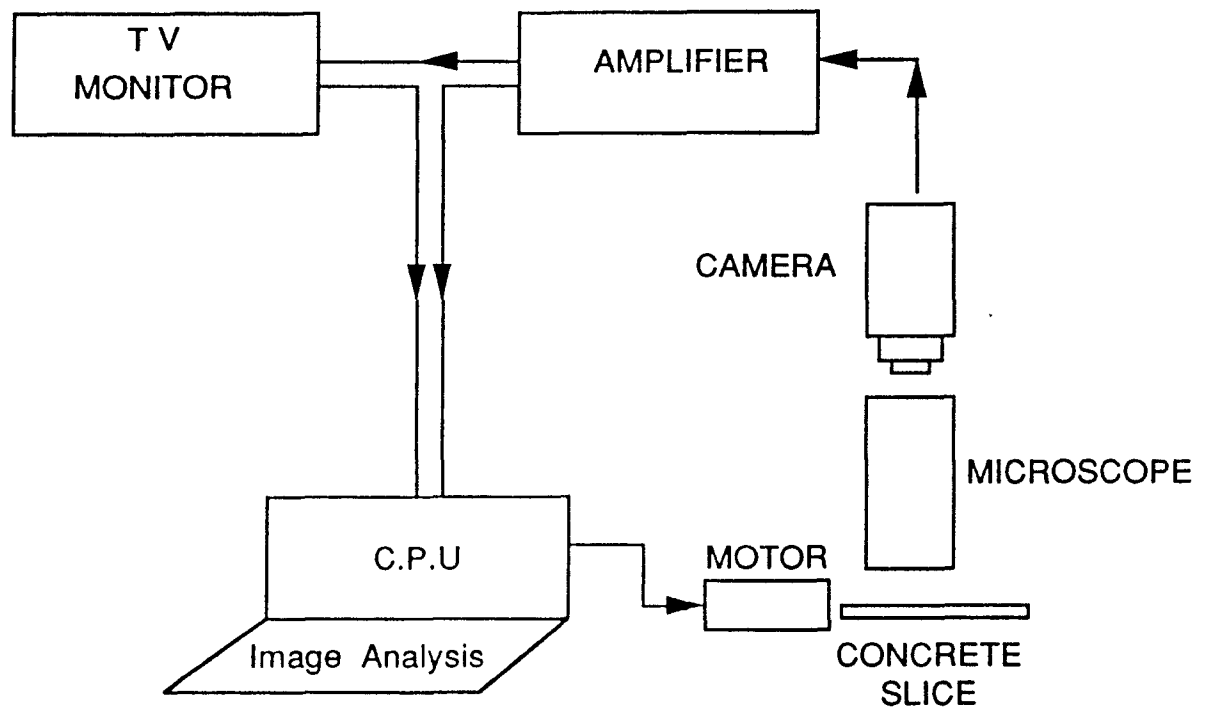


Figure 2.1: Configuration of Setup

DT2851 board. The DT2851 board is a High Resolution Frame Grabber, i.e. it is a 512×512 frame grabber designed for use on the IBM PC/AT. (A 512×512 frame consists of 512×512 pixels). DT-IRIS consists of subroutine libraries that are callable from BASIC, C, FORTRAN and PASCAL and which support all the functions of the DT2851 frame grabber [11]. In this thesis FORTRAN(version 5.0) was used along with subroutines from DT-IRIS FORTRAN library “ISFORLIB”. It was found that DT-IRIS was not compatible with earlier versions of FORTRAN. Subroutines from DT-IRIS perform the following categories of operations when called from FORTRAN programs :

- Acquisition of video frames into the DT2851 frame grabber frame-store memory buffers.
- Display of the DT2851 frame grabber’s frame-store memory buffers.
- Display and control of a display cursor.
- Storage and retrieval of images to and from disk files.

The DT2851 digitizes images with eight bits of resolution (i.e. $2^8 = 256$ level gray scale). For more detailed information about DT-IRIS and DT2851 board refer to the user manual [21,22].

2.6 Methodology

2.6.1 Methodolgy in Linear Traverse method

In this method the concrete specimen is cut, and the cut surface is polished with the help of finely graded abrasives. The plane, finely ground surface of the specimen is then viewed through a stationary microscope and measurements of air voids and the related parameters are made manually along parallel equidistant traverses [12]. In the Linear Traverse Method, the length of traverse across air voids

intercepted by the line of traverse is measured and the air void content is calculated by dividing this length of voids intercepted by the total length of traverse.

Thus the air content is calculated by means of equation (2.1):

$$A = \frac{\Delta v}{V} = \frac{\Sigma \Delta l}{L} \quad (2.1)$$

where A is the required air content, Δv is the volume of air, V is the volume of the sample, Δl is the length of air voids intercepted.

As can be seen from equation (2.1), this method is based on the principle that provided the bubbles are randomly arranged, a sufficiently large number of straight lines through any given specimen, will encounter a representative sample of the air bubbles, and of the total length of the lines, that fraction which is intercepted by voids is the same as the volume fraction of air in the sample.

2.6.2 Point Count Method

The Point Count Method is based upon statistical considerations and requires a finely ground cross section of the specimen. This method consists of placing a rectangular grid on the plane surface and counting each grid intersection that falls within a void. The air content is then calculated by dividing the number of intersections that fall within a void by the total number of grid intersections as given by equation (2.2):

$$A = \frac{S_v}{S_t} \quad (2.2)$$

where A is the reqd air content; S_v is the number of points falling within the section of air voids; and S_t is the total number of grid intersections.

In practice, a grid is created by means of mechanical stage capable of bilateral stepwise movements, mounted under a fixed binocular microscope. Counting of

points is done manually and the stage is shifted by a mechanical gear arrangement after each section under the microscope has been analyzed.

2.6.3 Automated Microscopical Determination of Air Content

In this method, the principle of the Linear Traverse Method has been used with a few modifications in the setup. Manual Supervision has been eliminated by the combined use of an Image Analyzing Software - DT-IRIS and a two phase motor attached to the stage of the microscope and operated by a software - MSTEP-5.

2.7 Image Analysis for Determination of Air Content

Entrained air voids can be distinguished from the concrete matrix because of the difference in depth between the air voids and the matrix and the fact that air voids are generally less than 1mm in size and are spherical. It is easy for the human eye to distinguish them with the help of a microscope but for the computer, a difference in mathematical values has to exist along with a threshold by which to be able to make a differentiation. This is exactly what is achieved by Image Processing. Each point in the image is given a value known as a pixel value depending upon the color intensity of that point. If a contrast can be created between the concrete matrix and the air voids, the contrast would result in a marked difference in pixel values.

This contrast is created in concrete by blackening the concrete surface and filling all the air voids with a white powder (figure 2.2.). Thus ideally an air void in the image has a pixel value of 255 and the concrete matrix ideally has a pixel value

of zero. But the concrete matrix is not completely black because of two reasons :

- The marker ink used may not be completely black, i.e it may have a dark blue tinge.
- The concrete matrix has traces of the white powder used to fill the air voids.

Therefore the pixel value of the concrete is generally around 100.

Similarly the air voids may not be completely white because the white powder used to fill them may not be truly white but may have a yellowish tinge.

Hence a threshold pixel value of 240 is set and any point having a pixel value above 240 is considered as an air bubble and correspondingly any value below 240 is considered as concrete. Figure 2.3 shows the pixel values of points as the line of traverse cross a bubble. This effectively demonstrates the reason for choosing a value of 240 as as a threshold.

2.8 Motor operating Software

The stage of the microscope is attached to a 2 phase motor operated by the software - MSTEP-5 made by Keithley Metrabyte. Metrabyte's MSTEP-5 is a plug in 2 axis stepper motor and incremental shaft encoder motion control board for the IBM PC/AT. The board is 12 inches long and requires a full length expansion slot in the computer. All communication with the MSTEP-5 is via I/O ports. The base I/O address for this board can be selected on a dipswitch and can be anywhere in the range 0 to 3F8 (hex). In this setup the base address was selected as &H330 or 816 (Dec).

This utility software is provided with a Microsoft Basic callable driver (MSTEP.BIN) for the control of the basic stepper and encoder functions. MSTEP.BIN contains functions that can be called from simple Basic programs to operate the

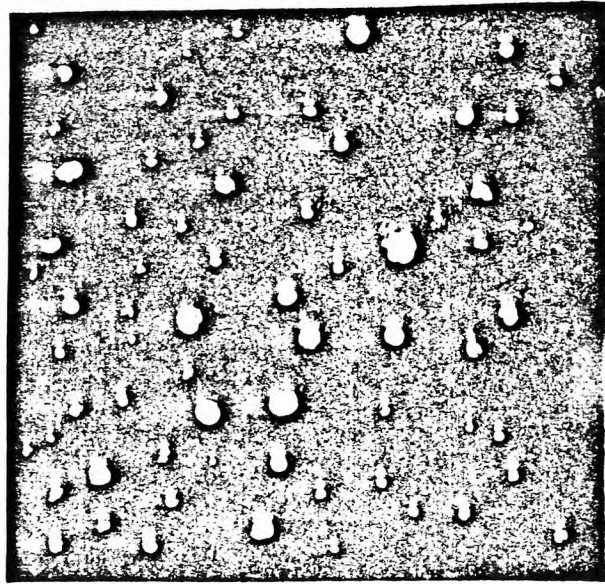


Figure 2.2: Diagram showing white air voids against the black concrete matrix

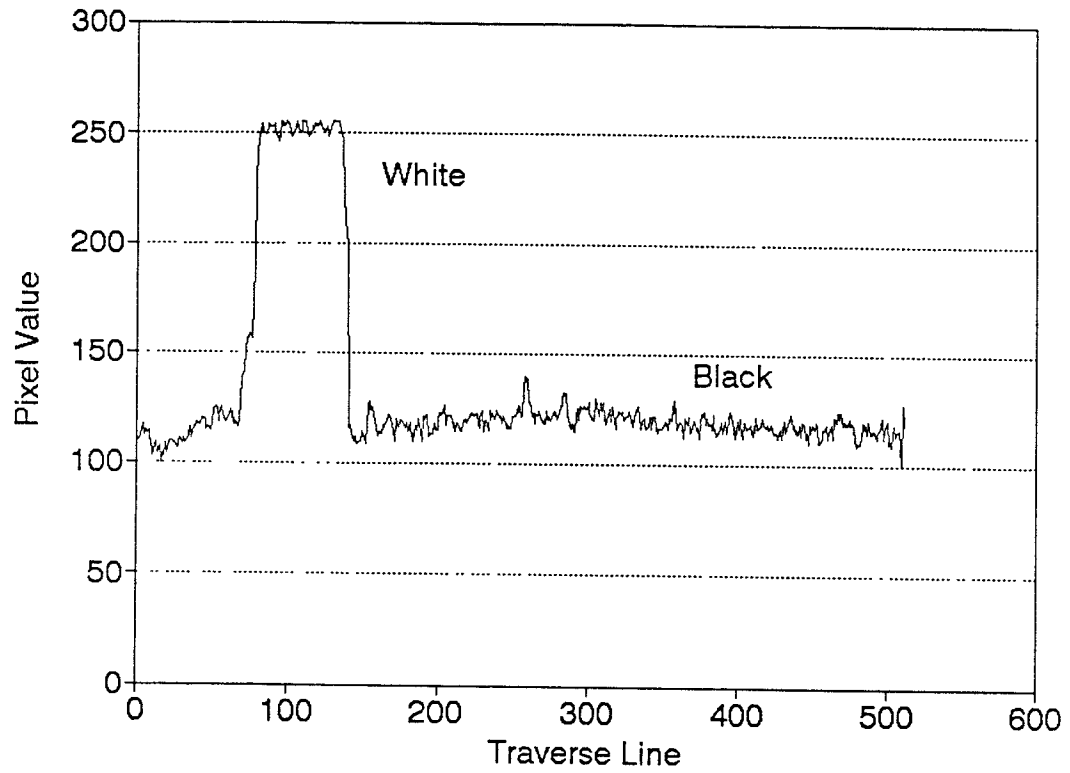


Figure 2.3: Graph of pixel points versus pixel values when the line of traverse crosses an air void

motor. A comprehensive demonstration program (DEMO.EXE) is also provided with options of all types of motor operations [23]

2.9 Explanation of Programs used

The process of digitizing the image (i.e. giving pixel values to each point of the image) is accomplished by calling subroutines from the DT-IRIS library. This process of calling the subroutines, analyzing the pixel values, recognizing the air voids and calculating the resultant parameters is done by a FORTRAN program MAIN1.FOR. This program calls subroutines from ISFORLIB.LIB which acquire an image, and digitize it. The program then analyzes the acquired data in order to calculate the total length of the air voids, the number of air voids, the number of chords in between the air voids in one frame (portion of the slice in view under the microscope) and stores this information in 3 files. One of which is B1.DAT which contains this information in a form which can be accessed by the computer(i.e. in two columns of data - one column containing the pixel number and the other containing the pixel values), the second file, BB1.DAT contains calculated data (i.e. bubble numbers, bubble size and the length of chord between the bubbles encountered in one frame) which can be read by the user, and the third file, GP1.DAT contains only the bubble sizes along with the number of voids of that size in two columns (This file is used for plotting the graph of “Bubble Size Vs Bubble Count”).

ASTM C-457 specifies that for the determination of air void parameters the total length of traverse should be minimum 100 inches with a concrete of maximum aggregate size of 1.5 inches. ASTM C-457 also specifies that the sample of the concrete to be analyzed should be obtained from at least three locations in the body of the concrete to ensure proper representation of the concrete sample. It

further states that best results are obtained if the selected traverse length is spread over the maximum of available prepared surface of concrete so as to compensate to the fullest degree for the heterogeneity of concrete. Hence to cover the required length of 100 inches, five slices of concrete were chosen from the top of the sample and each slice was so divided as to provide traverses of uniform length and a total traverse length of about 100 inches (figure 2.5).

Therefore an approximate distance of 20.57 inches was covered in each slice along equidistant traverses quarter of an inch apart. This 20.57 inches length is covered by four runs each of two batch programs : IMAGE.BAT and IMAGE2.BAT. These two programs are used alternately depending upon the direction in which the stage of the microscope has to be moved.

IMAGE.BAT runs the programs MAIN.EXE and BASICA MOTOR successively thirteen times (see figure 2.5.) Program (MAIN.FOR) analyzes one frame of 512 pixels. Similar programs, thirteen of them (MAIN1.FOR through MAIN13.FOR) perform identical tasks except that they create files with different names for the storage of data. After analysis of each frame, the BASIC program MOTOR which operates the two phase motor using functions from the software MSTEP-5 moves the stage so that the next frame comes into focus. The MSTEP-5 software also contains a demonstration program DEMO.EXE by which the stage can be brought to an extreme side before the start of the experiment.

After MAIN has been executed thirteen times, the batch program runs another program COMPACT which consolidates the results of these thirteen programs and gives the final result in 2 files : BBBB1.DAT and RUN1.DAT.

The batch program has to be executed eight times per slice. At the end of the eighth run the program COMBIN has to be executed. This program computes all the air content parameters of one particular slice. The total length of traverse in

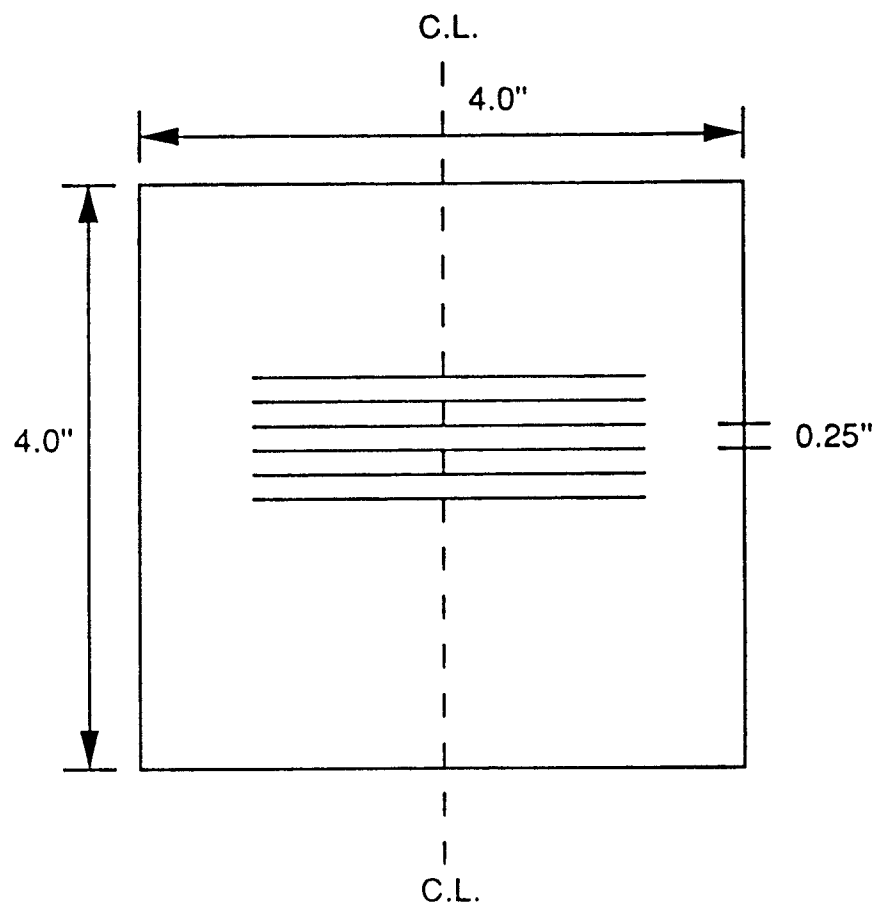


Figure 2.4: Diagram showing lengths of traverse on a single slice

a slice is thus 20.57 inches. Five such slices have to analyzed before the required length of 100 inches is covered. The program FINAL gives the final result, that is the resultant of the five slices.

See Appendix C for Program listings.

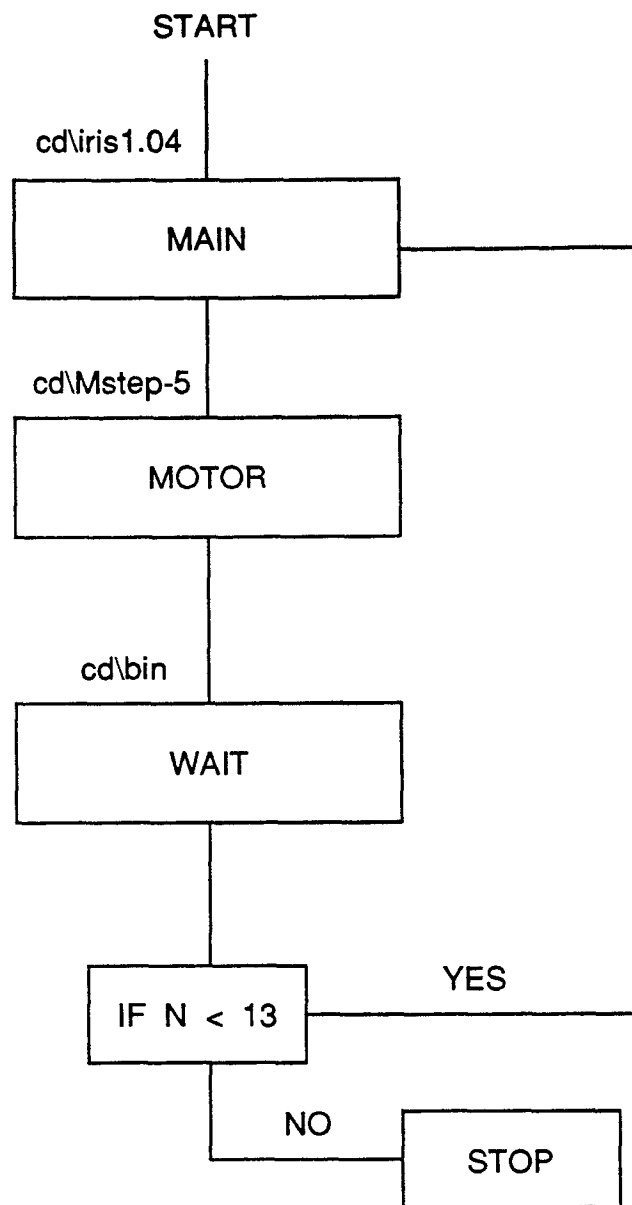


Figure 2.5: Flow Chart of the batch program IMAGE

Chapter 3

Experiments

3.1 Testing Program

Air Content in concrete and mortar was controlled by using an air entraining admixture known as MBVR manufactured by Master Builders. By varying the amount of MBVR added to each mix, a range of mixes with varying percentages of air were obtained. The air content was determined in the fresh as well as hardened state [24].

3.2 Air Content Measurements in Fresh Concrete

Two different devices were used to determine the percent of entrained air in fresh concrete:

- Precision Air Entrainment Meter (Model CT 126-A, manufactured by Soiltest) also known as the Pressure Meter.
- Fiber Optic System [23]

Four samples of concrete and five samples of mortar were tested with varying

amounts of AEA. The mix designs for concrete and mortar and the amount of AEA added for each sample are summarised in Table 3.1.

Specimen Type	Mix	AEA				
		0ml	2ml	5.5ml	10ml	15ml
Concrete	1:2.1:3.4:0.5	1	1	1	1	-
Mortar	1:2.1:1	1	1	1	1	1

Table 3.1 Experimental Program

In the Fiber Optic System, the syringe needle probe was moved around the large aggregate particles in the concrete. Ten readings were taken for each sample and the average of these ten results was used for comparison with each one of the values obtained by the Pressure Meter. Experimental results thus obtained are listed in Tables 4.1 to 4.10

Comparison of results obtained by the Pressure Meter and the fiber Optic system indicate a good degree of correlation in between the two techniques.

3.3 Measurement Technique in Hardened Concrete

3.3.1 Description of Testing Apparatus

The testing apparatus consists of four main parts. They are as follows:

- (1) The Computer IBM PC/AT with 640k RAM :

- (2) The Microscope (by Edmund Scientific Co.) The microscope has three levels of resolution : 40X, 60X and 100X. In this research a magnification of 40X was used. The ASTM C-457 specifies that the resolution of the microscope in the microscopical determination of air content and the related parameters should be such that smallest bubble distinguishable should be 20 microns. It was found that with a resolution of 40X the smallest bubble which could be distinguished was 10 microns. Hence a resolution of 40X was sufficient. The stage of the microscope is altered such that it can be moved along two rails in two directions by a two phase motor.
- (3) The two phase motor (by Keithley Metrabyte): This motor is connected to the computer and the power supply and can be operated by the software - MSTEP-5. The software MSTEP-5 is a plug-in two axis stepper motor and incremental board for the IBM PC/AT. This software is provided with a Microsoft Basic callable driver named MSTEP.BIN which contains functions which are callable from simple Basic programs to operate the motor.
- (4) The TV Camera and monitor(Hamamatsu)
- (5) The amplifier (Ikegami)

A high speed analog-to-digital converter converts the video signal from the TV camera to yield a digital picture made up of 512×512 pixels of 8 bits. This digital picture is stored in a digital frame memory. The digital image data to be analyzed are transferred from the digital frame memory to the computer by direct memory access. The final required result is obtained after this data is utilized by a series of programs as explained earlier in chapter 2. The configuration of this setup is shown in figures 3.1 and 3.2.

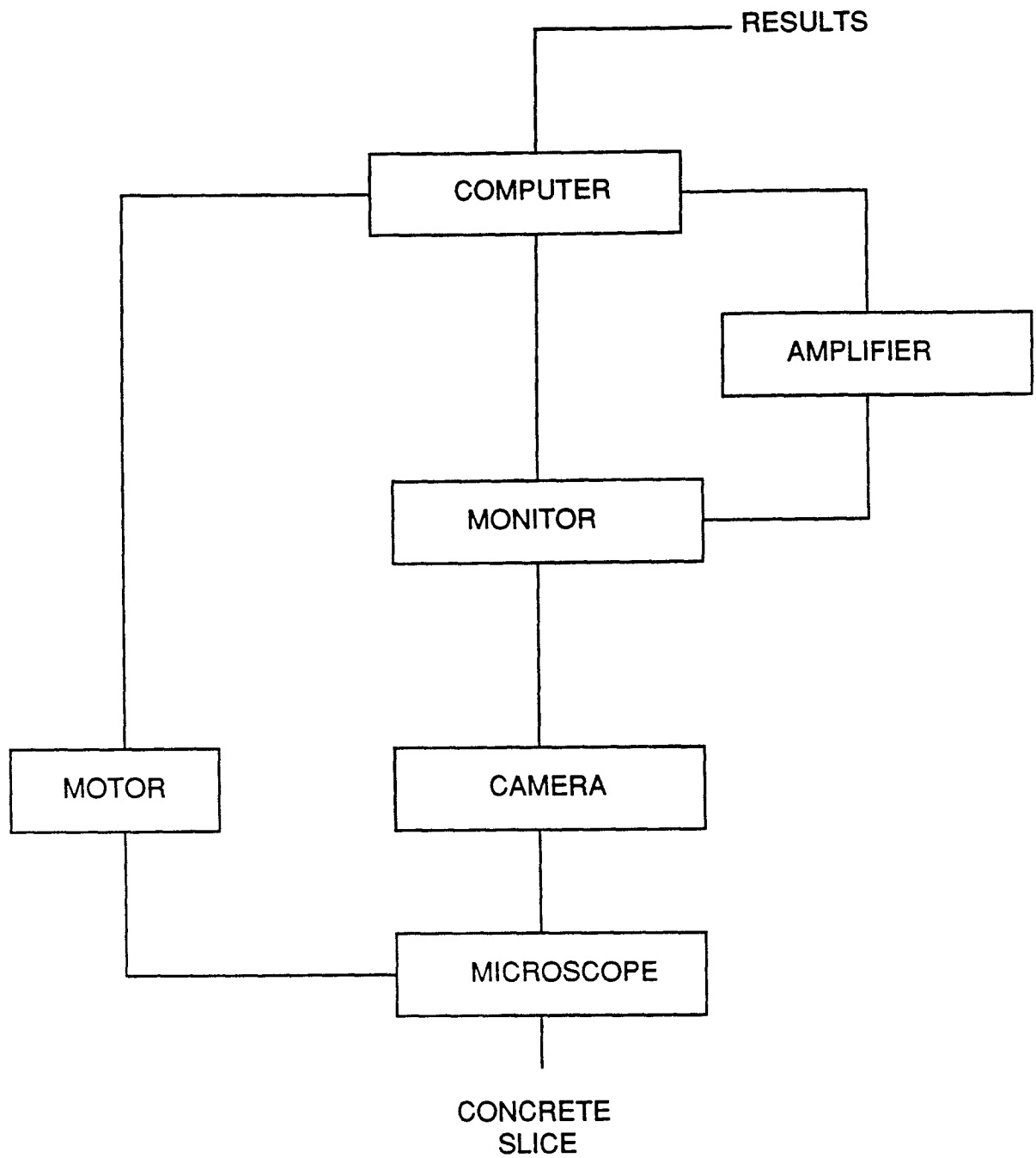


Figure 3.1: Schematic Diagram of the experimental Setup

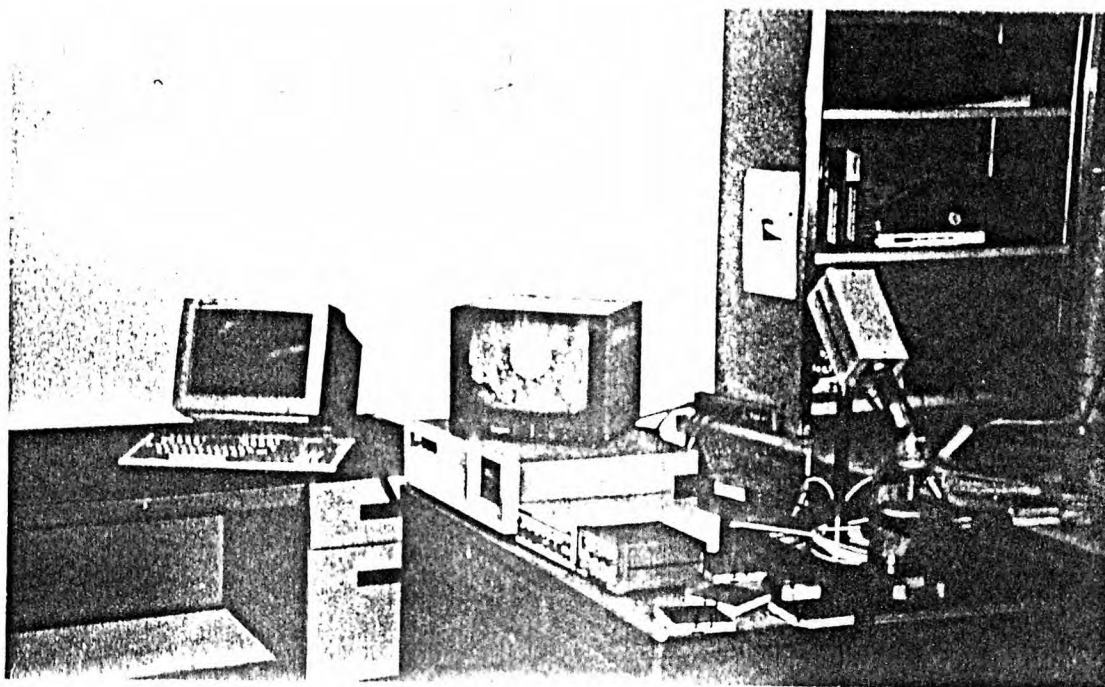


Figure 3.2: Photograph of the experimental Setup

3.4 Calibration of pixel length and motor

3.4.1 Determination of Spatial Resolution of a Pixel

The size of the physical area represented by a pixel is called the spatial resolution of the pixel. That is, the actual size of an object seen on the screen through the microscope can be calculated by multiplying the length in pixels by this resolution factor.

The principle used in the determination of the Spatial Resolution of a pixel is that the microscope lens has a constant focal length. That is, when any object is focused under the microscope it is at a fixed distance from the lens.

The length of a pixel was calibrated using an accurately graduated metallic vernier calliper. The graduated surface of the calliper was cleaned thoroughly with alcohol. Chalk was rubbed on the graduated surface so as to fill the graduations with chalk powder. Excess chalk was flicked off from the surface and the surface was wiped with a wet cotton swab. This surface of the calliper was then observed under the microscope and the program MAIN1.EXE was executed. The difference in the number of pixels between two consecutive divisions of the calliper was then noted and the spatial resolution of a pixel was calculated by dividing this difference by 0.025 inches which is the difference between two consecutive divisions of the callipers. These measurements were repeated a few times for accuracy and the average result was adopted.

$$63.66\bar{6} \text{ pixels} = 0.025'' \quad (3.1)$$

Therefore,

$$1 \text{ pixel} = 0.00039267'' = 3.9267 \times 10^{-4}'' \quad (3.2)$$

or

$$1 \text{ pixel} = 0.0099738 \text{ mm} = 9.9738 \times 10^{-3} \text{ mm} \quad (3.3)$$

or in terms of microns,

$$1 \text{ pixel} = 9.9738 \text{ microns} \quad (3.4)$$

3.4.2 Calibration of the motor

The number of cycles run by the motor has to be converted into the actual distance travelled by the stage of the microscope.

This was accomplished by trial runs of the motor with the vernier callipers in focus under the microscope. The number of steps needed to cross one division of 0.025 inches was obtained and with the help of this number, the number of steps needed to cross exactly one screen of 512 pixels was calculated.

$$0.025'' = 108.75 \text{ steps} \quad (3.5)$$

The microscope stage is required to move by one frame, that is,

$$1 \text{ frame} = 512 \text{ pixels} \times 0.00039267 = 0.2'' \quad (3.6)$$

Therefore,

$$0.2'' = 870 \text{ steps}$$

Therefore 870 steps are required to move the microscope stage by one frame.

3.5 Experimental Program

3.5.1 Preparation of Sample

Concrete to be tested is cast into a mould of size $4 \times 4 \times 12$ inches (fig 3.4). After demoulding the concrete is cured for two to three weeks before slicing. The

concrete is then cut with a diamond saw into slices of equal thickness. Five slices are cut from the top to the middle portion of the sample (fig 3.4). The top 1 inch of the specimen is not used for analysis as this portion contains a lot of entrapped bubbles which rise up from the deeper portions of the concrete during vibration. The slices to be analysed are polished with successively finer grinding sheets beginning with the grit no: 100 and going on upto grit no: 550. During polishing care should be taken so that existing air voids do not get destroyed due to the fine dust which comes out during polishing. For this, the surface to be polished should be cleaned with a fine brush after every few minutes during polishing. This process of polishing is called "lapping" and is a very significant step in the microscopical determination of air voids [25,26]. The purpose of lapping is to make the air void edges sharp and distinct. The concrete should be properly cured prior to the lapping process since surface defects are numerous when the paste is too weak. It is therefore a good practice to saw concrete slices and cure them for a few days before lapping [25]. After the slice is polished, the surface to be tested is cleaned with a very fine spray of water to remove any dust which may have accumulated in the air voids. The slice is then kept aside to dry.

Usually a ground surface of a concrete specimen contains components of nearly all shades of colour and brightness. This makes it impossible to assign a category of contrast positively to the air-void system. An analysis of the system suggested that it would be preferable to remove all natural contrasts by painting the surface black and then to create contrasts at the sites of air voids by filling them with a white powder [25].

The concrete specimen is examined methodically along parallel, equidistant traverses. These traverses are one-fourth of an inch apart. This distance between the traverses is maintained by metallic spacers one-fourth by one-fourth inch in cross

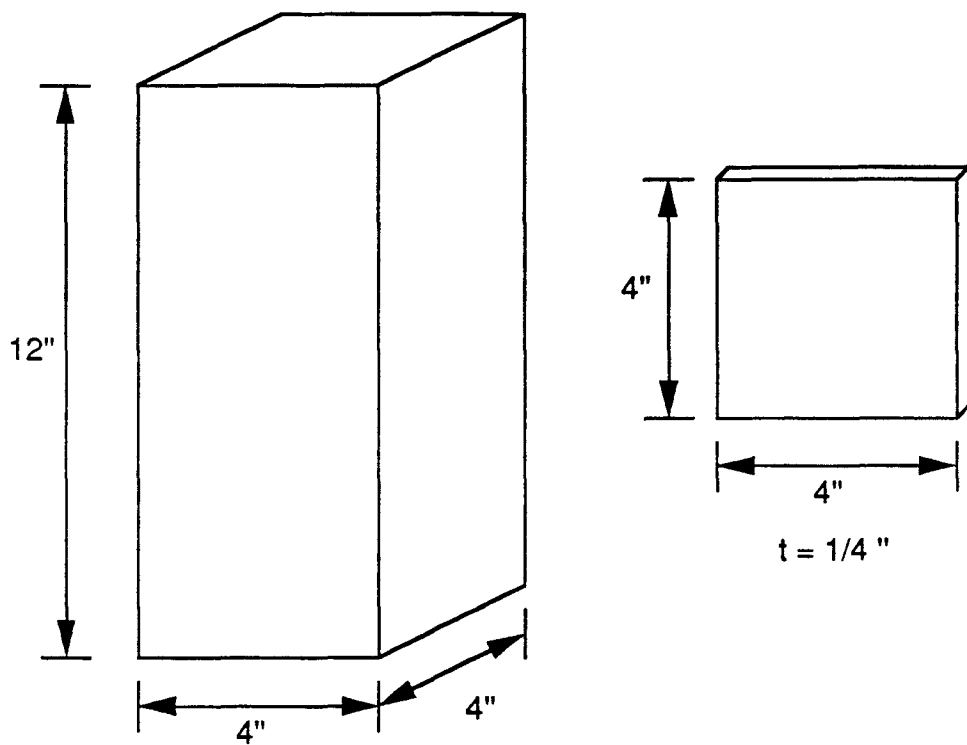


Figure 3.3: Diagram showing specimen with slices marking

section and four inches long. A sample prepared for analysis consists of 5 slabs to ensure adequate sampling throughout the thickness of the specimen. It has been shown by several researchers a total traverse length of 100 inches was sufficient to obtain results with a standard error of less than 0.4 % [12,13]. Brown and Pierson have shown this length of traverse is adequate to establish the air content of concrete containing aggregate as coarse as one and half inches [12].

Therefore each slab was so divided so as to provide a uniform length of 20.57 inches and a total length of above 100 inches.

3.6 Experimental Procedure

3.6.1 Determination of Paste Content

To calculate the paste content of concrete by this method, the following procedure is to be followed :

- (1) Blacken only the large aggregate of the polished concrete slice as carefully as possible and leave the rest of slice as is (fig 3.5).
- (2) Switch on the computer, amplifier, and the monitor two to three hours prior to actually starting the experiment. After switching on the amplifier, it is noticed that the image is not steady. In order to obtain a steady image the program DISPLAY should be executed. This program can be executed from the root directory as well as the directory : IRIS1.04. Focus the slice to be viewed by means of the focussing screw to side of the microscope stage.
- (3) After the amplifier and the camera have been on for approximately two hours, the gain has to be adjusted to the required level. This can be accomplished by means of IRIS-TUTOR. On the c: prompt change directory to

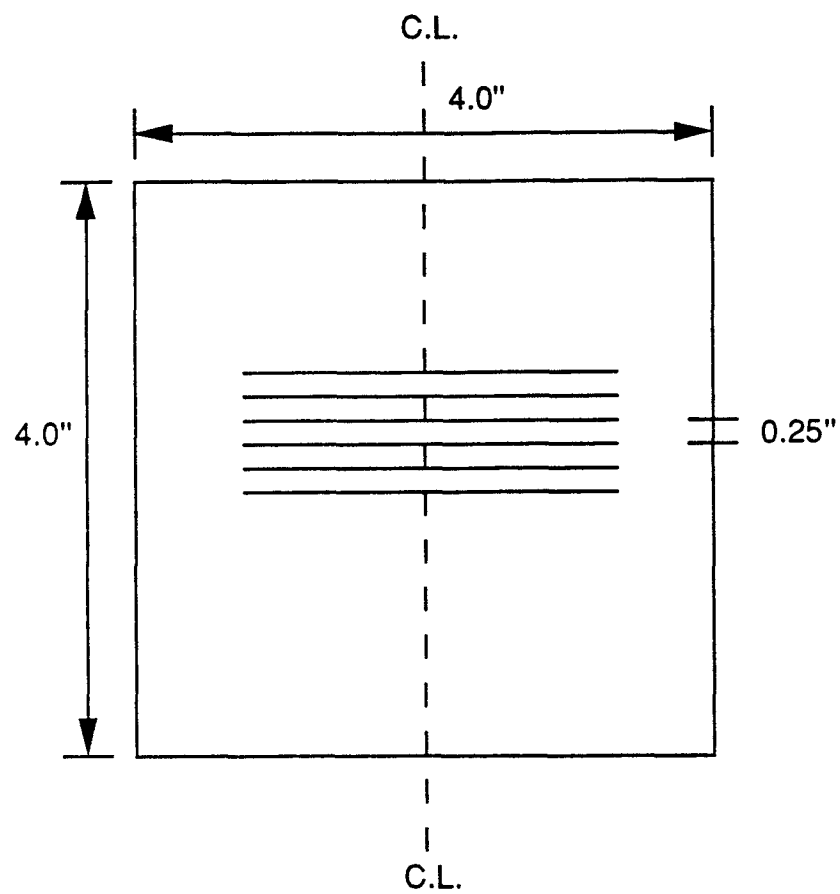


Figure 3.4: Diagram showing traverse lengths on each slice

IR-TUTOR. Execute the program IR.EXE. After entering the IRIS-TUTOR

type the following commands :

```
sync external
clear buffer 1
acquire 1 frame to buffer 1
display buffer 1
place_cursor
```

- (4) At this point a cursor will be visible on the screen. Move the cursor by means of the cursor keys and note the pixel values at the junction of white and black points. There should be a distinct difference in the pixel values. The white points should have a pixel value well above 240 (a value of about 250 has been found to be satisfactory) and the black points should have a pixel value well below 240 (about 100). If this is not so, clear buffer 1, then increase or decrease gain and repeat the above procedure to check the pixel values again. This process is to be repeated till the required pixel values are obtained. This is the optimum level of the gain.
- (6) Make sure that the stage of the microscope is at one of the extreme ends. Switch on the power supply for the motor.
- (7) Execute the program PASTE.BAT or PASTE2.BAT depending on the direction in which the microscope stage has to be moved. The execution of this program results in the formation of 13 files (PC1.DAT to PC13.DAT) in the directory IM-DATA and one resultant file (PASTE1.DAT) in the directory RESULTS. Rename PASTE1.DAT to PASTE2.DAT and delete all the files in the directory IM-DATA. These files have to be deleted otherwise the execution of the next program will give an error since the next program i.e. PASTE or PASTE2 generates files with the same names.

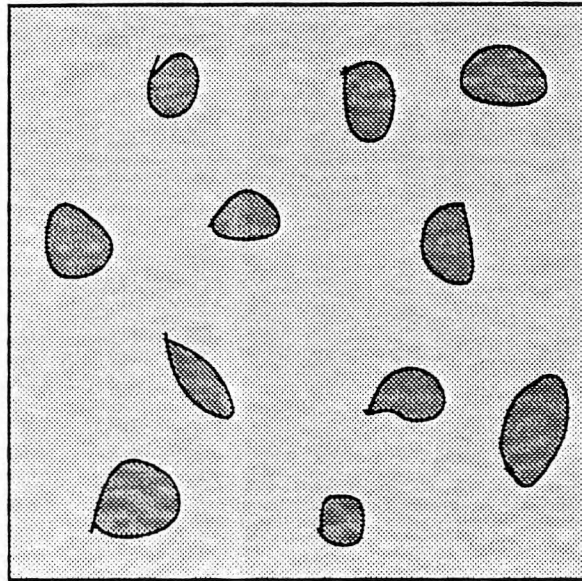


Figure 3.5: Diagram showing prepared Concrete surface for determination of paste content

(8) Repeat step (7) till eight files PASTE2.DAT to PASTE9.DAT are formed.

Execute the program PUNE.EXE to obtain the cumulative result of Slice 1 in the file PSLICE1.DAT. Rename PSLICE1.DAT to PSLICE2.DAT to avoid any errors or overwriting in the execution of the next program.

Repeat steps (7) and (8) for four more slices to obtain the final result of all five slices in the file PFINAL.DAT. It is to be noted that the above mentioned technique only slightly overestimates the paste content since it does not distinguish between the fine aggregates and the cement pastes. The percentage error in the paste content calculated by the above method was found to be 5.1 %, for which the appropriate corrections are given in Appendix A

3.6.2 Determination of Air Content

- (1) The surface of the slice which has been used for the calculation of paste content is then fully blackened with a permanent black ink using a thick marker. At this stage white chalk sticks are finely pulverised for the consequent stage of specimen preparation. After making sure that the surface has dried properly, the crushed chalk is rubbed onto the surface making certain that the chalk powder is entering the air voids. The excess chalk is flicked off the surface of the slice with the help of a cotton swab. After the chalk powder has settled in the voids wipe the surface gently with a damp cotton swab.

As a result of this procedure a concrete slice is obtained which has a totally black surface and air voids which are filled with white chalk powder. See Fig 3.6. Thus this contrast of black concrete and white air voids helps in distinguishing the edges of the air voids in Image Analysis.

- (2) Follow steps 2 through 6 from the section 3.6.1 (determination of Paste Content).
- (3) Execute the program IMAGE.BAT or IMAGE2.BAT depending on the position of the stage. The execution of this program results in the formation of three sets of data files in the directory IM-DATA and two files in the directory RESULTS. One set BBX.DAT consists of thirteen files ($X = 1$ to 13) formed because of execution of the program MAIN.EXE thirteen times in the batch file IMAGE. This set of thirteen files BX.dat is then used by the computer to form the resultant data file. The second set BBX.DAT consists of thirteen files which can be viewed by the user. The third set GPX.DAT consists of files which are used to plot the graphs of Bubble Size Vs Bubble Count. The two files in the RESULTS directory : BBBB.DAT and RUN.DAT contain the resultant of all the individual files.
- (4) Rename all the files in the directory IM-DATA and store them in a floppy disk before deleting all files in this directory to avoid the generation of any errors or overwriting during the execution of the next batch program. In the directory RESULTS rename RUN.DAT to RUN2.DAT and rename BBBB.DAT to SECT2.DAT. Now the next batch program should be run and the process repeated. The programs IMAGE.BAT and IMAGE2.BAT are to be executed alternately.
- (5) The data files in the directory IM-DATA should again be renamed and stored as before. The RUN.DAT file should now be renamed to RUN3.DAT and BBBB.DAT to SECT3.DAT.

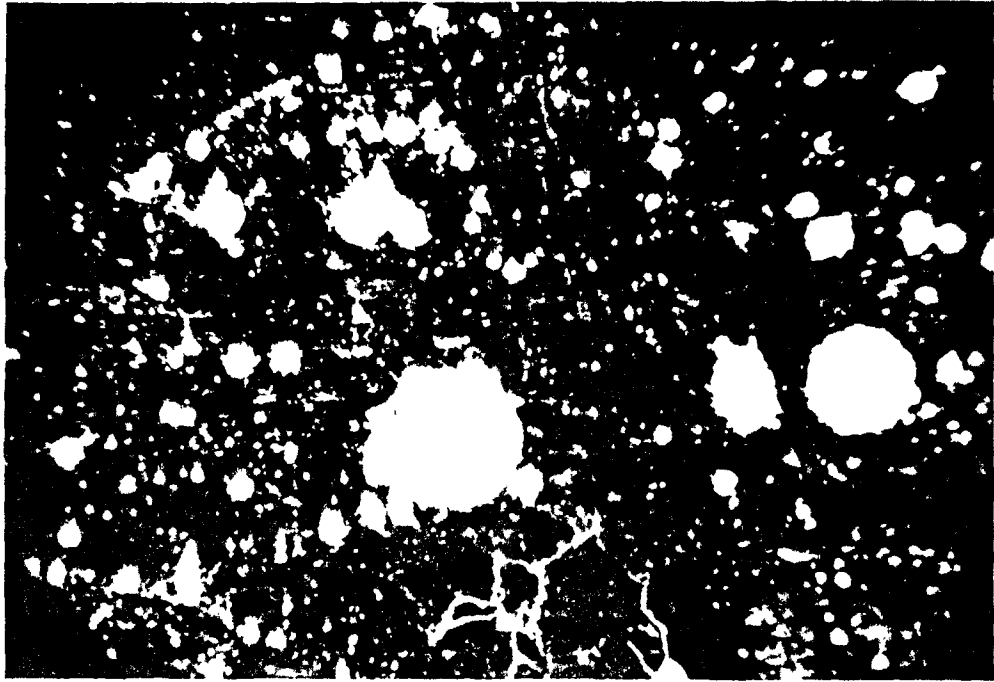


Figure 3.6: Photograph of prepared slice seen through the microscope with 40X magnification for the determination of air content

- (5) This process should be repeated eight times till RUN2.DAT, RUN3.DAT, .., RUN9.DAT and SECT2.DAT, SECT3.DAT, .., SECT9.DAT are formed. After these eight sets of files are formed, run the program COMBIN.EXE. This results in the formation of two more files : RESULT.DAT and XSLICE.DAT. These files contain the resultant data of the entire slice. Rename these files to RESULT2.DAT AND XSLICE2.DAT.

This whole process should be repeated for 4 more slices till the files : RESULT2.DAT, RESULT3.DAT, .., RESULT6.DAT are formed. To get the final result of the concrete specimen, now run the program FINAL.EXE. The required results can be obtained from the file : OUTPUT.DAT.

Chapter 4

Results and Discussion

4.1 Results for Air Content

This chapter presents the experimental results, their analysis and a discussion of the observed trends. Concrete and mortar samples were tested both in the hardened as well as in the fresh state. Experimental program is depicted in Table 3.1.

Experiments were carried out on concrete and mortar with varying amounts of AEA [10]. It was observed that in any mix, larger amounts of AEA produced increased amounts of entrained air. Tables 4.1 through 4.5 list test results obtained from air content measurements of fresh mortar. Tables 4.6 through 4.9 depict the same for fresh concrete. These samples were then cast into molds to be tested in the hardened state.

Air content of all the samples tested in the fresh and hardened states are compared in Table 4.10. These results are further compared in figures 4.1 through 4.3. Results indicate that an increase in air content is possible by increasing the dosage of admixture. Many researchers have shown that this increase depends on many characteristics such as the cement type, type of AEA, mixing time, water-cement ratio etc [17-19].

Results also indicate that, in general, the air content in hardened concrete is lower than in fresh Concrete. This can be explained by the fact that some of the less stable bubbles are lost during compaction [1,2,17].

4.2 Results for other Parameters

Many parameters other than the total air content such as the Spacing Factor, Specific Surface, and Mean Chord Length affect the potential resistance of the concrete to freezing and thawing [2,7,13]. The automated microscopical method which is developed during the course of this thesis, is capable of computing the following parameters :

- (1) Total Air Content of sample
- (2) Total number of Bubbles
- (3) Size of each bubble
- (4) Mean Chord Length
- (5) Specific Surface
- (6) Spacing Factor

Table 4.11 lists results from calculations of the above mentioned.

4.3 Size Distribution

Air content parameters obtained for each slice with a traverse length of 20.57 inches as well as the cumulative results obtained from five slices representing the total values were plotted by a commercially available software (QUATTRO-PRO).

Bubble Size Distribution curves were plotted against the number of bubbles. Bubble sizes represent dimensions less than a specified value. For instance, 75 microns, 150 microns etc. These curves were plotted for each slice (traverse length = 20.57 inches), as well as for the entire specimen (traverse length = 103 inches). Data representing the Bubble Size Grading for the entire specimen were plotted by combining and sorting according to the size distribution of data from each slice.

Fig 4.4 shows the Bubble Size Distribution for the mortar specimen with no MBVR (AEA). Figures 4.5 through 4.9 show the Size Distribution for each slice (traverse length = 20.57 inches) of the same mortar. Subsequent figures i.e. figures 4.10 through 4.33 show the Size Distribution of Mortar with MBVR (AEA).

Figure 4.34 through 4.42 shows the Bubble Size Distributions for the concrete specimen with no MBVR (AEA). Figures 4.43 through 4.61 represent the bubble Size Distribution for samples of concrete with MBVR(AEA).

It can be seen that the total number of bubbles are much larger for specimens which are air entrained. Also the percentage of small bubbles is greater in the case of specimens with MBVR. This is because the air in specimens without an AEA is largely entrapped air which consists of large irregular air voids and are formed due to insufficient compaction. Air in specimens with AEA consists of small and spherical, regularly spaced voids which are stabilized by the AEA. Increasing amounts of AEA result in larger number of bubbles, reduced Spacing Factor and larger Specific Area. (In our experiments, mortar with 2 ml AEA and mortar with 15 ml AEA did not conform to this general rule). Larger Specific Area can be explained by the fact that, with an AEA, a larger air content is produced with a lot of small air voids. AEA stabilizes smaller bubbles and prevents them from fusing to form larger voids thus increasing the number of bubbles and therefore reducing the Spacing Factor between the voids.

4.4 Comparison between Air Entrainment in Concrete and Mortar

It is reported by many researchers that the air content in mortar is expected to be higher in mortar than in concrete [20]. This is explained by them according to the following facts :

- (1) If we consider a sample of concrete having an air content of 7 %, this is equivalent to the matrix of the concrete containing about 13 % (since matrix of concrete is about 50 % of the total volume of concrete) air by volume, since all the volume of air, entrained and entrapped is present only in the matrix of the concrete [19].
- (2) It has been proved that an increase in the water cement ratio leads to greater air entrainment along with a decrease in the specific area of bubbles. Since mortar has a greater water cement ratio as compared to concrete at a comparable state of fluidity(workability), it is suggested that mortar would have a higher air content but larger bubbles (because of the increase in specific area of bubbles) [7].
- (3) It has frequently been stated that an increase in the sand content results in an increase in air entrainment. For example an increase in the sand content by 5 % will lead to an increase in the air content by 1 to 1.5 %. Mortar certainly has a greater sand content than concrete, it is therefore expected that the air content in mortar is higher than the air content in concrete.

Therefore, according to the above mentioned mechanisms, it can be stated that the air content in mortar is higher than the air content in concrete for the same amount of AEA. Our experiments indicated the same. The specific surface

of mortar was also observed to be less than that of concrete thus indicating the presence of larger bubbles in mortar .

File name	Fiber Optic Reading	Pressuremeter Reading
DF10.WK1	3.11 %	4.1 %
DF11.WK1	3.55 %	
DF12.WK1	3.86 %	
DF13.WK1	1.93 %	
DF14.WK1	2.74 %	
Df15.WK1	2.44 %	
DF16.WK1	2.26 %	
DF17.WK1	2.62 %	
DF18.WK1	* %	
DF19.WK1	* %	

Fiber Optic Average : 3.00 %

(* In this test only eight tests were carried out by the fiber optic sensor)

Table 4.1 Mortar with no AEA, Date of test : 3-14-91

File name	Fiber Optic Reading	Pressuremeter Reading
DF10.WK1	3.66 %	4.1 %
DF11.WK1	3.51 %	
DF12.WK1	3.89 %	
DF13.WK1	4.01 %	
DF14.WK1	3.53 %	
Df15.WK1	3.33 %	
DF16.WK1	3.30 %	
DF17.WK1	4.18 %	
DF18.WK1	4.08 %	
DF19.WK1	3.85 %	

Fiber Optic Average : 3.73 %

Table 4.2 Mortar with 2 ml MBVR (AEA) ; Date of test : 3-14-91

File name	Fiber Optic Reading	Pressuremeter Reading
DF10.WK1	5.03 %	4.60 %
DF11.WK1	4.99 %	
DF12.WK1	5.22 %	
DF13.WK1	4.47 %	
DF14.WK1	5.95 %	
Df15.WK1	4.76 %	
DF16.WK1	3.79 %	
DF17.WK1	5.25 %	
DF18.WK1	5.75 %	
DF19.WK1	4.19 %	

Fiber Optic Average : 4.96 %

Table 4.3 Mortar with 5.5 ml MBVR ; Date of test : 3-15-91

File name	Fiber Optic Reading	Pressuremeter Reading
DF10.WK1	5.41 %	5.50 %
DF11.WK1	4.68 %	
DF12.WK1	5.08 %	
DF13.WK1	4.97 %	
DF14.WK1	5.05 %	
Df15.WK1	5.99 %	
DF16.WK1	5.18 %	
DF17.WK1	5.95 %	
DF18.WK1	6.46 %	
DF19.WK1	5.60 %	

Fiber Optic Average : 5.44 %

Table 4.4 Mortar with 10ml MBVR ; Date of test : 3-19-91

File name	Fiber Optic Reading	Pressuremeter Reading
DF10.WK1	6.10 %	6.00 %
DF11.WK1	6.16 %	
DF12.WK1	6.22 %	
DF13.WK1	5.78 %	
DF14.WK1	6.86 %	
Df15.WK1	6.35 %	
DF16.WK1	6.34 %	
DF17.WK1	5.02 %	
DF18.WK1	6.84 %	
DF19.WK1	6.33 %	

Fiber Optic Average : 6.20 %

Table 4.5 Mortar with 15 ml MBVR ; Date of test : 3-20-91

File name	Fiber Optic Reading	Pressuremeter Reading
DF10.WK1	2.22 %	2.2 %
DF11.WK1	2.49 %	
DF12.WK1	2.42 %	
DF13.WK1	2.45 %	
DF14.WK1	2.43 %	
Df15.WK1	2.32 %	
DF16.WK1	2.32 %	
DF17.WK1	2.27 %	
DF18.WK1	2.23 %	
DF19.WK1	2.04 %	

Fiber Optic Average : 2.32 %

Table 4.6 Concrete with no MBVR ; Date of test : 10-5-91

2.2) Concrete with 2 ml MBVR (AEA) ; Date of test : 10-16-90

File name	Fiber Optic Reading	Pressuremeter Reading
DF10.WK1	3.87 %	4.0 %
DF11.WK1	4.37 %	
DF12.WK1	5.80 %	
DF13.WK1	4.52 %	
DF14.WK1	4.87 %	
Df15.WK1	3.77 %	
DF16.WK1	4.40 %	
DF17.WK1	3.88 %	
DF18.WK1	5.00 %	
DF19.WK1	3.87 %	

Fiber Optic Average : 4.43 %

File name	Fiber Optic Reading	Pressuremeter Reading
DF10.WK1	4.96 %	5.50 %
DF11.WK1	5.17 %	
DF12.WK1	6.15 %	
DF13.WK1	5.92 %	
DF14.WK1	5.23 %	
Df15.WK1	6.61 %	
DF16.WK1	5.62 %	
DF17.WK1	7.68 %	
DF18.WK1	7.26 %	
DF19.WK1	5.95 %	

Fiber Optic Average : 6.05 %

Table 4.8 Concrete with 5.5 ml MBVR ; Date of test : 10-19-91

File name	Fiber Optic Reading	Pressuremeter Reading
DF10.WK1	4.96 %	6.30 %
DF11.WK1	5.96 %	
DF12.WK1	5.72 %	
DF13.WK1	5.89 %	
DF14.WK1	4.67 %	
Df15.WK1	4.86 %	
DF16.WK1	5.10 %	
DF17.WK1	6.23 %	
DF18.WK1	6.19 %	
DF19.WK1	5.75 %	

Fiber Optic Average : 5.53 %

Table 4.9 Concrete with 10 ml MBVR ; Date of test : 10-22-91

AEA	0 ml	2 ml	5.5 ml	10 ml	15 ml
Fresh Concrete					
a) Fiber Optic	2.32 %	4.43 %	6.05 %	5.53 %	*
b) Pressure Meter	2.2 %	4.0 %	5.50 %	6.30 %	*
Hardened Concrete	2.06 %	4.4 %	4.28 %	4.96 %	*
Fresh Mortar					
a) Fiber Optic	3.0 %	3.73 %	4.96 %	5.44 %	6.20 %
b) Pressure Meter	4.1 %	4.1 %	4.6 %	5.5 %	6.00 %
Hardened Mortar	2.2 %	3.46 %	4.69 %	5.48 %	5.07 %

Table 4.10 Comparison of Results of Mortar and Concrete in the fresh and hardened State

(* Tests with 15 ml AEA were not conducted for concrete due to lack of time)

S. #	MBVR ml	Air Content	Specific Surface mm^2/mm^3	Mean Chord Length mm	Spacing Factor mm
Concrete					
1	0	2.06	*	*	*
2	2	4.4 %	*	*	*
3	5.5	4.28 %	762	0.138	0.0046
4	10	4.96 %	863	0.122	0.0037
Mortar					
1	0	2.22 %	404	0.260	0.0197
2	2	3.46 %	783	0.134	0.0081
3	5.5	4.69 %	563	0.187	0.0093
4	10	5.48 %	565	0.186	0.0096
5	15	5.07 %	446	0.236	0.0127

Table 4.11 Results of other parameters of concrete and mortar

(* At the time these tests were conducted the system was not developed enough so as to be able to calculate these parameters.)

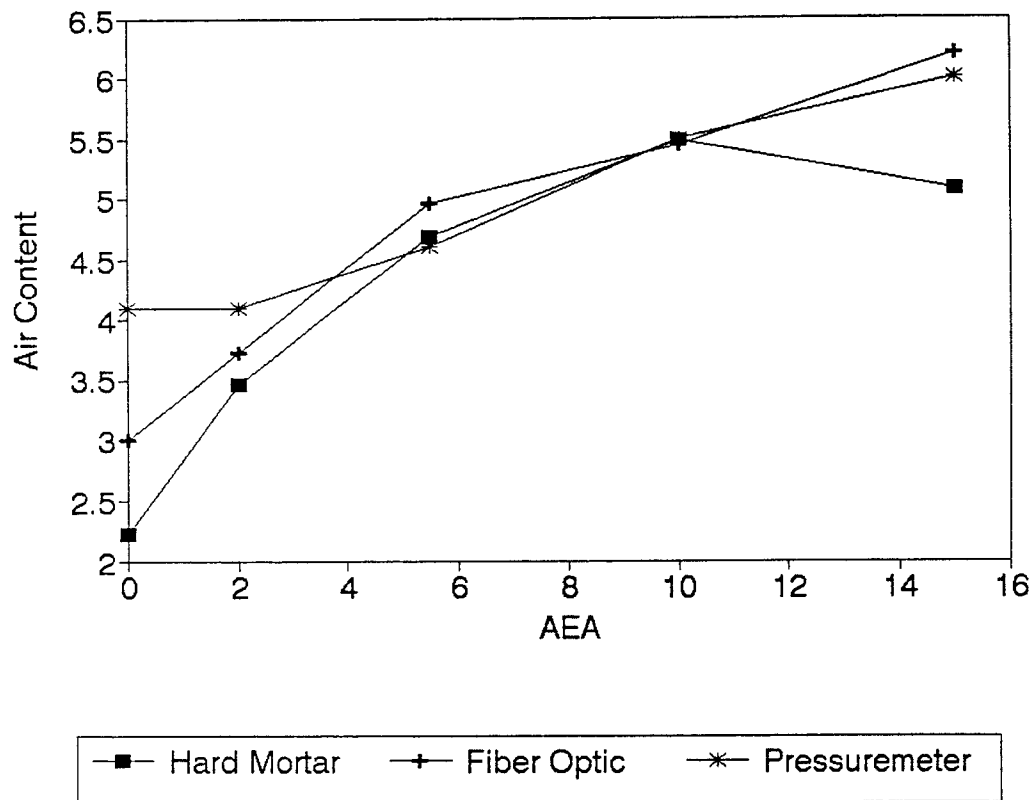


Figure 4.1: Graph showing results of mortar in the hardened state and in the fresh state (Fiber Optic and Pressure Meter results)

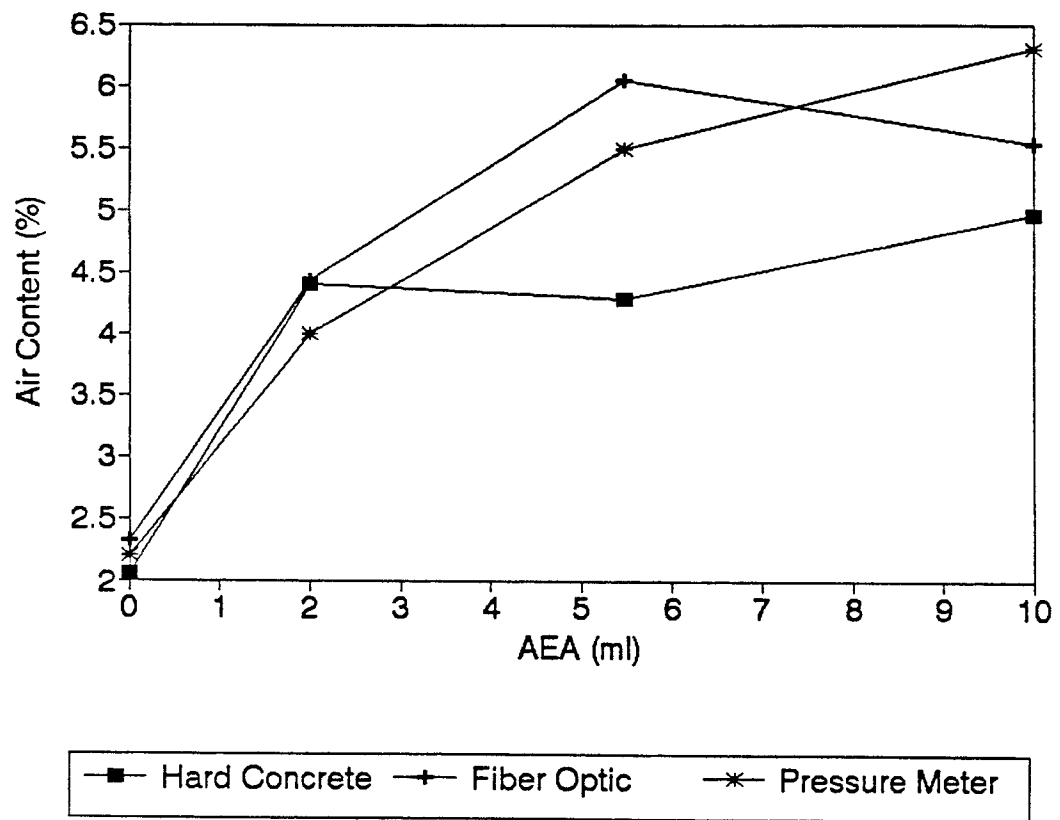


Figure 4.2: Graph showing results of concrete in the fresh and hardened state

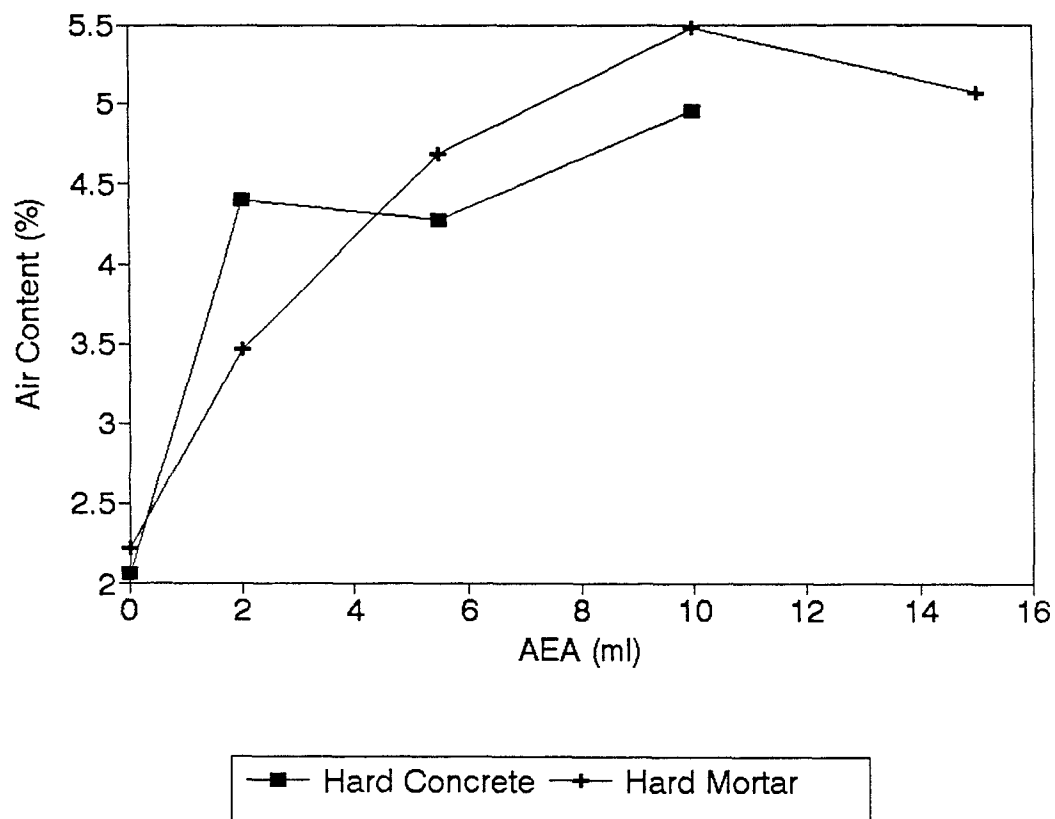


Figure 4.3: Graph showing air contents of concrete and mortar with different amounts of AEA

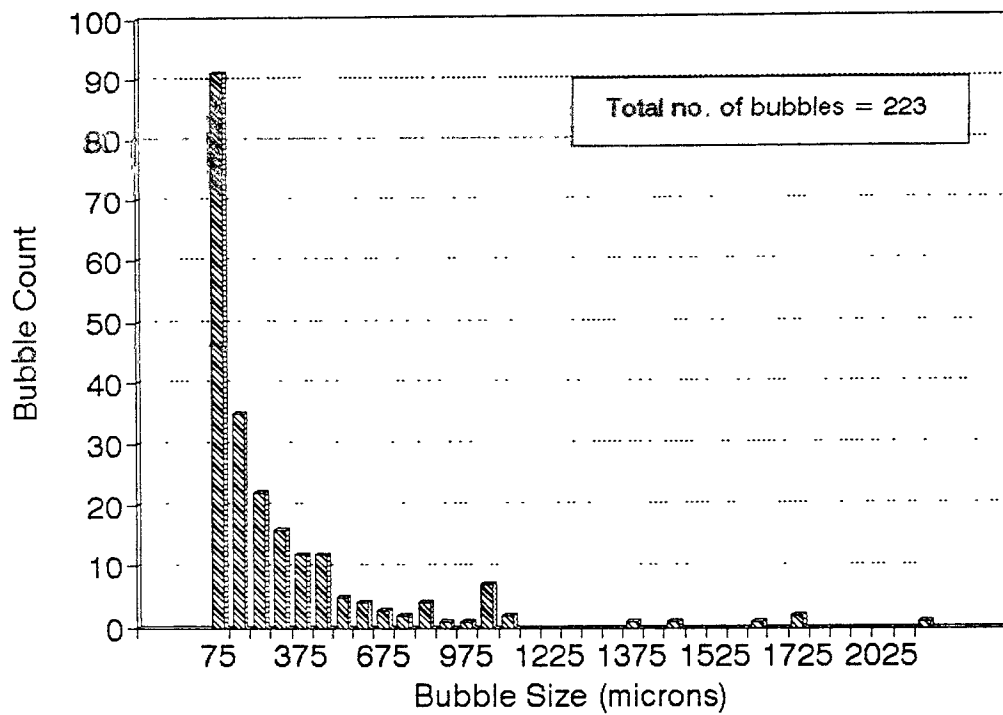


Figure 4.4: Graph showing the Bubble Size Distribution for mortar with no AEA (traverse length = 103 inches)

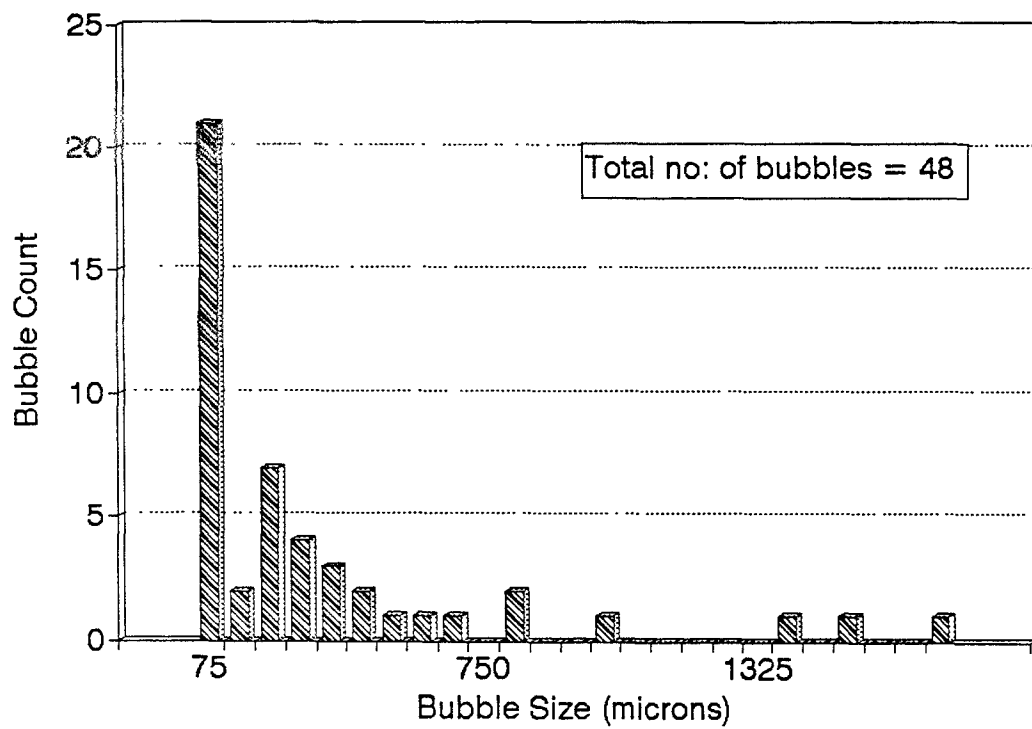


Figure 4.5: Graph showing the Bubble Size Distribution for Slice # 1 of the mortar specimen with no AEA (traverse length = 20.57 inches)

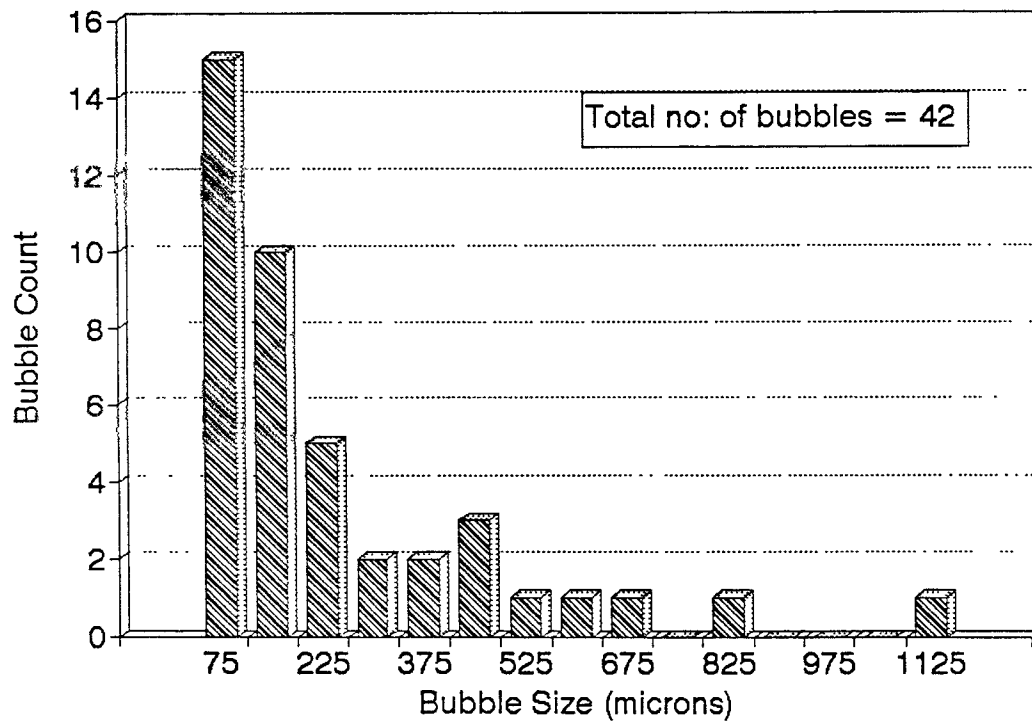


Figure 4.6: Graph showing the Bubble Size Distribution for Slice # 2 of the mortar specimen with no AEA (traverse length = 20.57 inches)

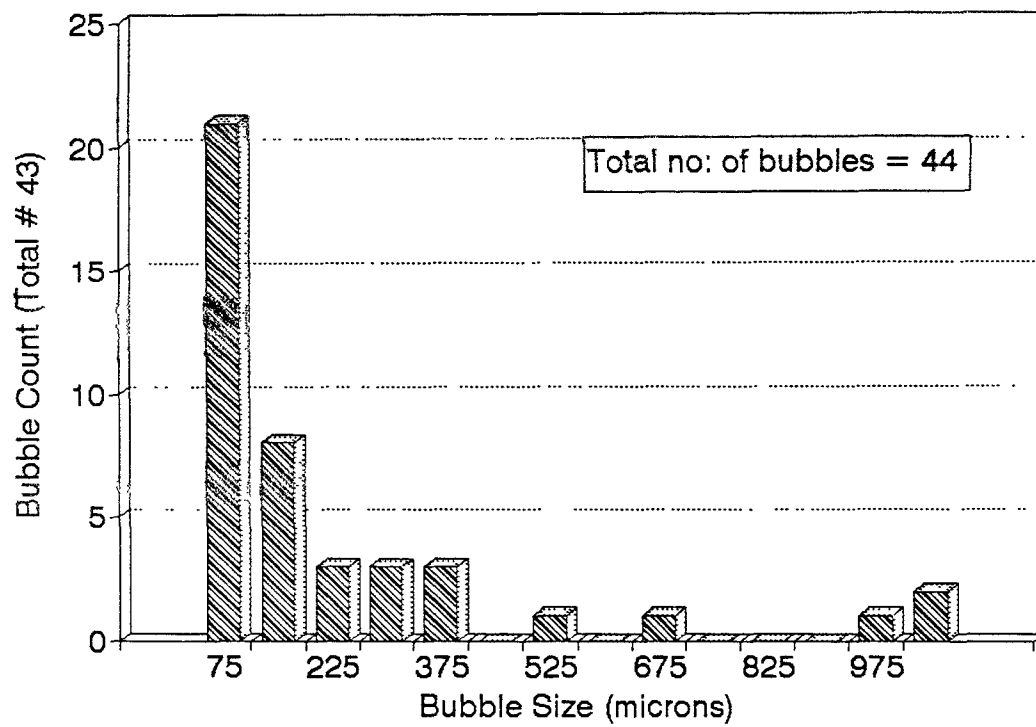


Figure 4.7: Graph showing the Bubble Size Distribution for Slice # 3 of the mortar specimen with no AEA (traverse length = 20.57 inches)

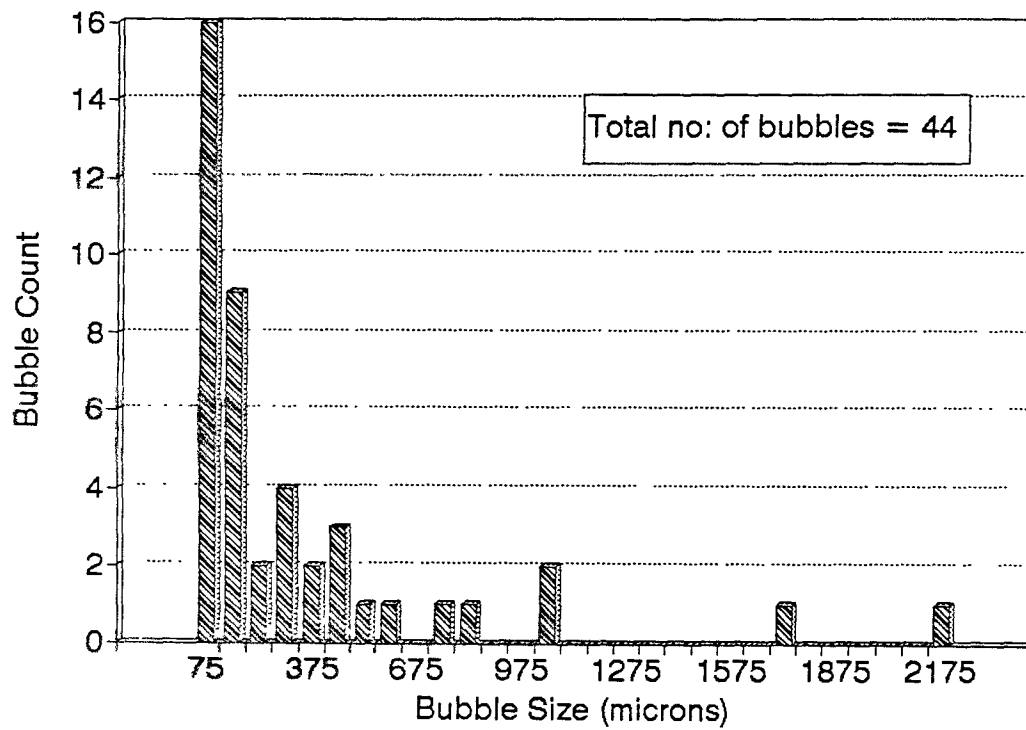


Figure 4.8: Graph showing the Bubble Size Distribution for Slice # 4 of the mortar specimen with no AEA (traverse length = 20.57 inches)

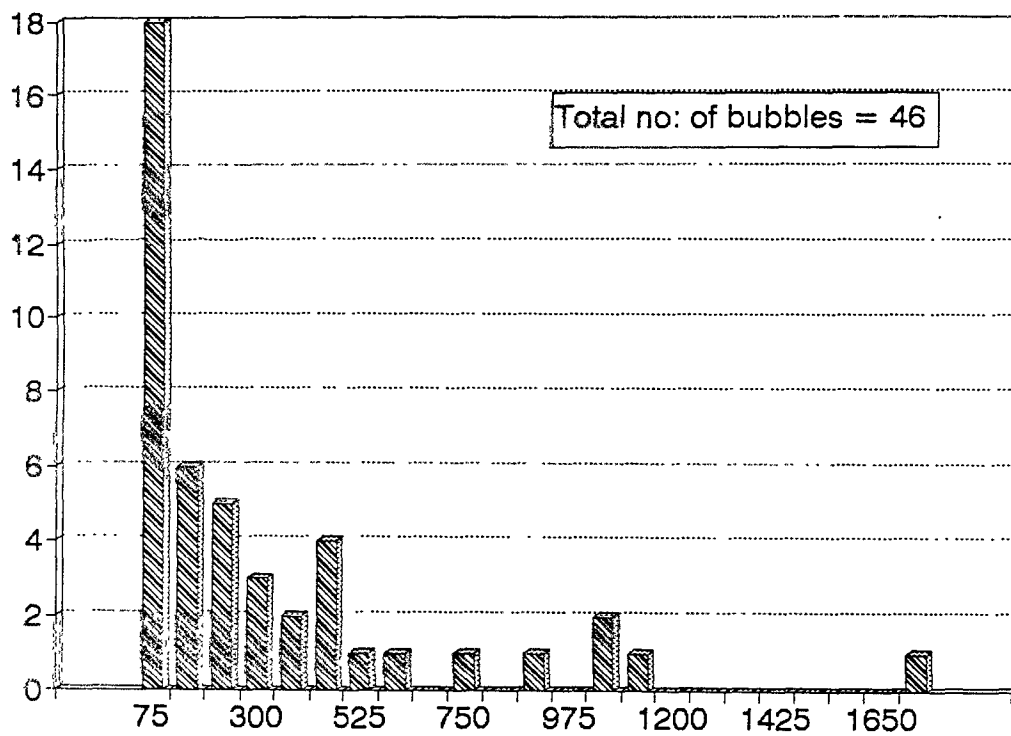


Figure 4.9: Graph showing the Bubble Size Distribution for Slice # 5 of the mortar specimen with no AEA (traverse length = 20.57 inches)

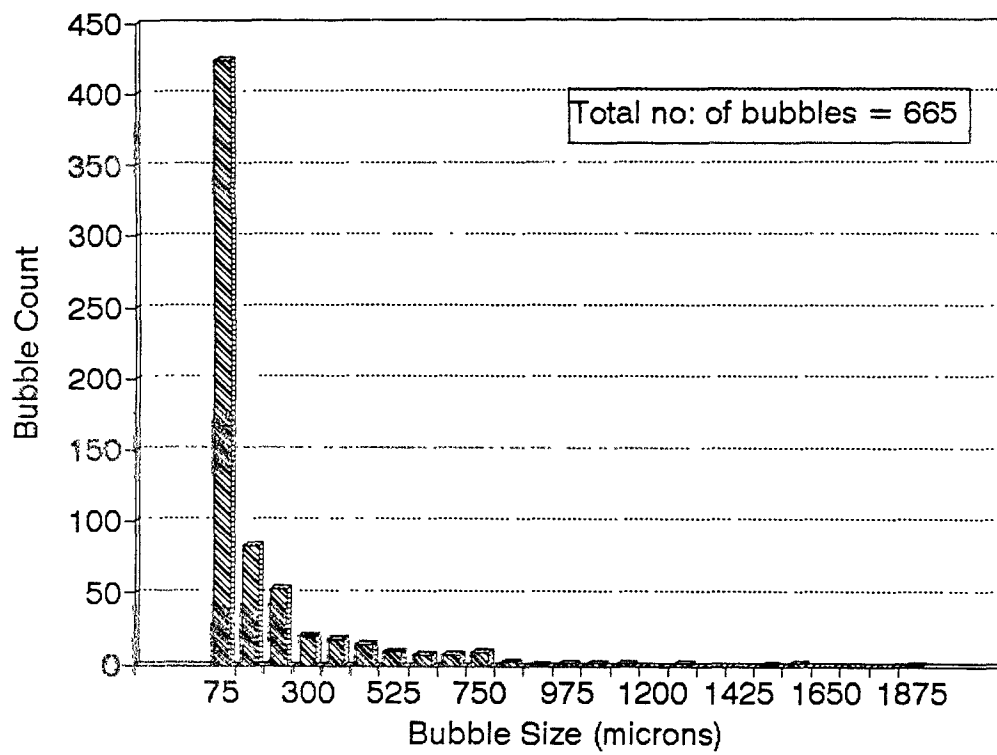


Figure 4.10: Graph showing the Bubble Size Distribution for mortar with 2 ml AEA (traverse length = 103 inches)

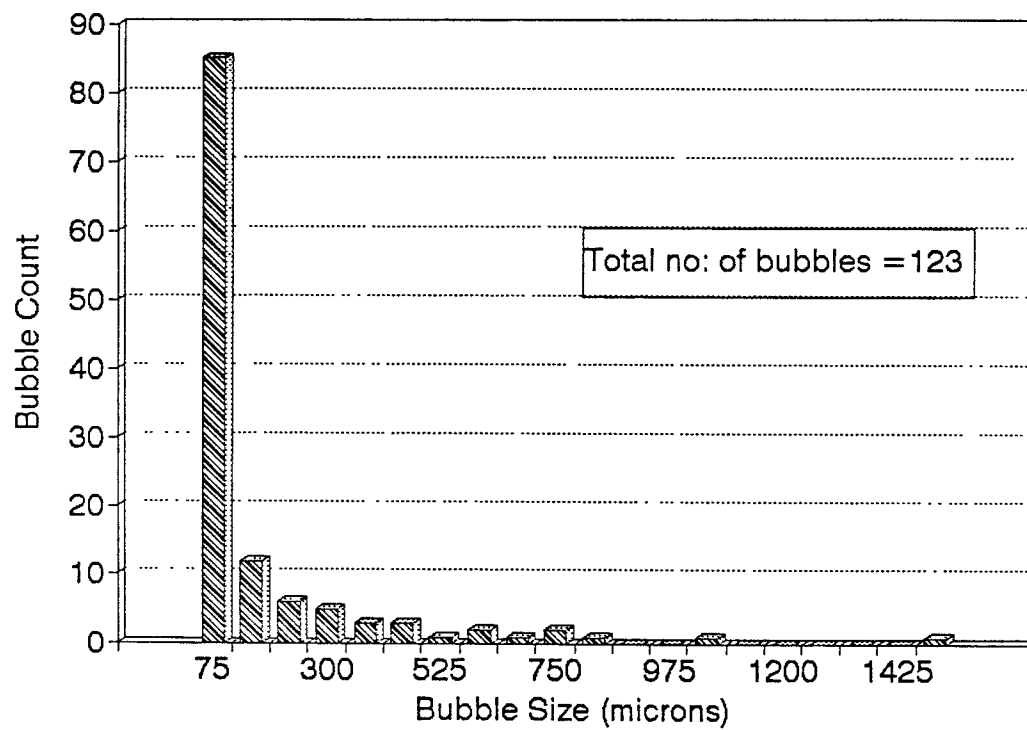


Figure 4.11: Graph showing the Bubble Size Distribution for Slice # 1 of the mortar specimen with 2 ml AEA (traverse length = 20.57 inches)

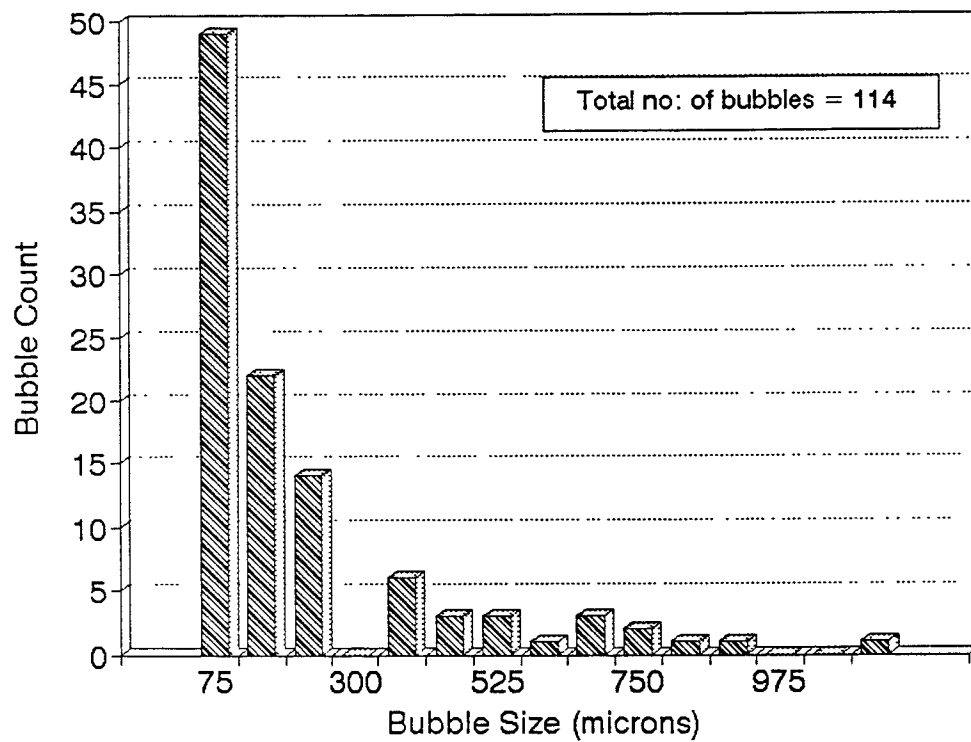


Figure 4.12: Graph showing the Bubble Size Distribution for Slice # 2 of the mortar specimen with 2 ml AEA (traverse length = 20.57 inches)

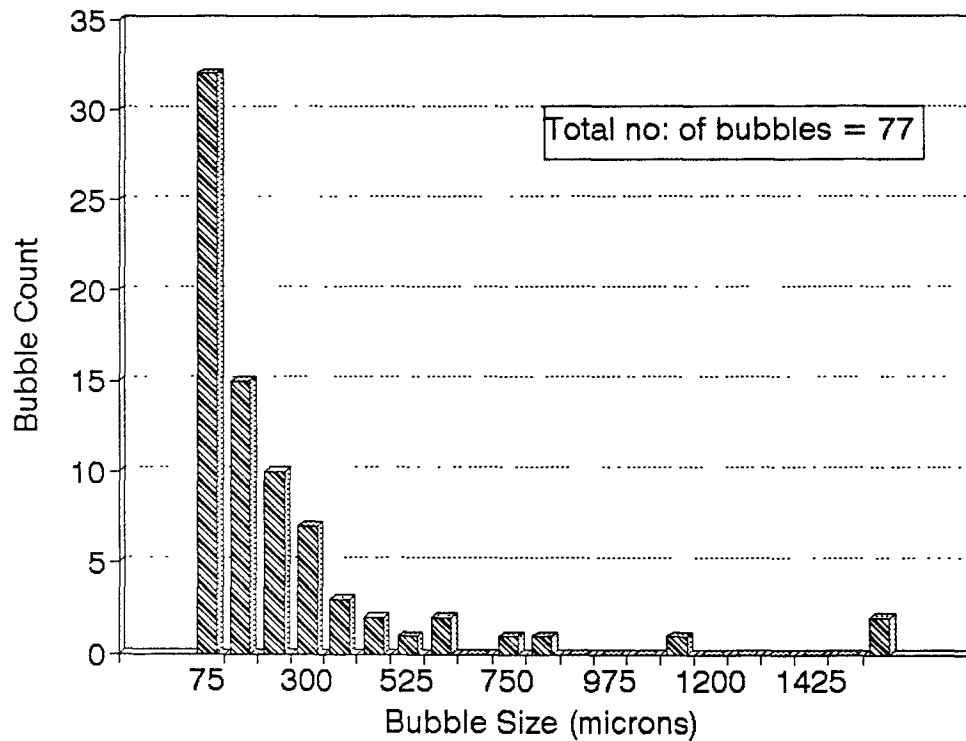


Figure 4.13: Graph showing the Bubble Size Distribution for Slice # 3 of the mortar specimen with 2 ml AEA (traverse length = 20.57 inches)

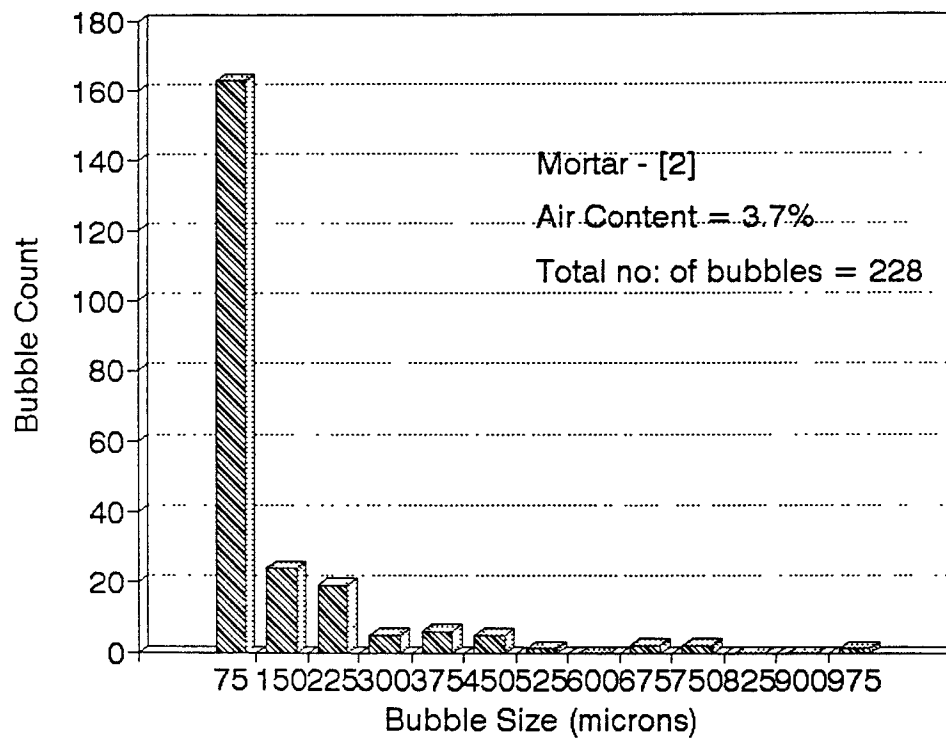


Figure 4.14: Graph showing the Bubble Size Distribution for Slice # 4 of the mortar specimen with 2 ml AEA (traverse length = 20.57 inches)

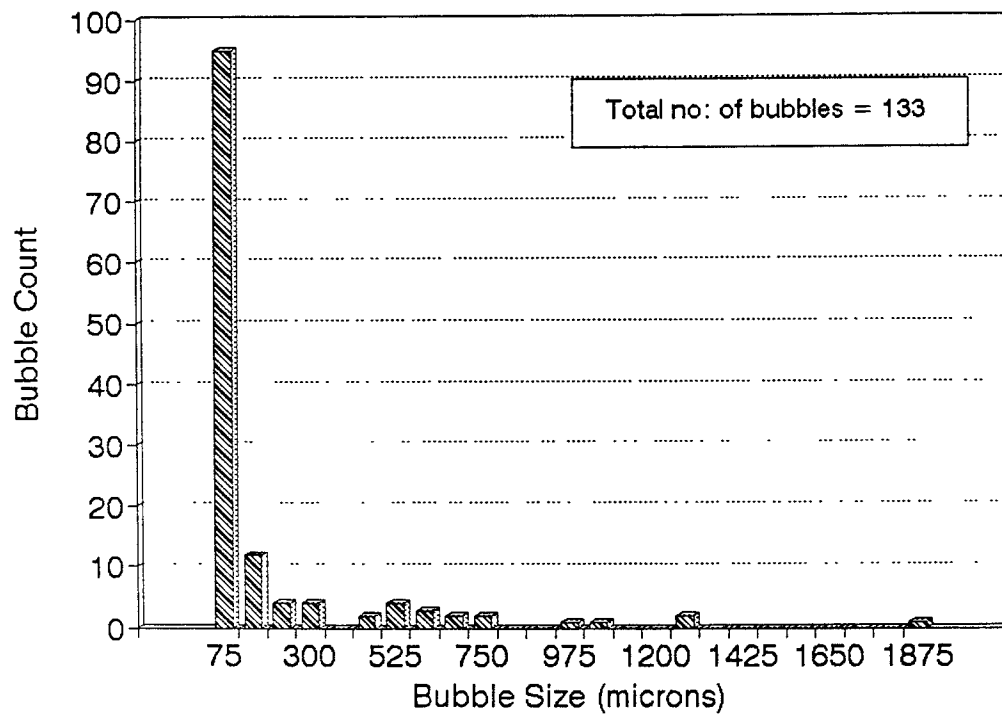


Figure 4.15: Graph showing the Bubble Size Distribution for Slice # 5 of the mortar specimen with 2 ml AEA (traverse length = 20.57 inches)

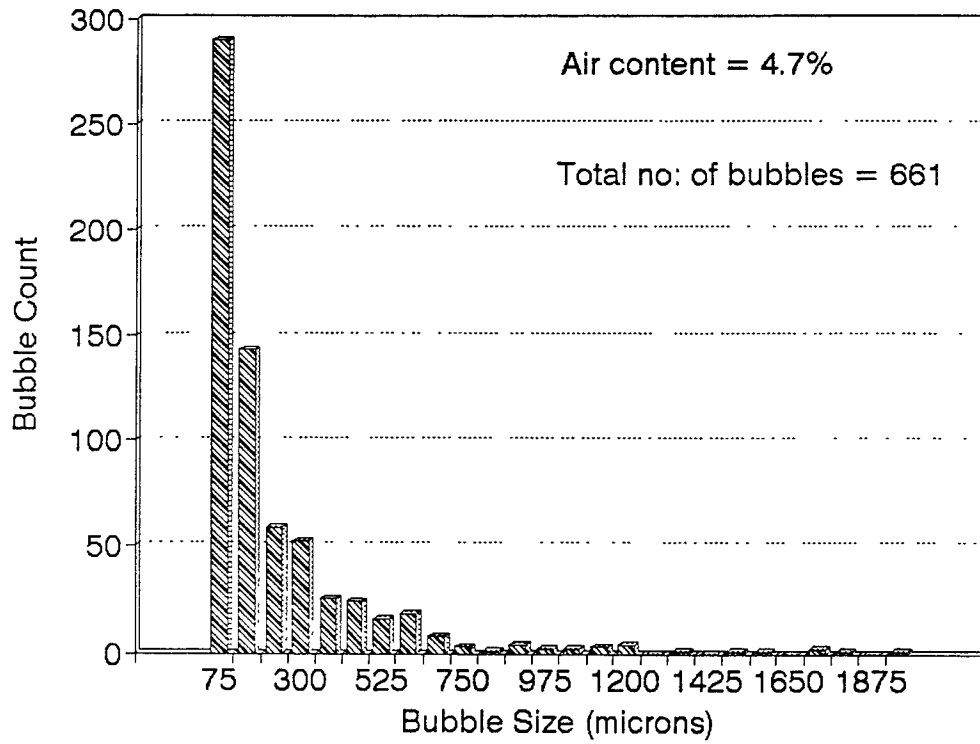


Figure 4.16: Graph showing Bubble Size Distribution for mortar with 5.5 ml AEA (traverse length = 103 inches)

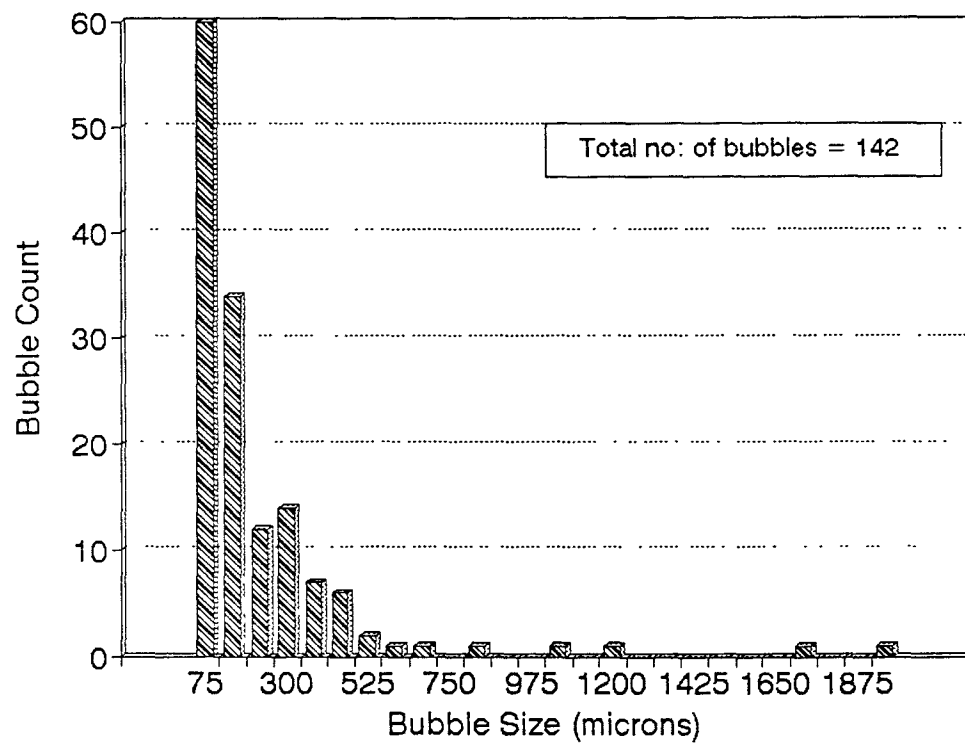


Figure 4.17: Graph showing Bubble Size Distribution for Slice # 1 of mortar with 5.5 ml AEA (traverse length = 20.57 inches)

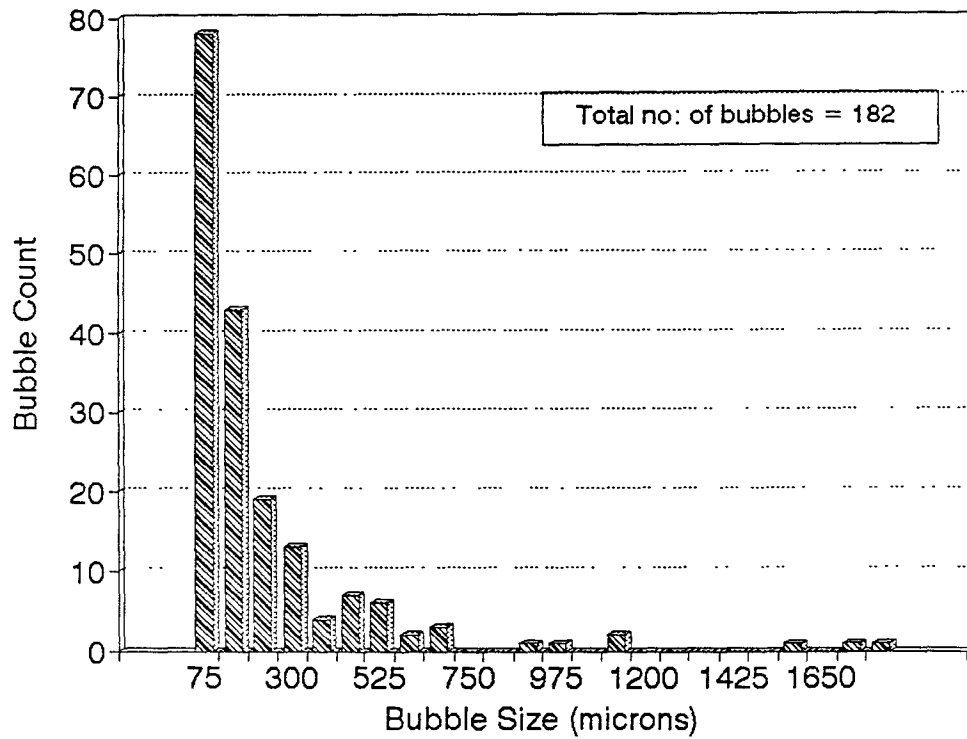


Figure 4.18: Graph showing Bubble Size Distribution for Slice # 2 of mortar with 5.5 ml AEA (traverse length = 20.57 inches)

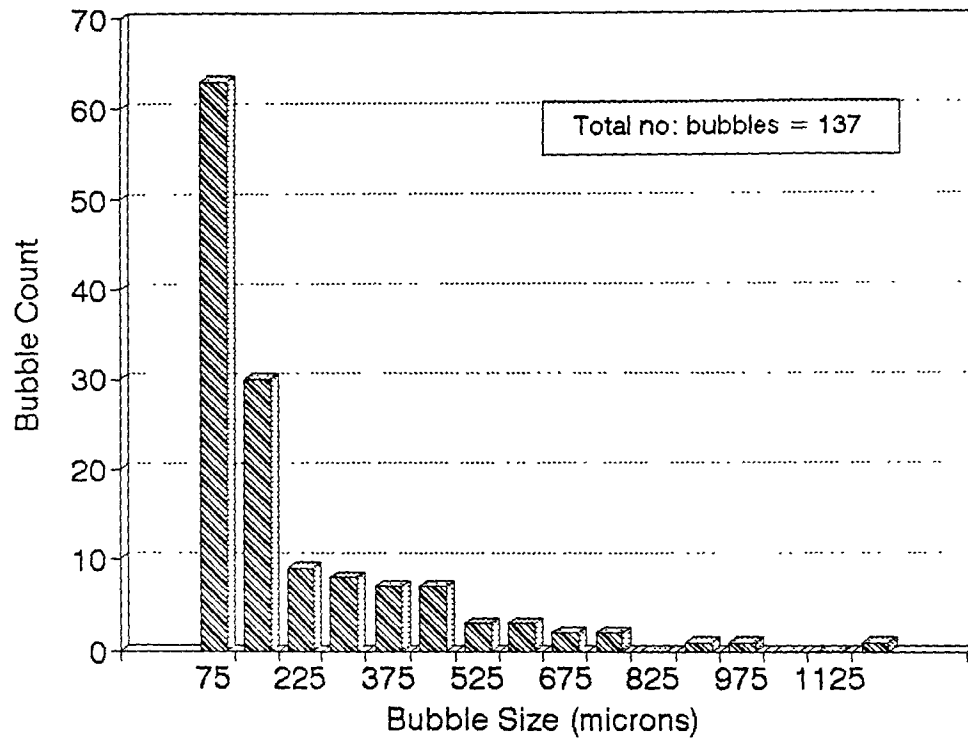


Figure 4.19: Graph showing Bubble Size Distribution for Slice # 3 of mortar with 5.5 ml AEA (traverse length = 20.57 inches)

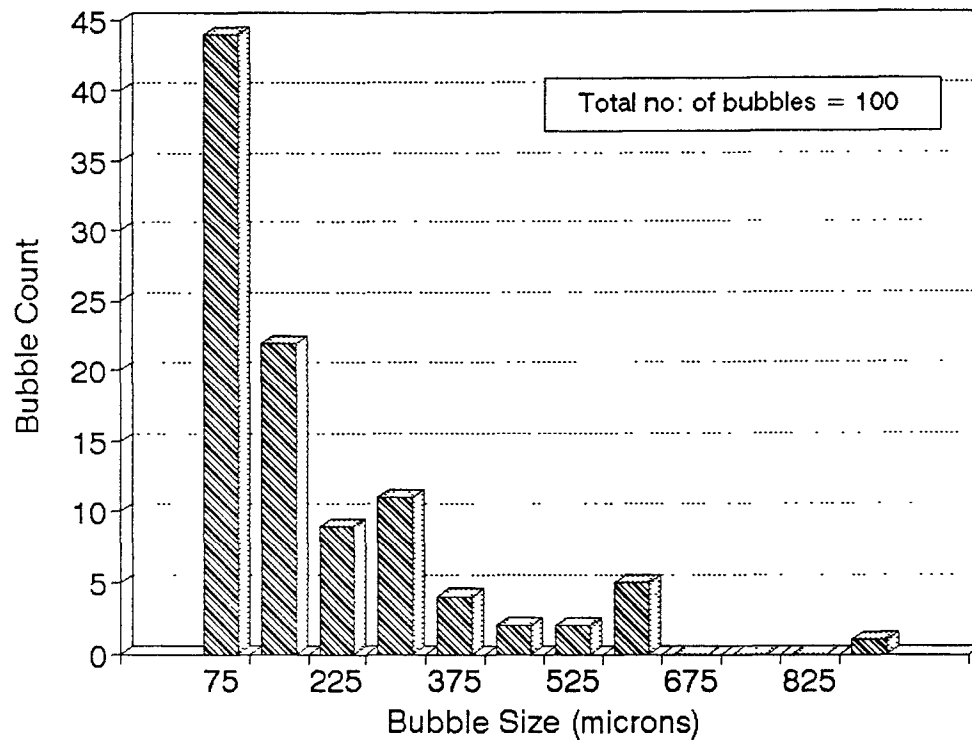


Figure 4.20: Graph showing Bubble Size Distribution for Slice # 4 of mortar with 5.5 ml AEA (traverse length = 20.57 inches)

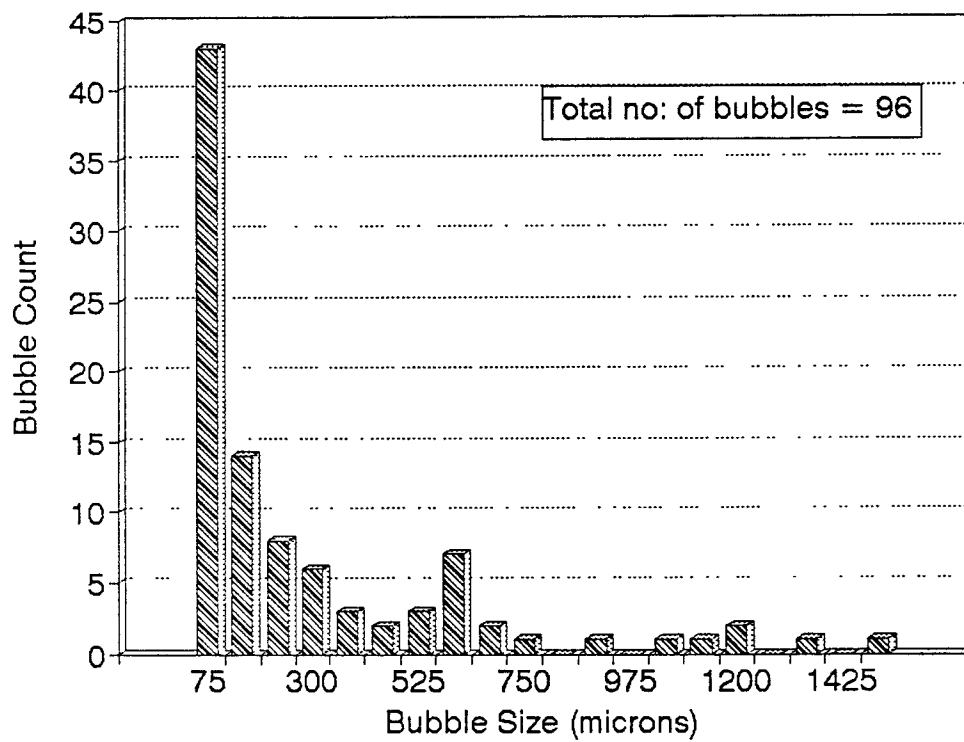


Figure 4.21: Graph showing Bubble Size Distribution for Slice # 5 of mortar with 5.5 ml AEA (traverse length = 20.57 inches)

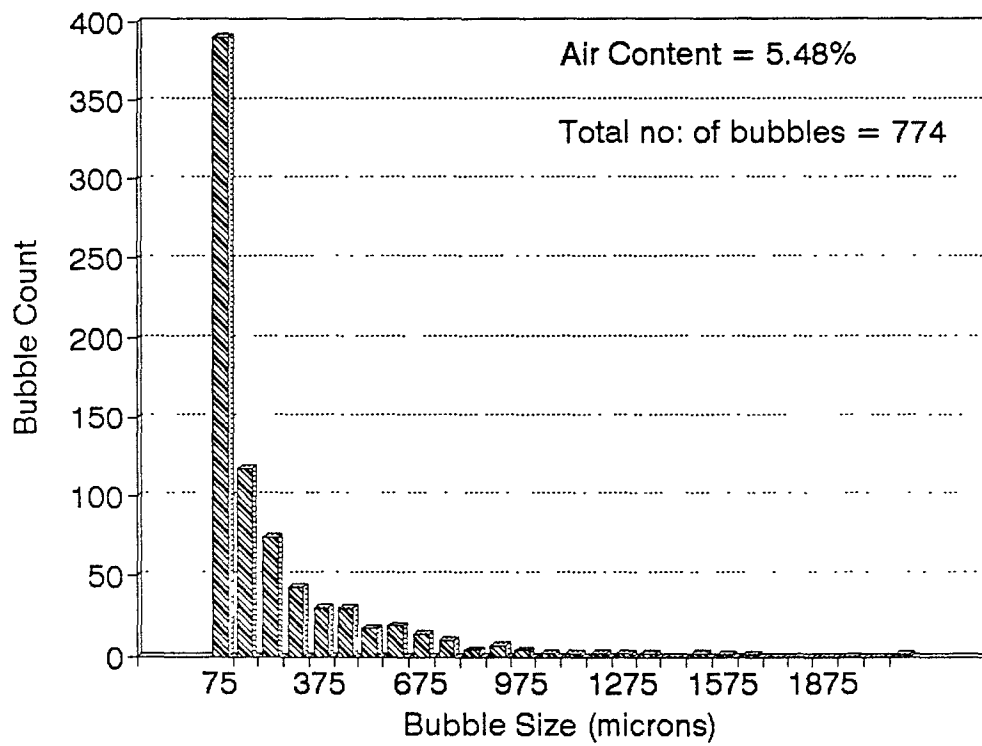


Figure 4.22: Graph showing Bubble Size Distribution for mortar with 10 ml AEA (traverse length = 103 inches)

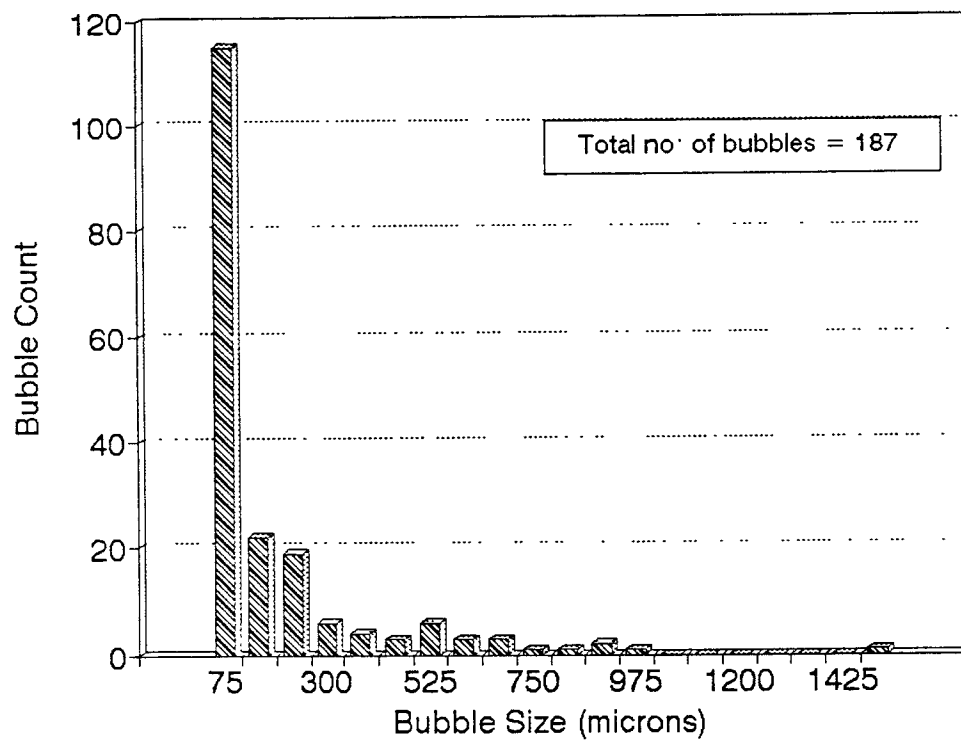


Figure 4.23: Graph showing Bubble Size Distribution for Slice # 1 of mortar with 10 ml AEA (traverse length = 20.57 inches)

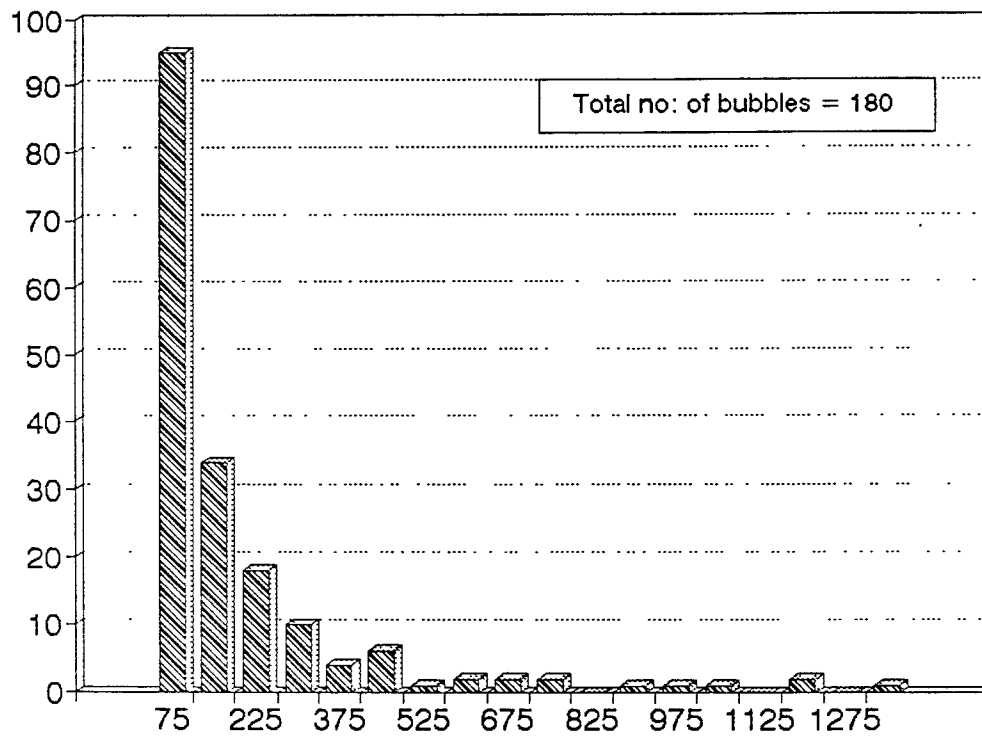


Figure 4.24: Graph showing Bubble Size Distribution for Slice # 2 of mortar with 10 ml AEA (traverse length = 20.57 inches)

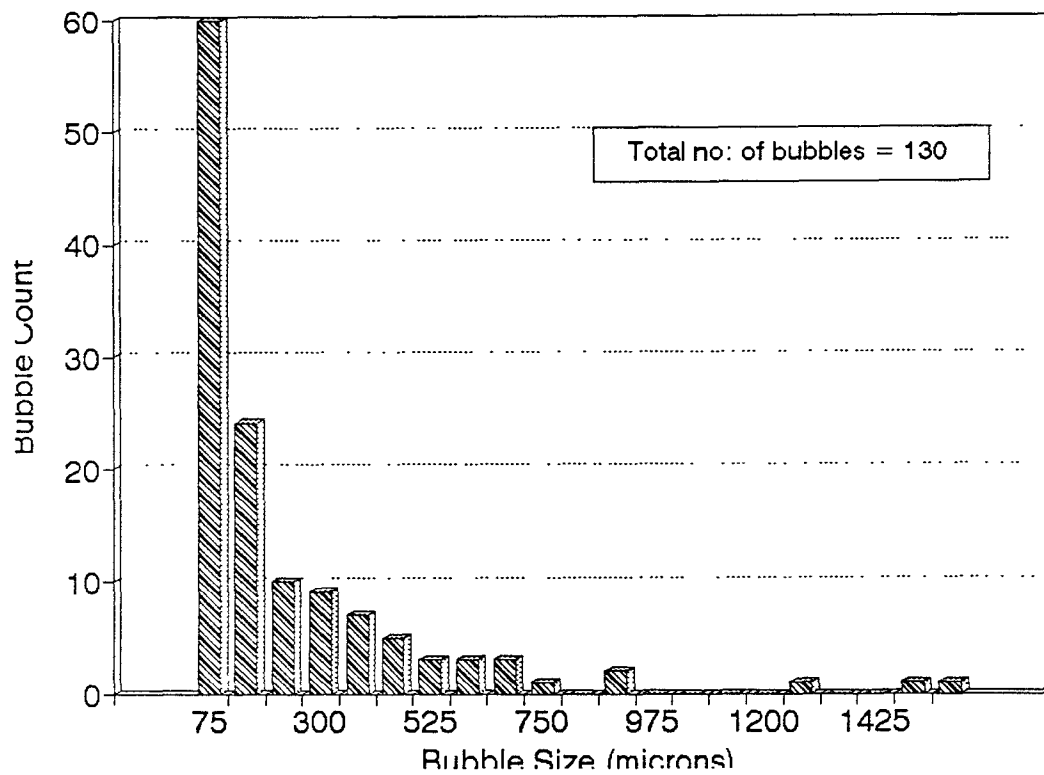


Figure 4.25: Graph showing Bubble Size Distribution for Slice # 3 of mortar with 10 ml AEA (traverse length = 20.57 inches)

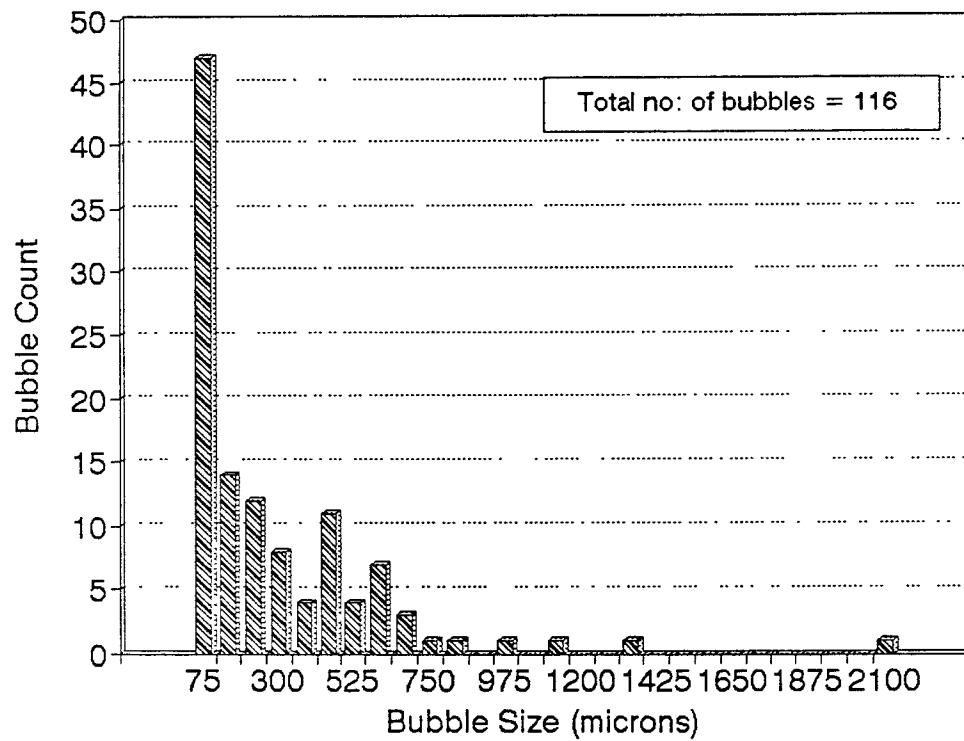


Figure 4.26: Graph showing Bubble Size Distribution for Slice # 4 of mortar with 10 ml AEA (traverse length = 20.57 inches)

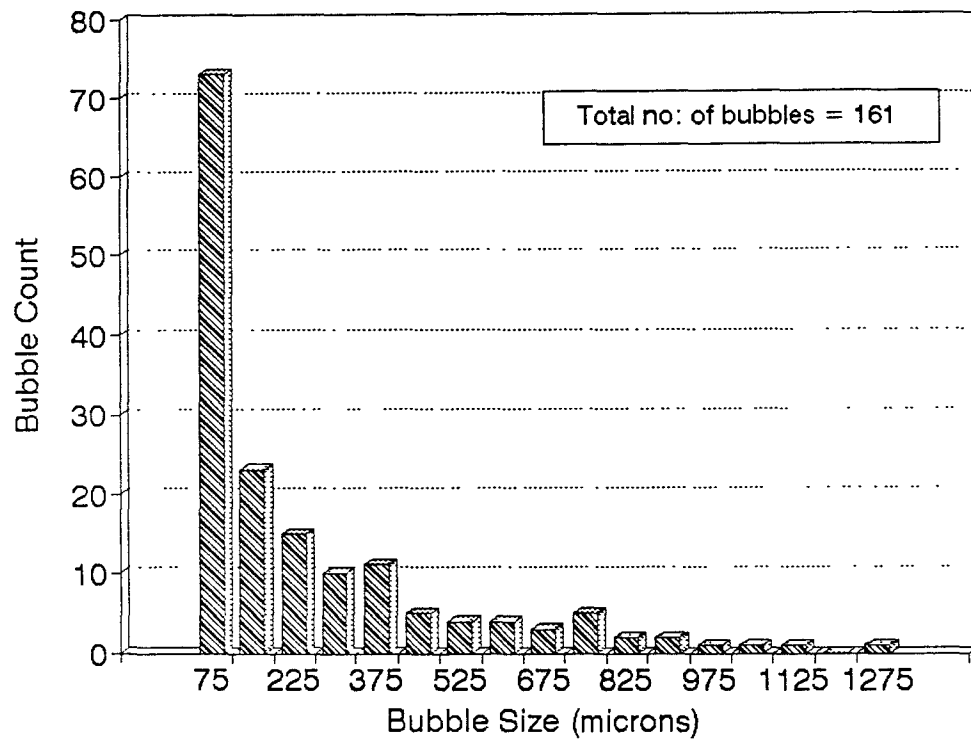


Figure 4.27: Graph showing Bubble Size Distribution for Slice # 5 of mortar with 10 ml AEA (traverse length = 20.57 inches)

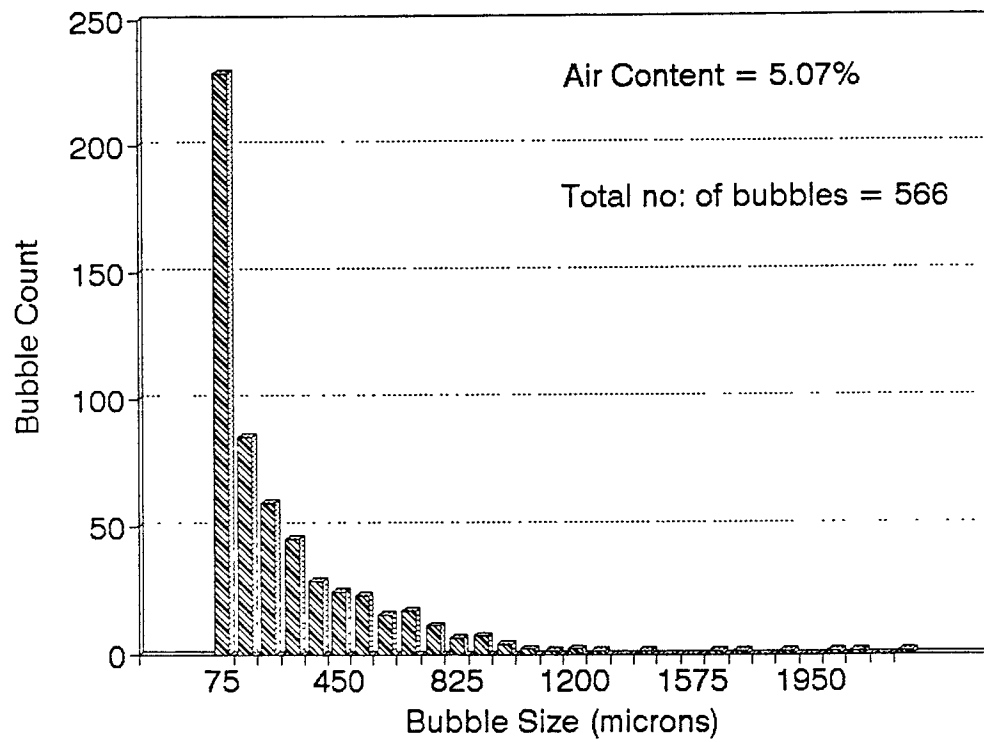


Figure 4.28: Graph showing Bubble Size Distribution for mortar with 15 ml AEA (traverse length = 103 inches)

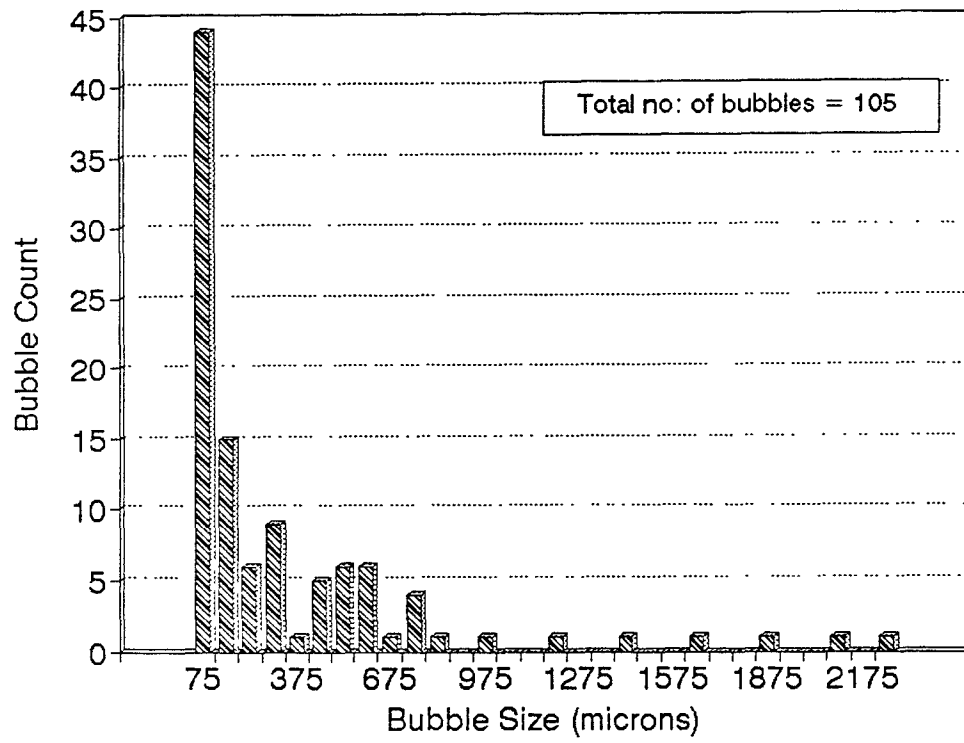


Figure 4.29: Graph showing Bubble Size Distribution for Slice # 1 of mortar with 15 ml AEA (traverse length = 20.57 inches)

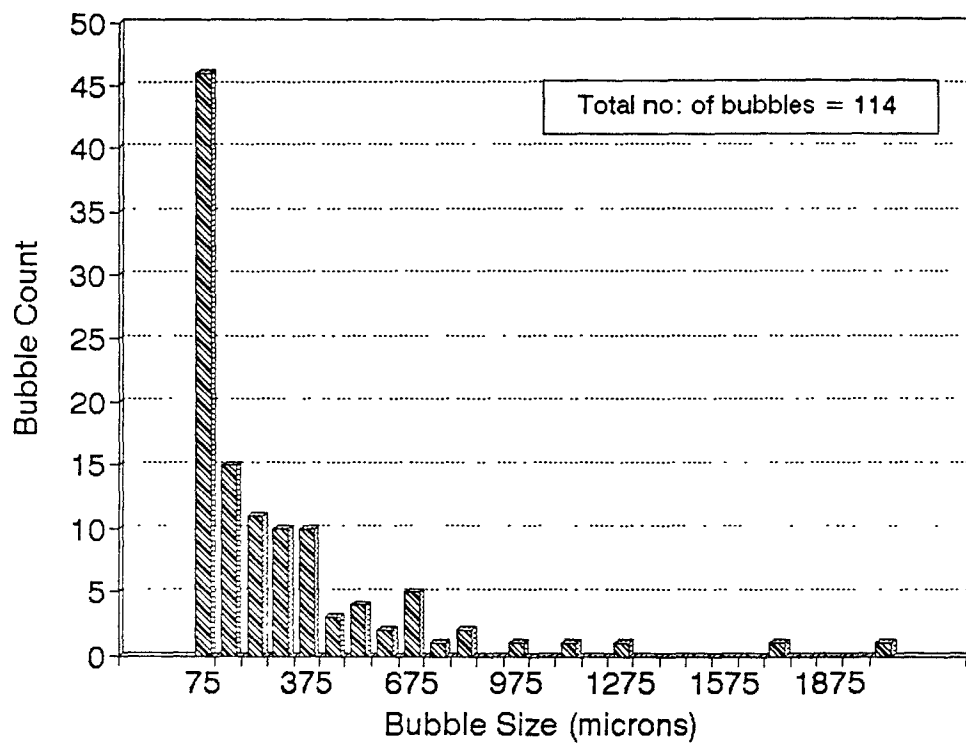


Figure 4.30: Graph showing Bubble Size Distribution for Slice # 2 of mortar with 15 ml AEA (traverse length = 20.57 inches)

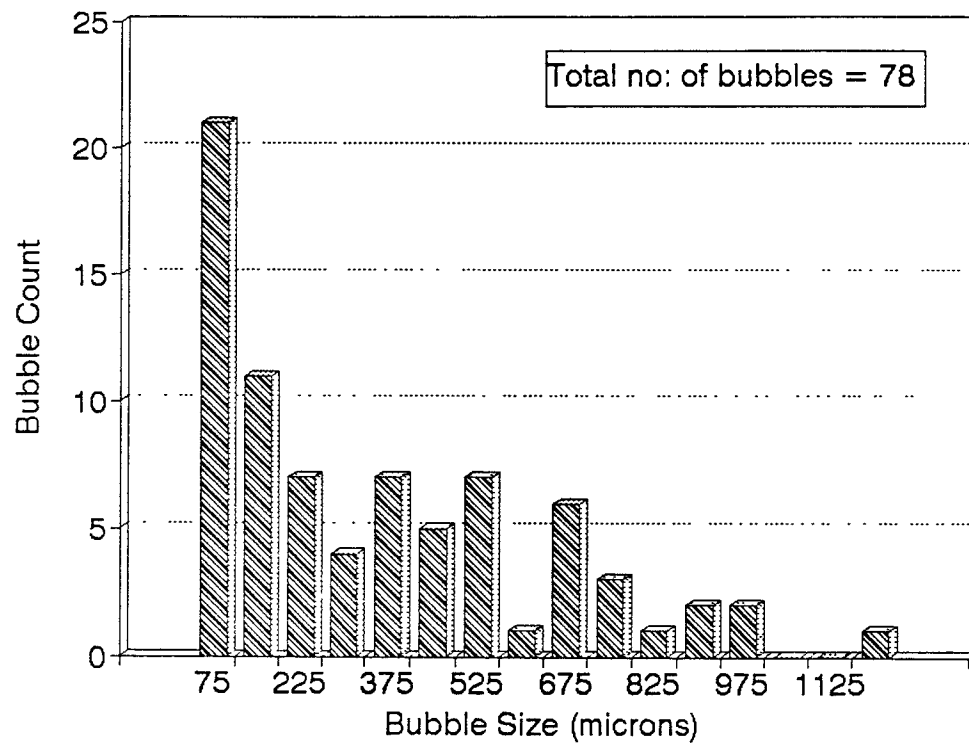


Figure 4.31: Graph showing Bubble Size Distribution for Slice # 3 of mortar with 15 ml AEA (traverse length = 20.57 inches)

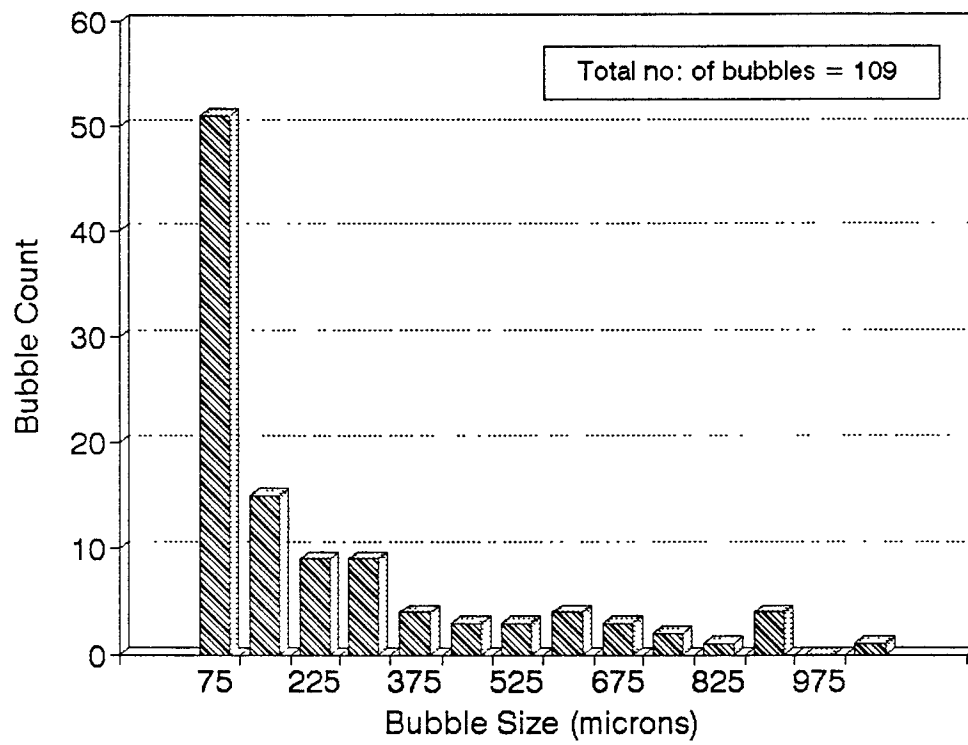


Figure 4.32: Graph showing Bubble Size Distribution for Slice # 4 of mortar with 15 ml AEA (traverse length = 20.57 inches)

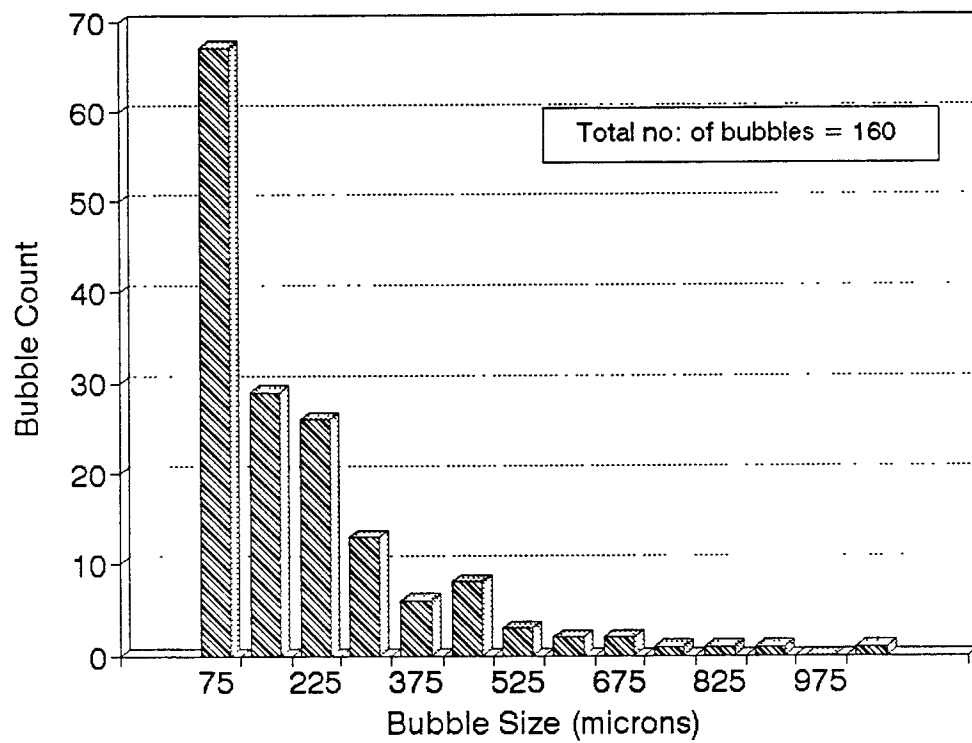


Figure 4.33: Graph showing Bubble Size Distribution for Slice # 5 of mortar with 15 ml AEA (traverse length = 20.57 inches)

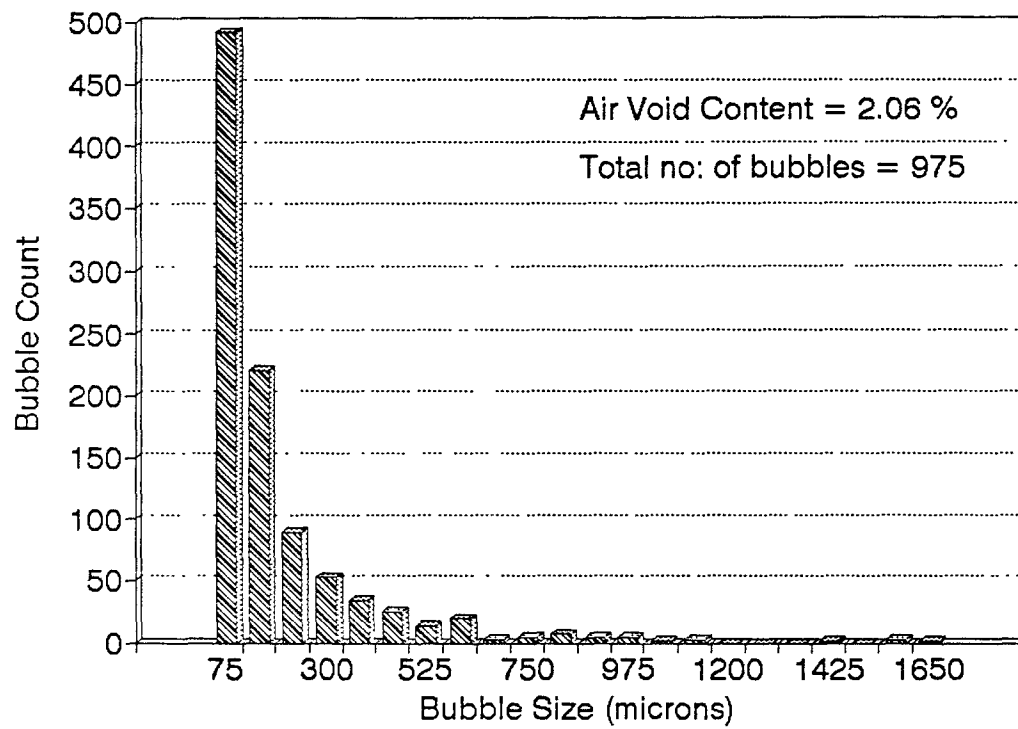


Figure 4.34: Graph showing Bubble Size Distribution for concrete with no AEA (traverse length = 100.5 inches)

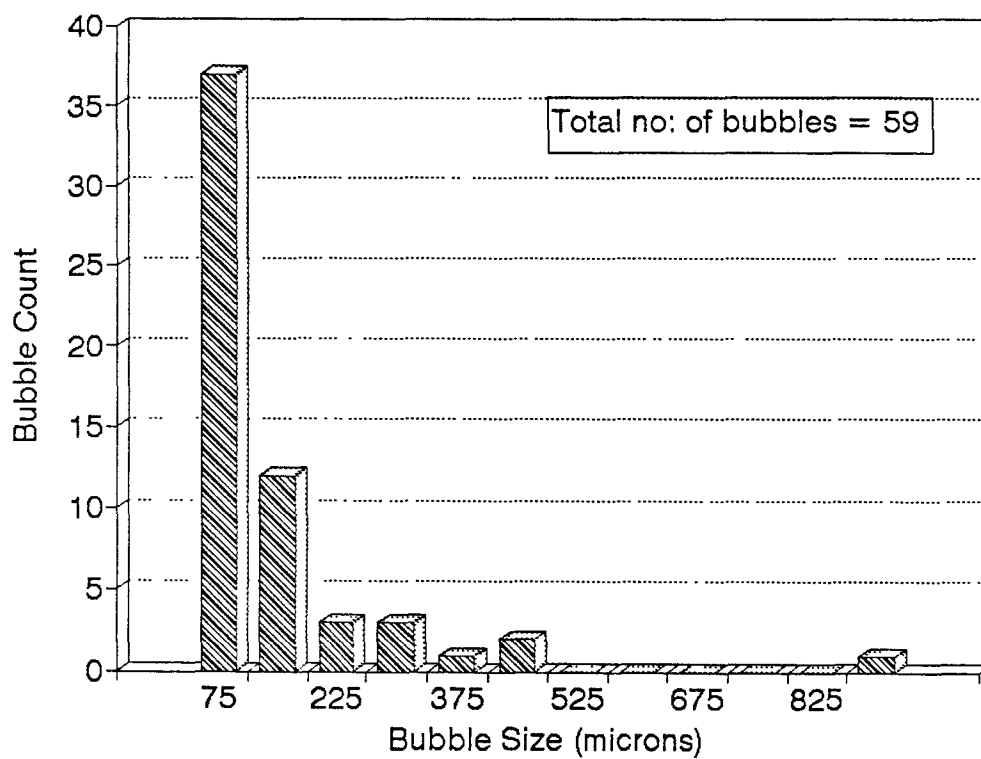


Figure 4.35: Graph showing Bubble Size Distribution for Slice # 1 of concrete with no AEA (traverse length = 13.96 inches)

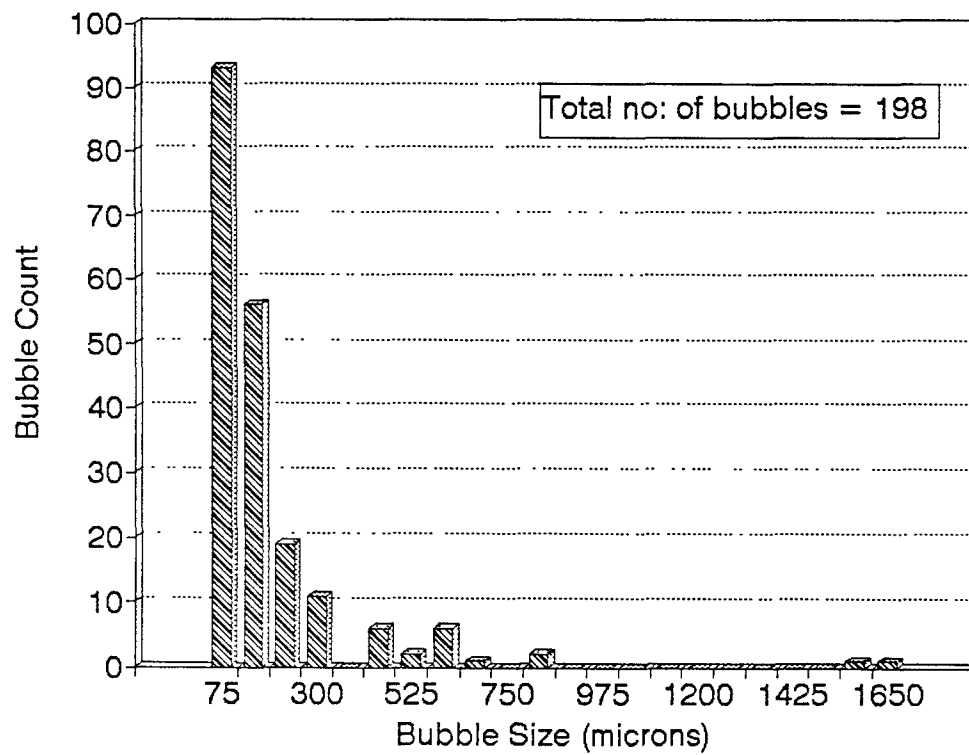


Figure 4.36: Graph showing Bubble Size Distribution for Slice # 2 of concrete with no AEA (traverse length = 13.96 inches)

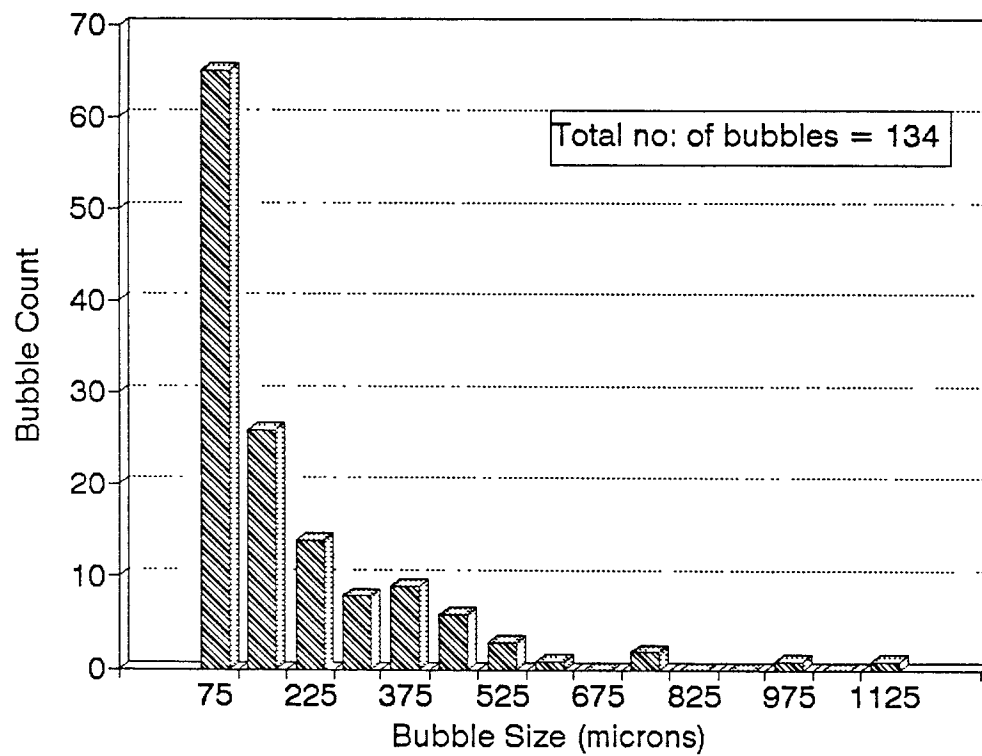


Figure 4.37: Graph showing Bubble Size Distribution for Slice # 3 of concrete with no AEA (traverse length = 13.96 inches)

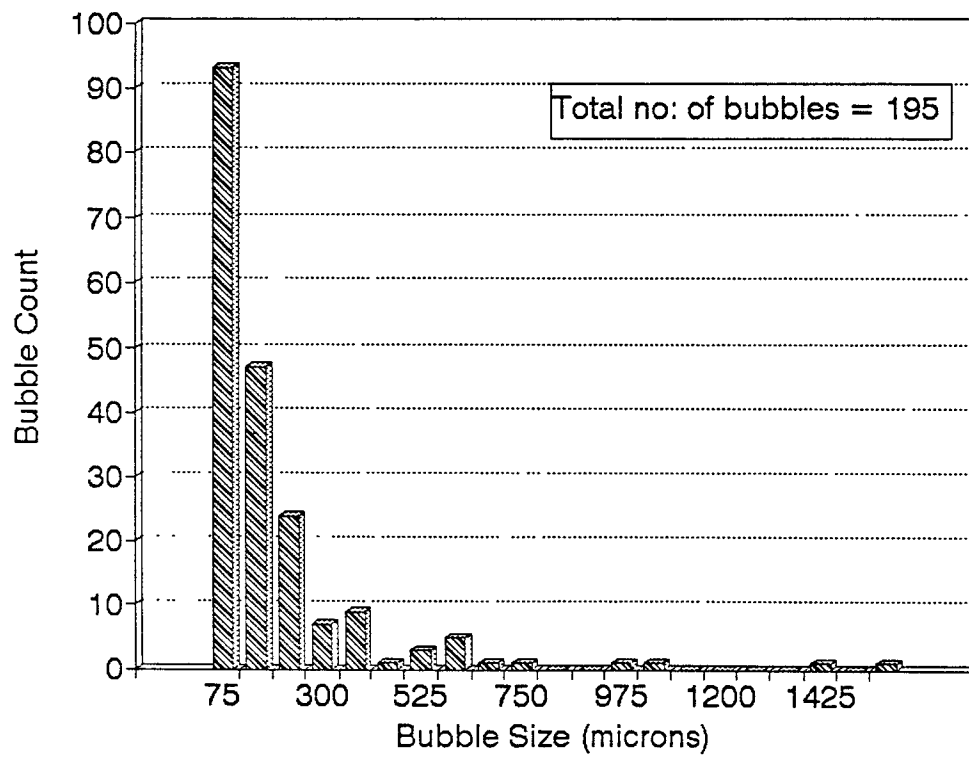


Figure 4.38: Graph showing Bubble Size Distribution for Slice # 4 of concrete with no AEA (traverse length = 13.96 inches)

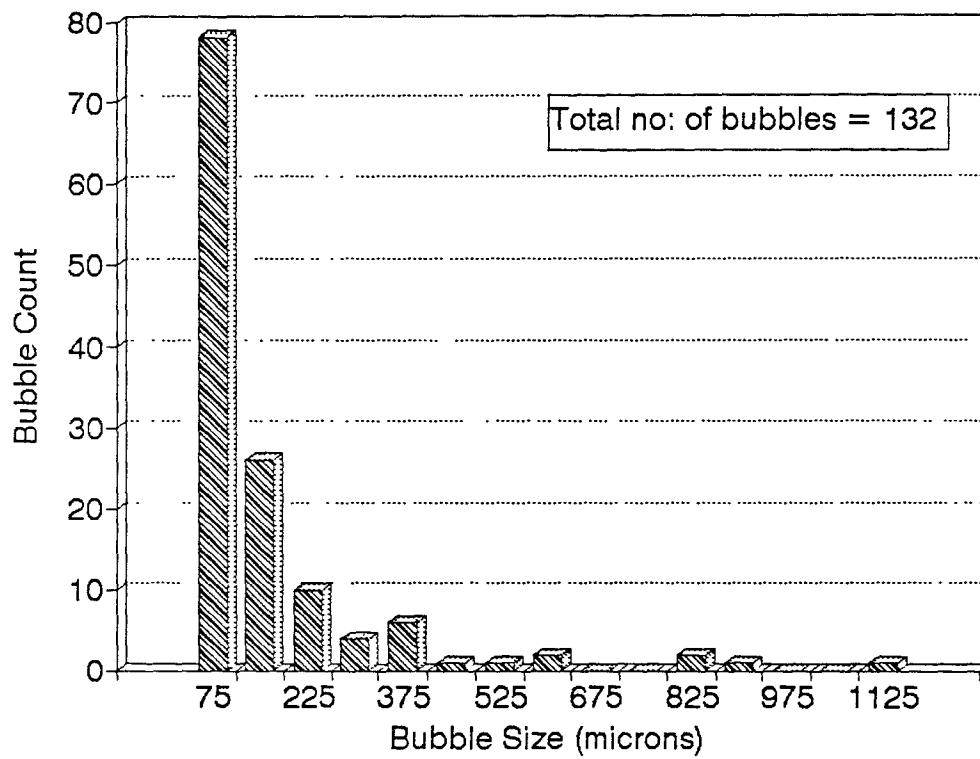


Figure 4.39: Graph showing Bubble Size Distribution for Slice # 5 of concrete with no AEA (traverse length = 13.96 inches)

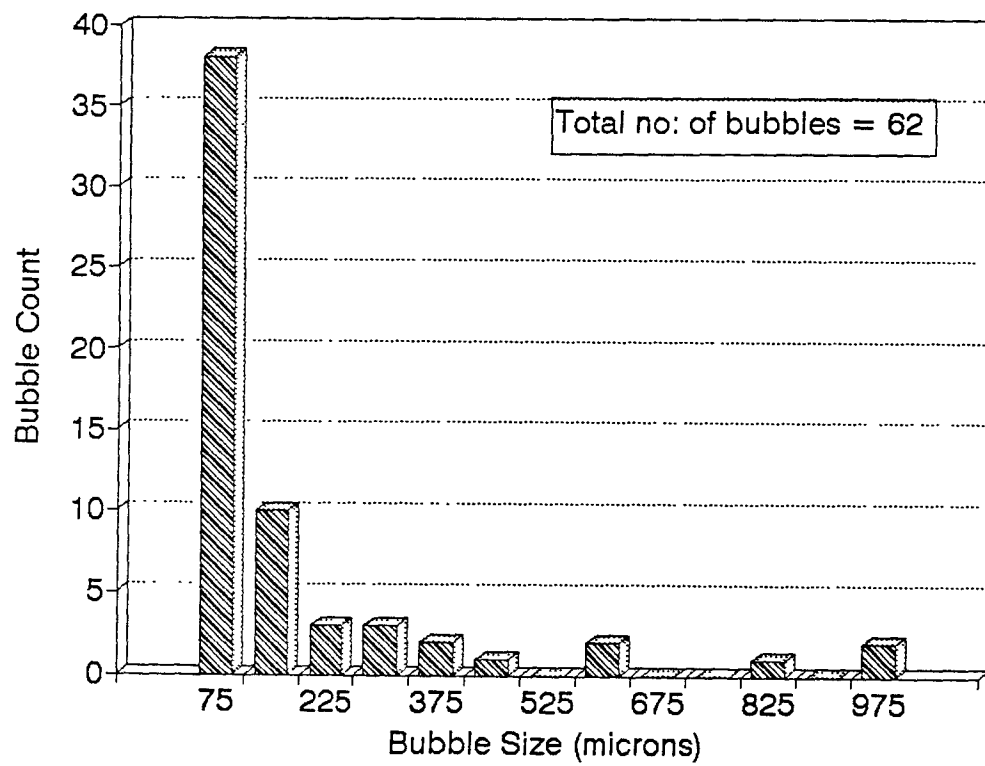


Figure 4.40: Graph showing Bubble Size Distribution for Slice # 6 of concrete with no AEA (traverse length = 13.96 inches)

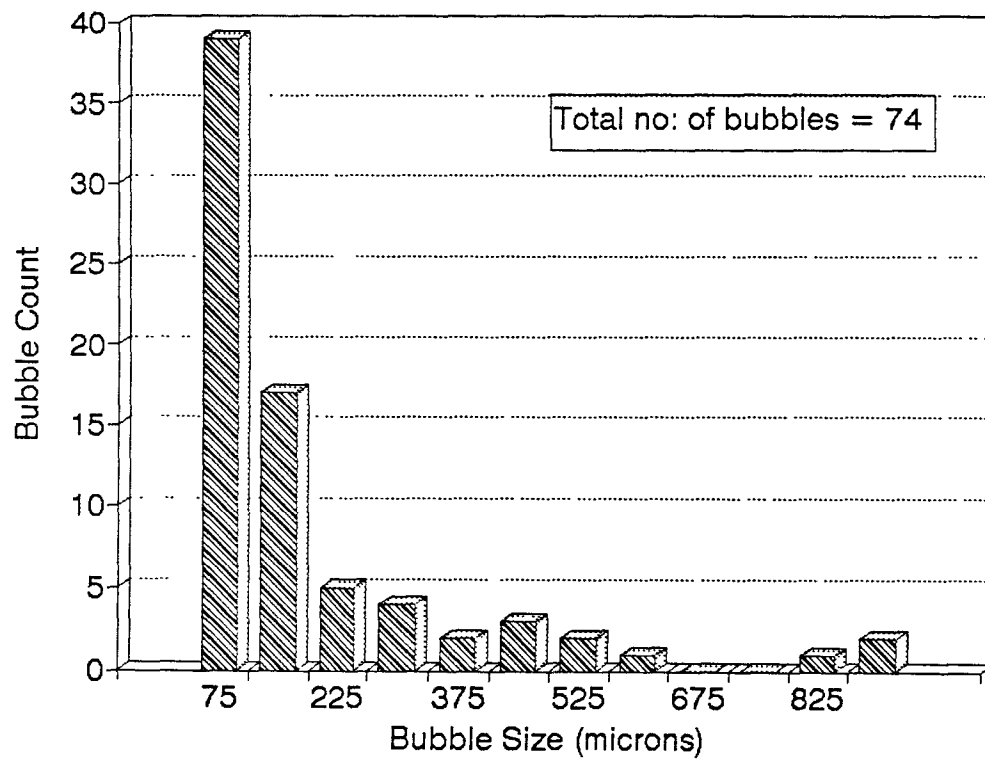


Figure 4.41: Graph showing Bubble Size Distribution for Slice # 7 of concrete with no AEA (traverse length = 13.96 inches)

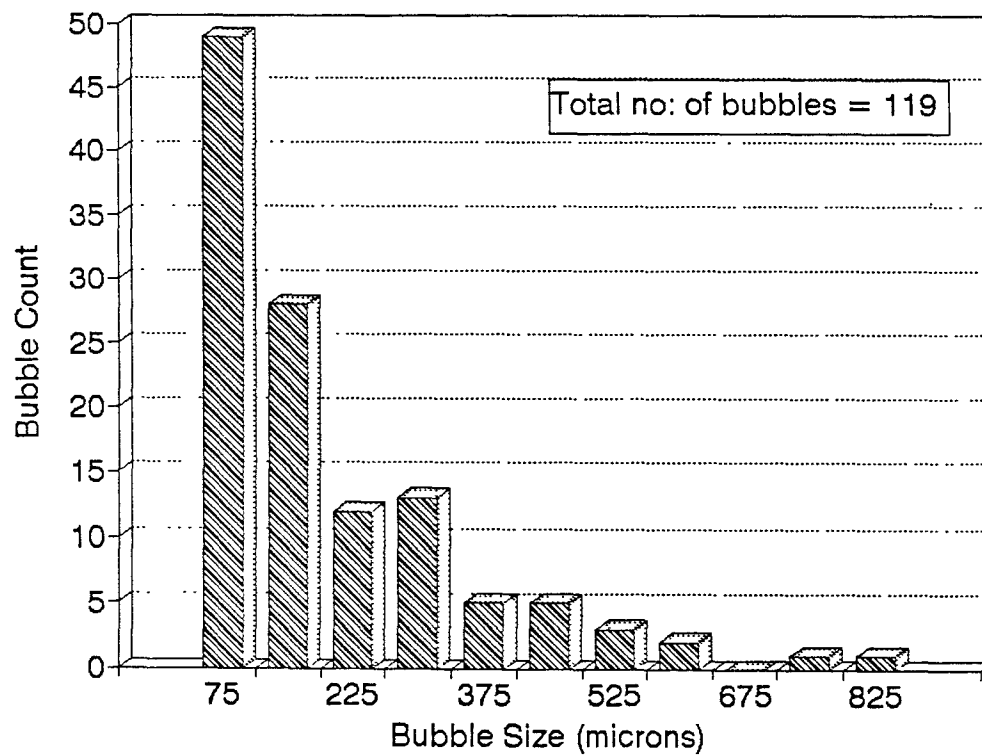


Figure 4.42: Graph showing Bubble Size Distribution for Slice # 8 of concrete with no AEA (traverse length = 13.96 inches)

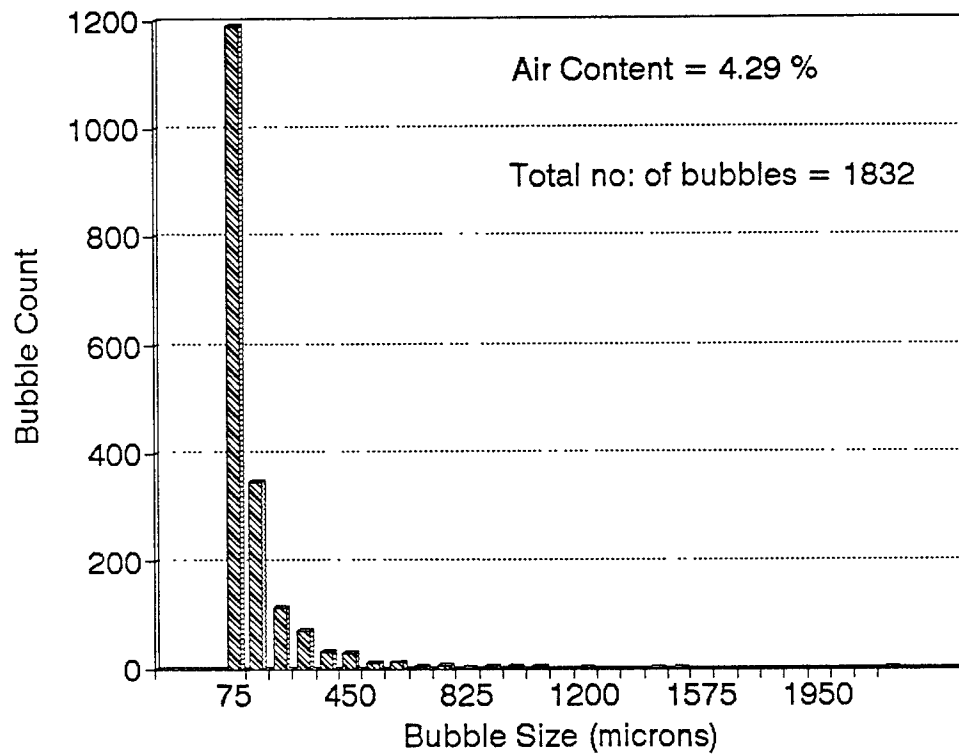


Figure 4.43: Graph showing Bubble Size Distribution for concrete with 2 ml AEA (traverse length = 100.5 inches)

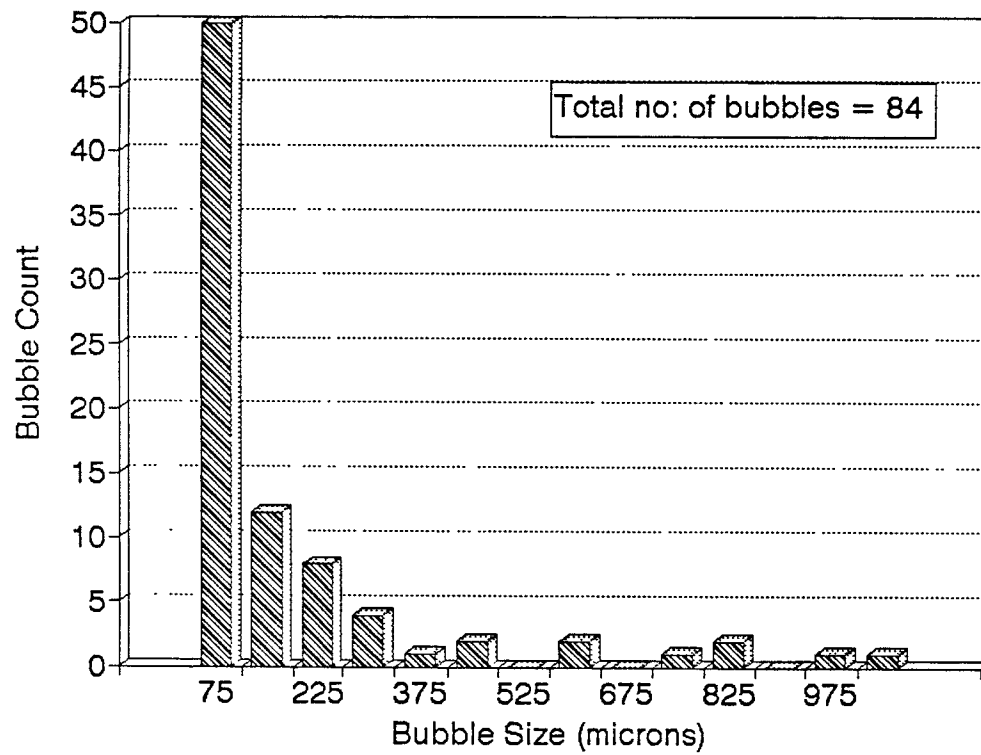


Figure 4.44: Graph showing Bubble Size Distribution for Slice # 1 of concrete with 2 ml AEA (traverse length = 13.96 inches)

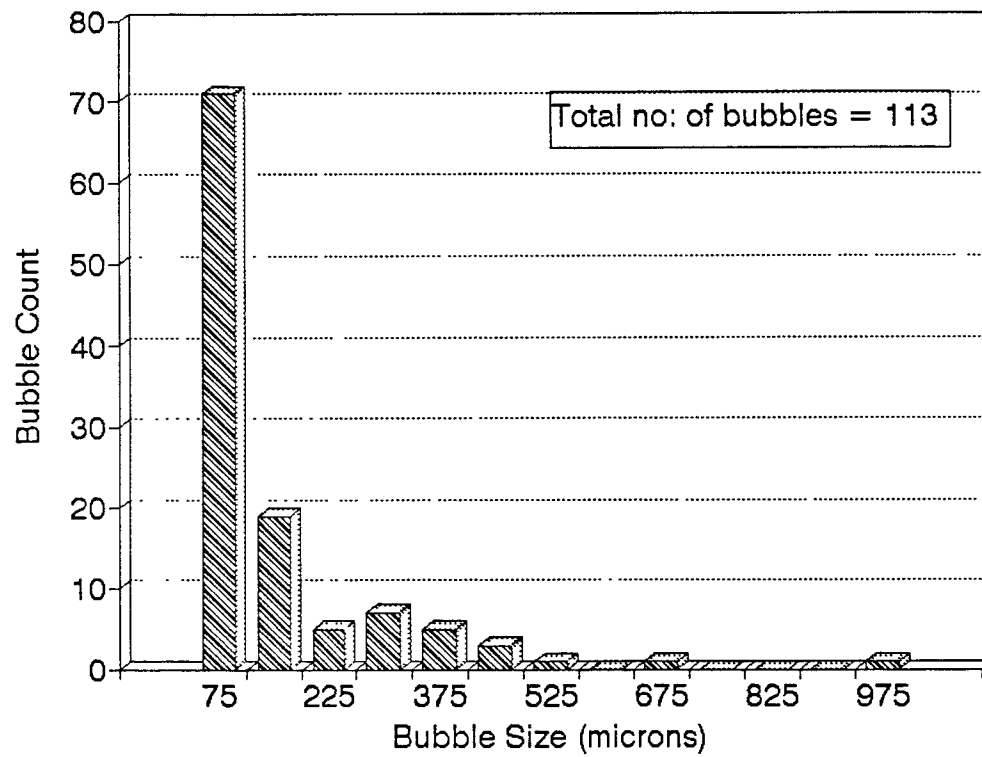


Figure 4.45: Graph showing Bubble Size Distribution for Slice # 2 of concrete with 2 ml AEA (traverse length = 13.96 inches)

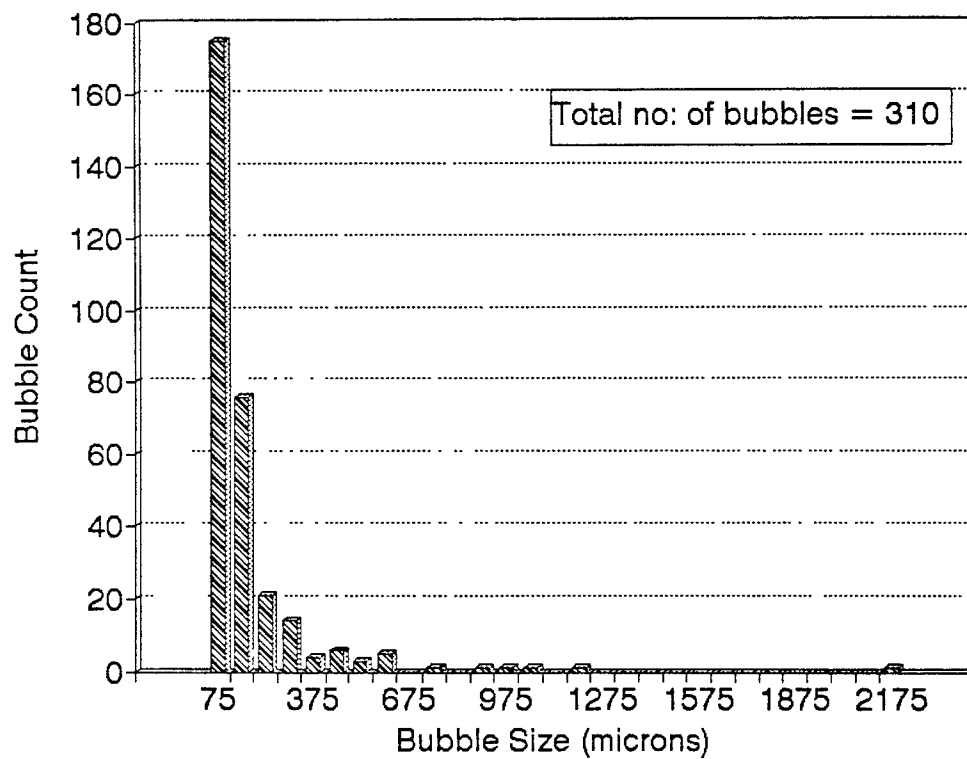


Figure 4.46: Graph showing Bubble Size Distribution for Slice # 3 of concrete with 2 ml AEA (traverse length = 13.96 inches)

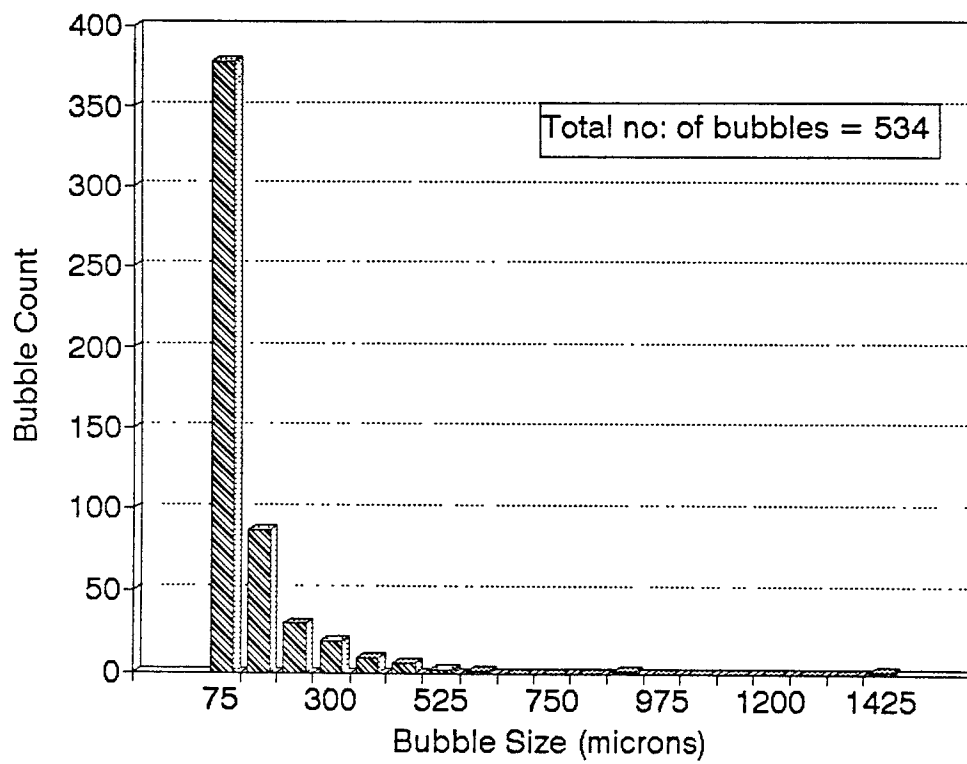


Figure 4.47: Graph showing Bubble Size Distribution for Slice # 4 of concrete with 2 ml AEA (traverse length = 13.96 inches)

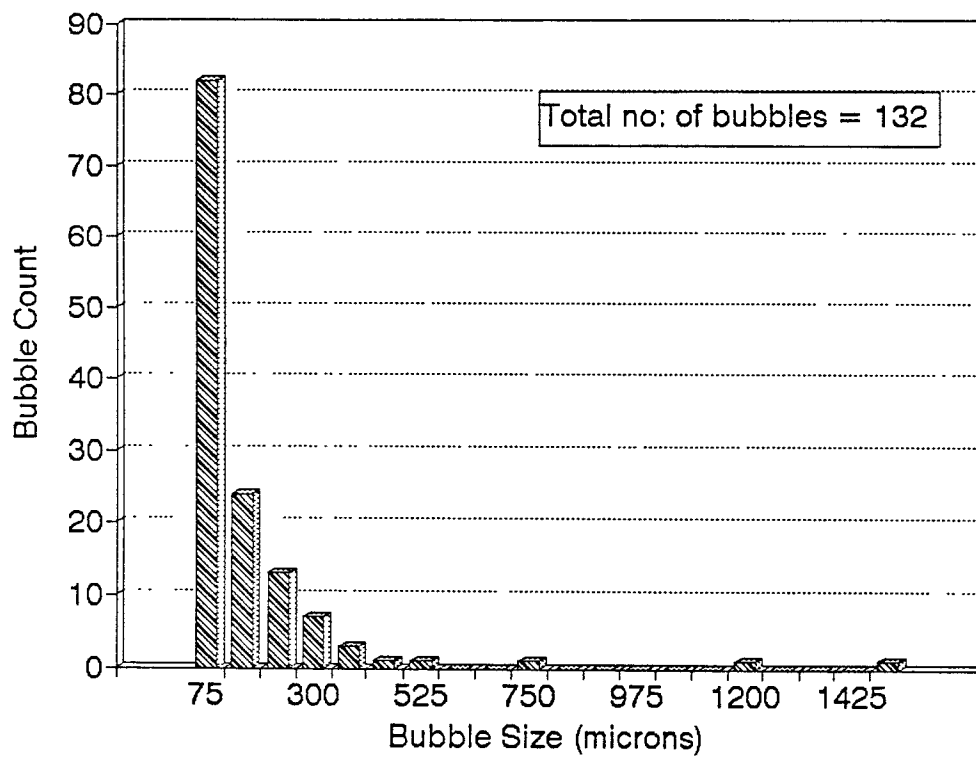


Figure 4.48: Graph showing Bubble Size Distribution for Slice # 5 of concrete with 2 ml AEA (traverse length = 13.96 inches)

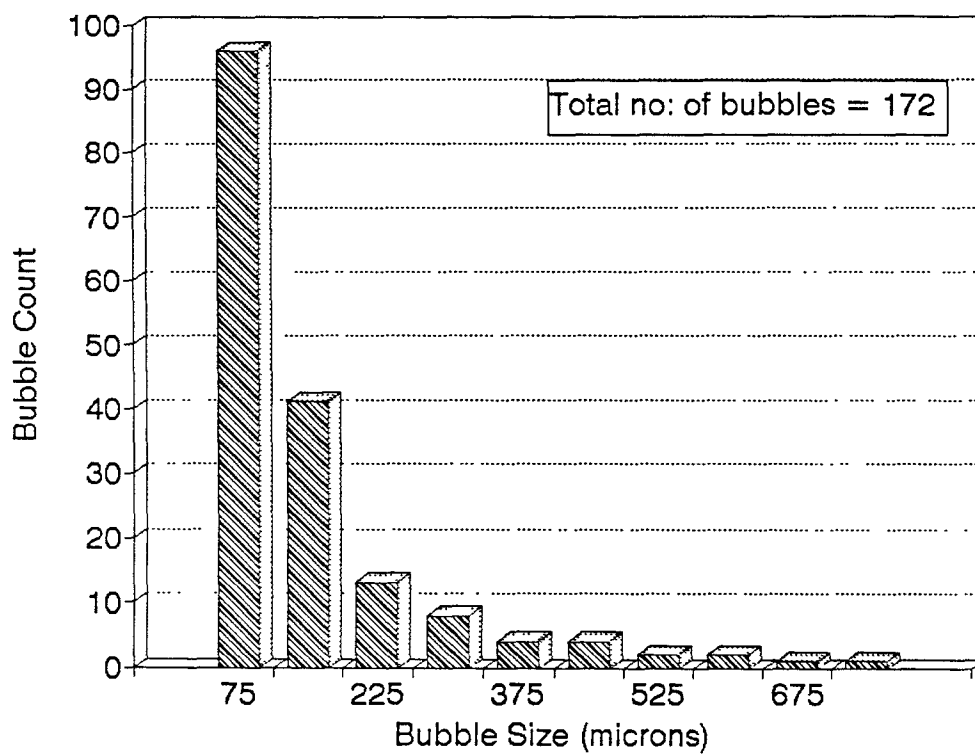


Figure 4.49: Graph showing Bubble Size Distribution for Slice # 6 of concrete with 2 ml AEA (traverse length = 13.96 inches)

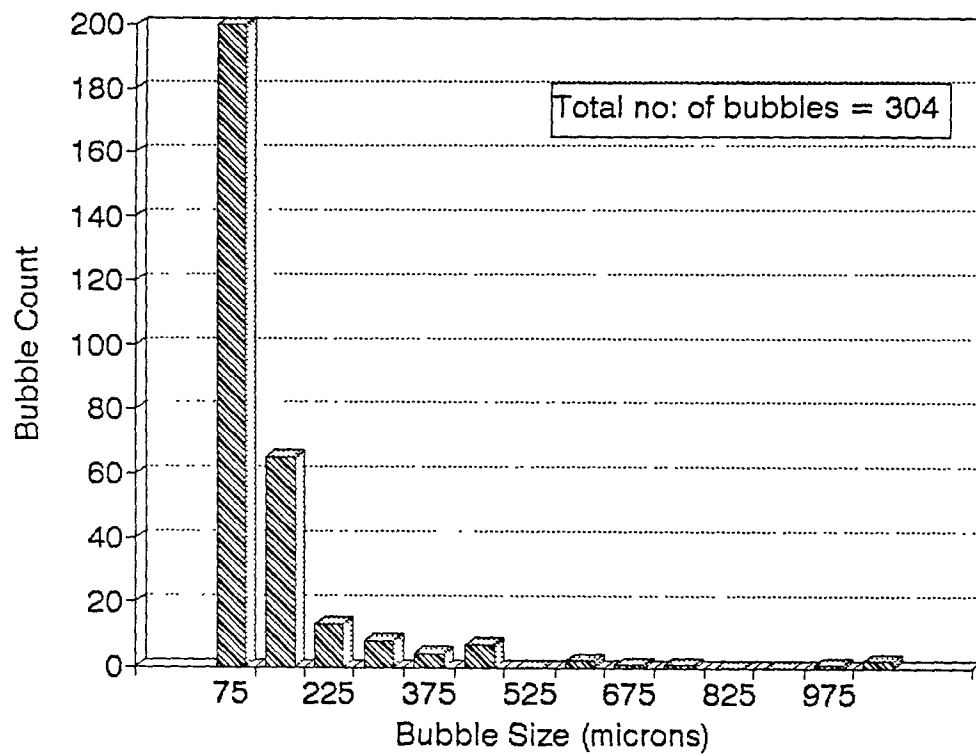


Figure 4.50: Graph showing Bubble Size Distribution for Slice # 7 of concrete with 2 ml AEA (traverse length = 13.96 inches)

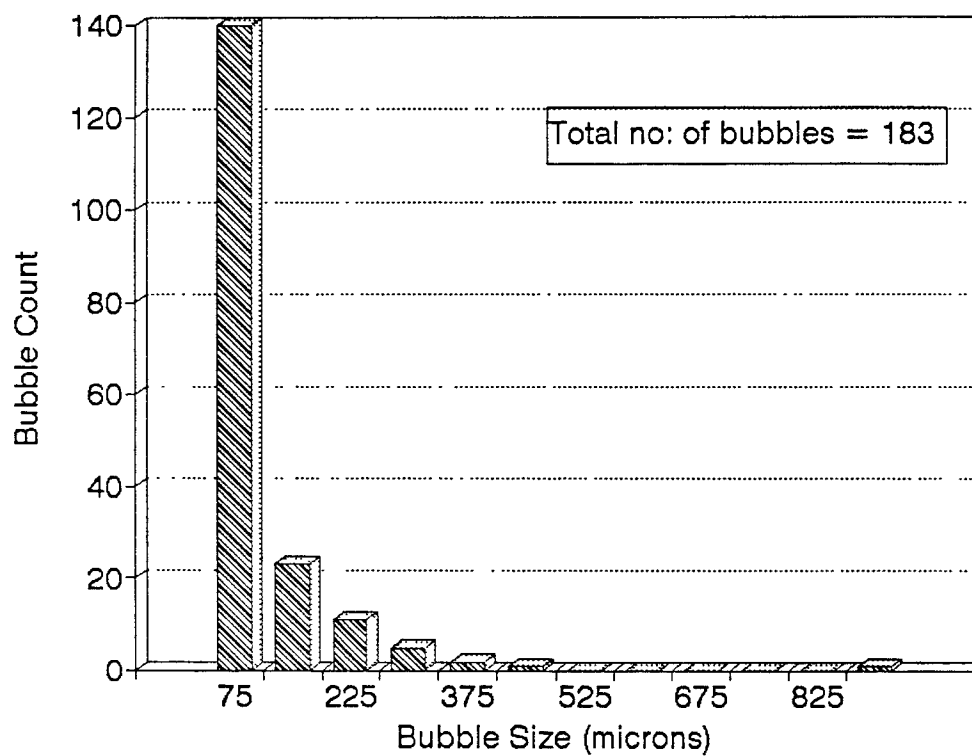


Figure 4.51: Graph showing Bubble Size Distribution for Slice # 8 of concrete with 2 ml AEA (traverse length = 13.96 inches)

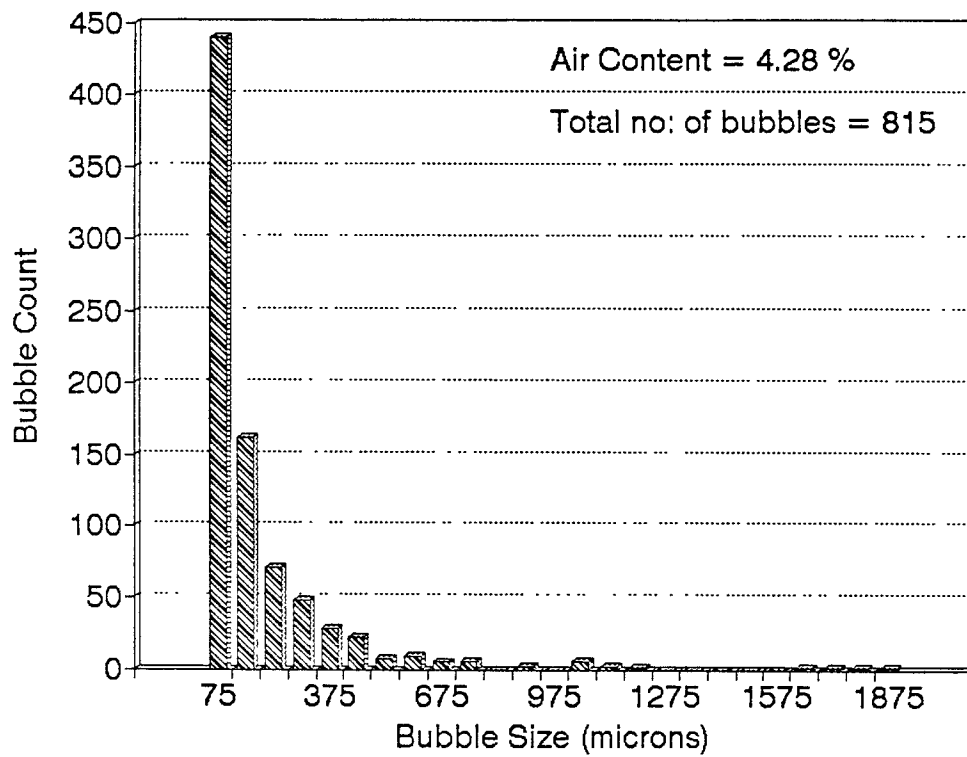


Figure 4.52: Graph showing Bubble Size Distribution for concrete with 5.5 AEA (traverse length = 103 inches)

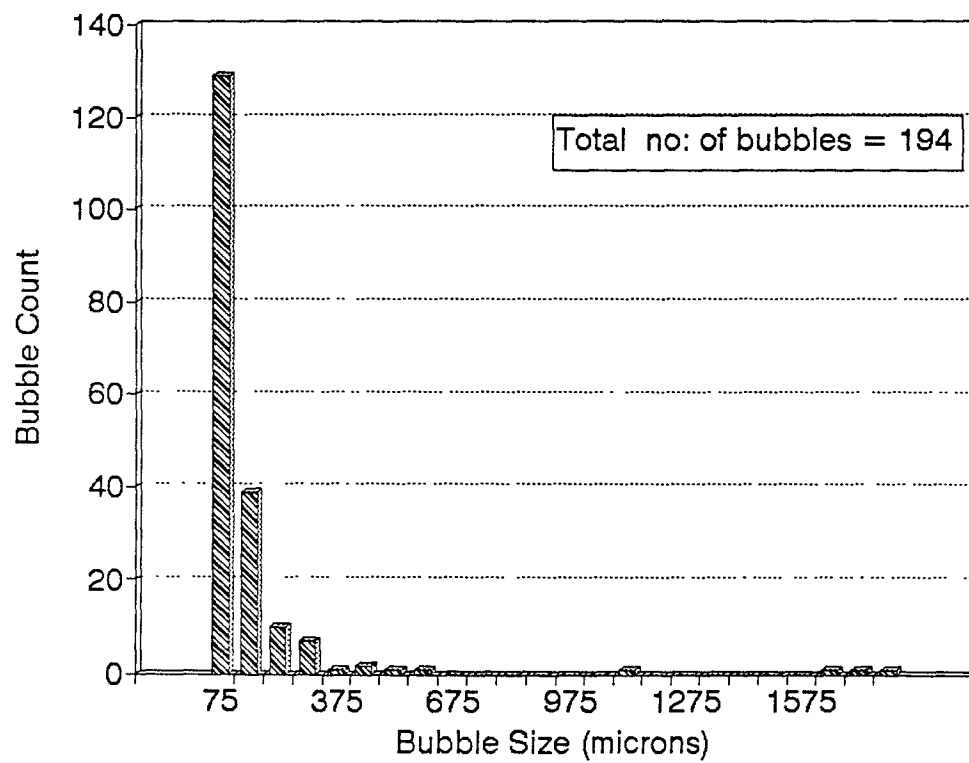


Figure 4.53: Graph showing Bubble Size Distribution for Slice # 1 of concrete with 5.5 AEA (traverse length = 20.57 inches)

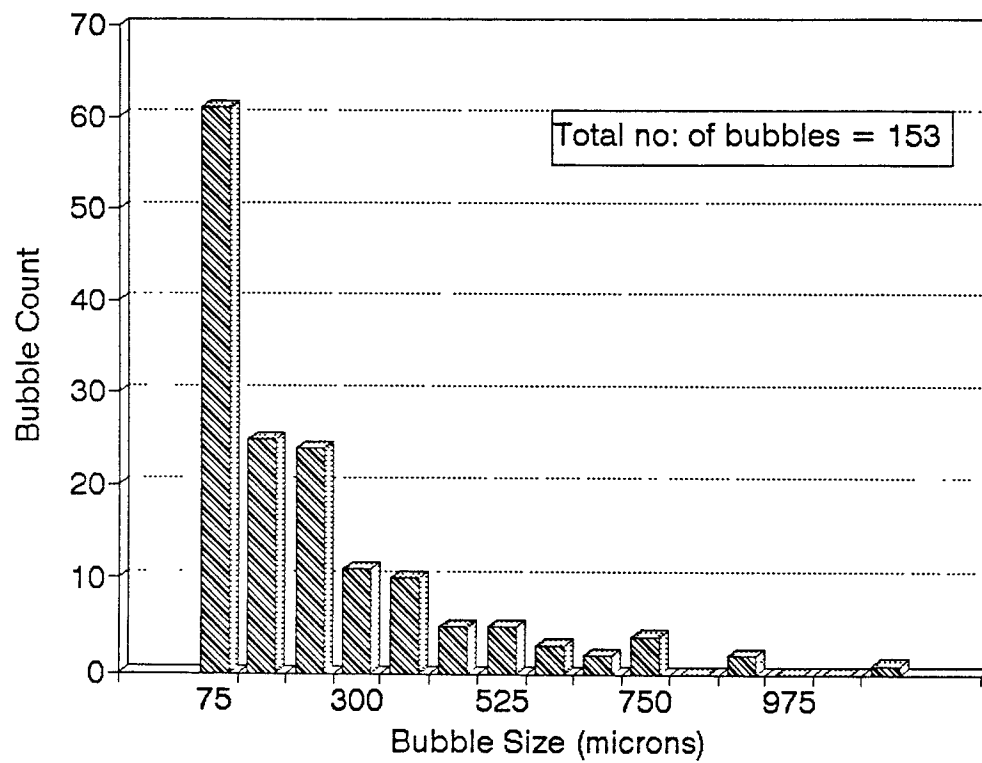


Figure 4.54: Graph showing Bubble Size Distribution for Slice # 2 of concrete with 5.5 AEA (traverse length = 20.57 inches)

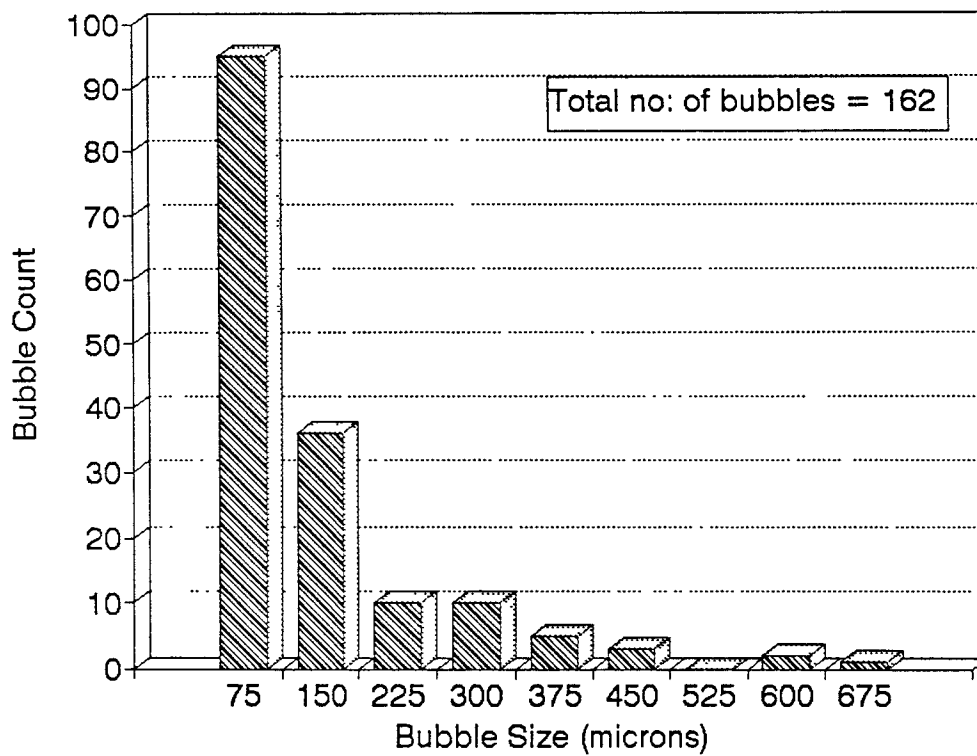


Figure 4.55: Graph showing Bubble Size Distribution for Slice # 3 of concrete with 5.5 AEA (traverse length = 20.57 inches)

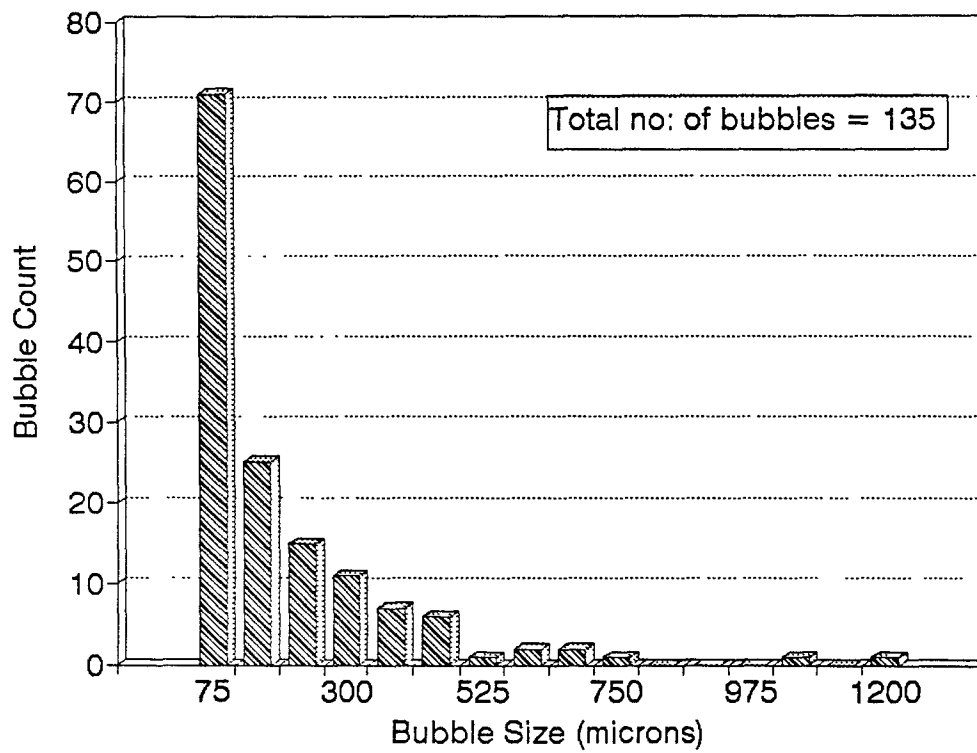


Figure 4.56: Graph showing Bubble Size Distribution for Slice # 4 of concrete with 5.5 ml AEA (traverse length = 20.57 inches)

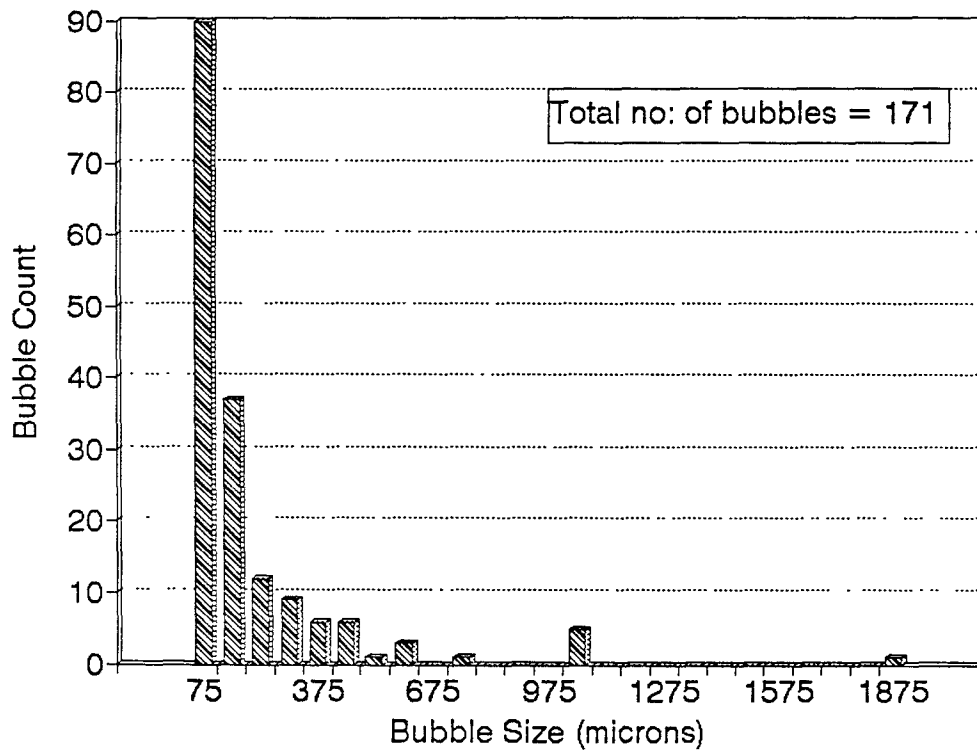


Figure 4.57: Graph showing Bubble Size Distribution for Slice # 5 of concrete with 5.5 AEA (traverse length = 20.57 inches)

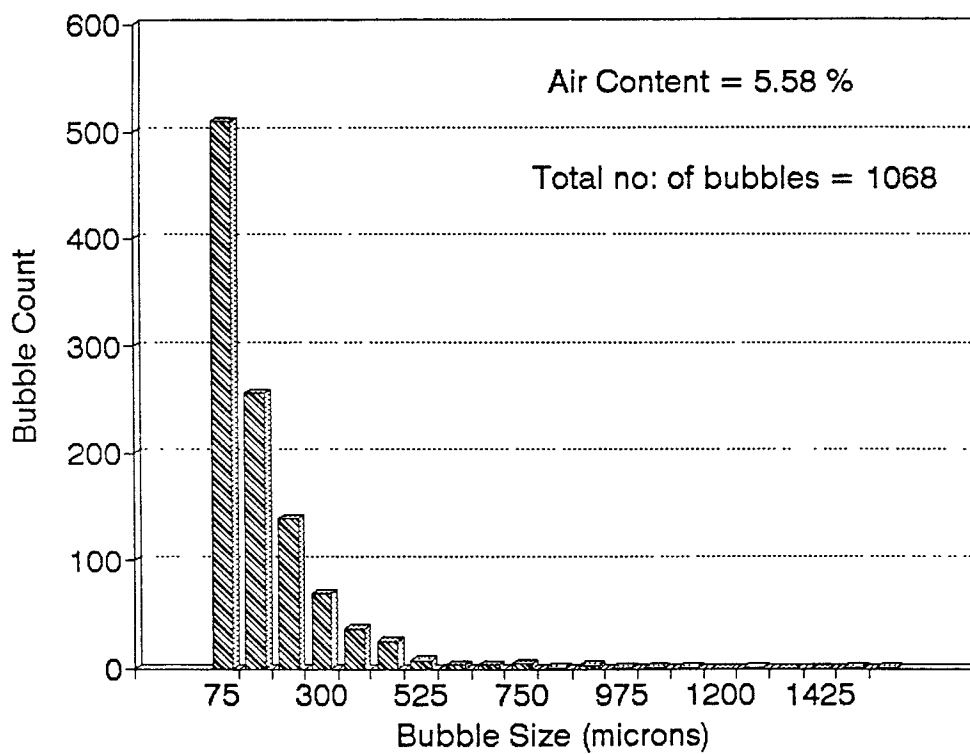


Figure 4.58: Graph showing Bubble Size Distribution for concrete with 10 AEA (traverse length = 103 inches)

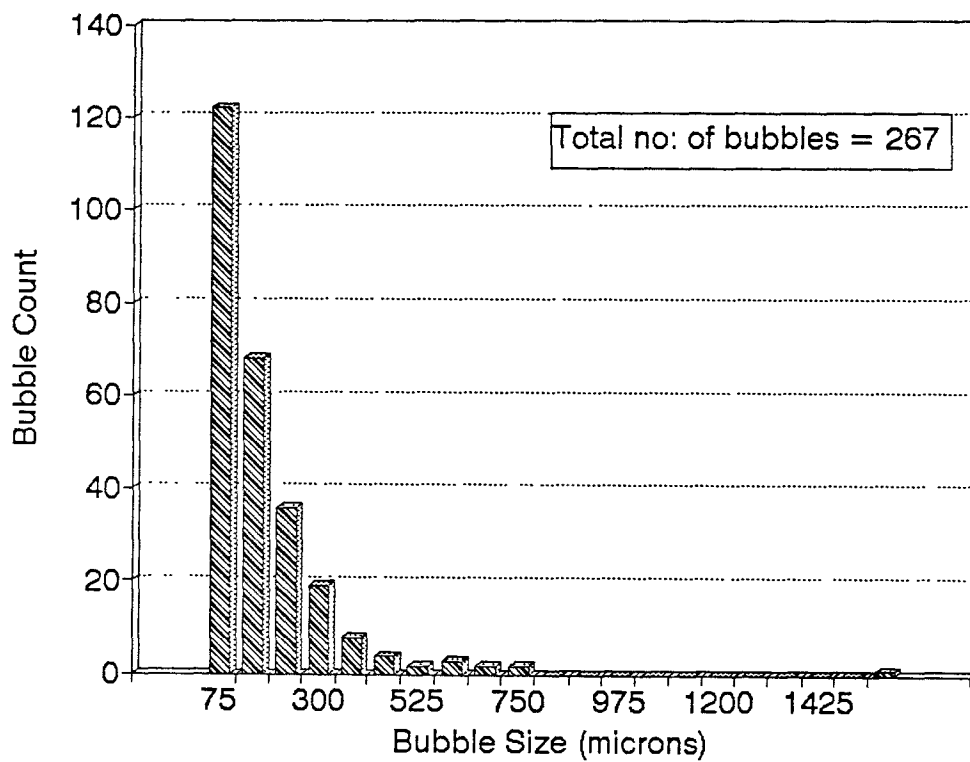


Figure 4.59: Graph showing Bubble Size Distribution for Slice # 1 of concrete with 10 AEA (traverse length = 20.57 inches)

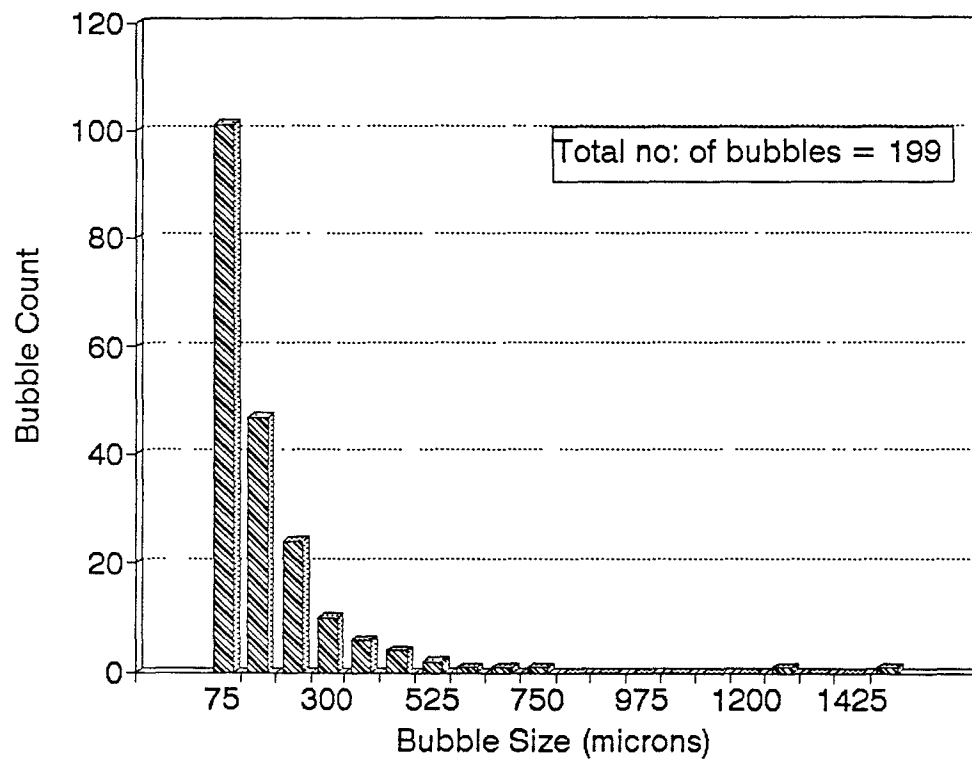


Figure 4.60: Graph showing Bubble Size Distribution for Slice # 2 of concrete with 10 AEA (traverse length = 20.57 inches)

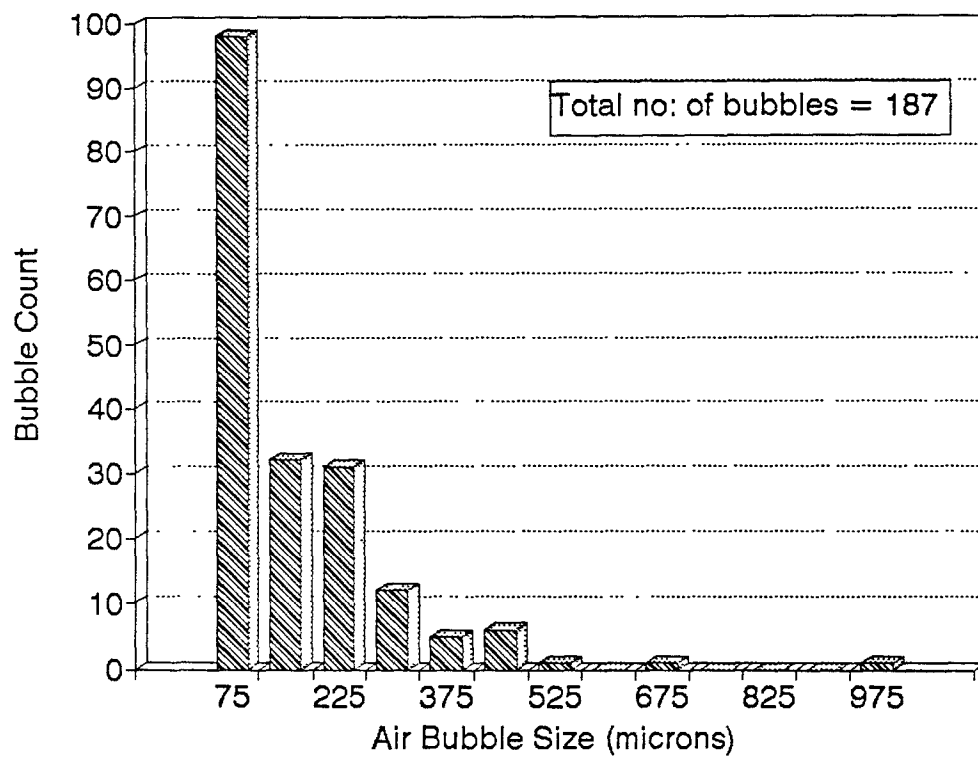


Figure 4.61: Graph showing Bubble Size Distribution for Slice # 3 of concrete with 10 AEA (traverse length = 20.57 inches)

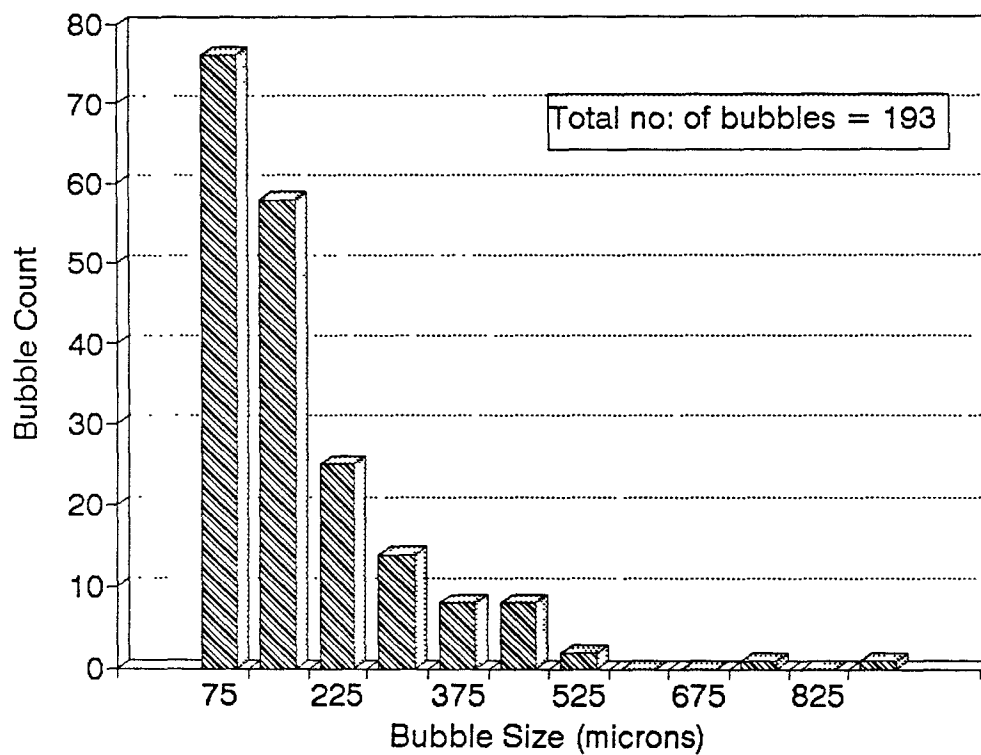


Figure 4.62: Graph showing Bubble Size Distribution for Slice # 4 of concrete with 10 AEA (traverse length = 20.57 inches)

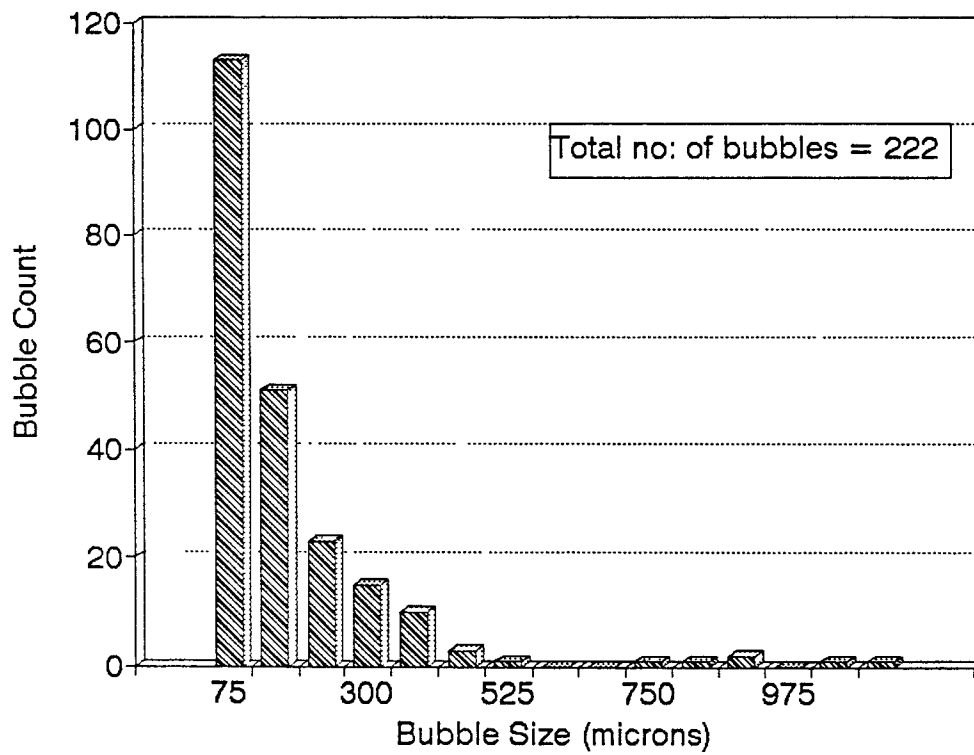


Figure 4.63: Graph showing Bubble Size Distribution for Slice # 5 of concrete with 10 AEA (traverse length = 20.57 inches)

Chapter 5

Concluding Remarks

5.1 Conclusions

Based on the results obtained in this investigation, the following conclusions can be drawn :

- (1) The automated system which was developed and tested in this thesis, is reliable and worth further usage.
- (2) Larger amounts of AEA produce larger amounts of entrained air.
- (3) Increasing amounts of AEA result in larger number of bubbles, reduced Spacing Factor, and larger Specific Area.
- (4) The air content in mortar is higher than the air content in concrete for the same amount of AEA.
- (5) The Specific Surface Area of voids in Mortar is less than that of voids in concrete thus indicating the presence of larger voids in mortar.

5.2 Future Research

The automated system developed is new and requires further research.

Possible future research could involve :

- (1) This system could be further developed so that the result could be obtained with fewer runs of the batch program. This would reduce further the time required to calculate the air content and required parameters.
- (2) A better Image Processing software could be tried which could also detect the shape of the void thus differentiating between giving the percentage of entrapped and entrained air.

Bibliography

- (1) "Freezing and Thawing of Concrete - Mechanisms and Control", Cordon, William A., ACI Monograph No. 3, Published jointly by ACI and The IOWA State University Press., c1965.
- (2) "Concrete - Properties and Manufacture", Akroyd, T. N. W., Published by Pergamon Press Inc., c1962.
- (3) "Durability of Concrete", *ACI Publications SP-47*, 1975, [385p.]
- (4) ASTM C 231, Annual Book of ASTM Standards, Vol 4.02, 1989.
- (5) "Properties of Concrete", T.C. Powers, Published by John Wiley & Sons, Inc., c1968.
- (6) Kenneth C. Hover, "Some Recent Problems with Air-Entrained Concrete", *Cement, Concrete and Aggregates*, Vol 11, No. 1, Summer 1989, pp. 67-72.
- (7) Manning, D. G., "Where Have All the Bubbles Gone?", *Concrete International*, Vol 3, No. 8, Aug 1980, pp. 99-103.
- (8) Burg, G. R. U., "Slump Loss, Air Loss, and Field Performance of Concrete", *ACI Journal, Proceedings*, Vol 80, No. 4, July-Aug 1983, pp. 332-339.

- (9) Gay, F.T., "A Factor Which May Affect Differences in the Determined Air Content of Plastic and Hardened Air-Entrained Concrete", *Proceedings of the Fourth International Conference on Cement Microscopy*, Las Vegas, March 28-April 1982, pp. 292-296.
- (10) ASTM C 457, Annual Book of ASTM Standards, Vol 4.02, 1989
- (11) Richard C. Mielenz & V.E. Walkodoff, "Optical Measurement of Air Voids in Hardened Concrete", *Journal of the American Concrete Institute*, Oct 1958.
- (12) L.S. Brown and C.U. Pierson, "Linear Traverse Technique for Measurement of Air in Hardened Concrete", *Journal of the American Concrete Institute*, Vol 22, No. 2, Oct 1950.
- (13) B.W. Langan and M.A. Ward, "Determination of the Air Void System Parameters in Hardened Concrete - An Error Analysis", *ACI Journal, Proceedings*, Vol 83, No. 6, Nov-Dec 1986, pp. 943-952
- (14) Computer Methods in Image Analysis, J. K. Aggarwal, Richard O. Duda, Azriel Rosenfeld.
- (15) "An Introduction to Digital Image Processing", Wayne Niblack, Published by Englewood Cliffs, Prentice Hall International, c1986.
- (16) "Digital Image Processing", Castleman, Kenneth R., Published by Englewood Cliffs, N.J.: Prentice Hall International, c1979.
- (17) "Digital Image Processing", Baxes, Gregory A.
- (18) "Vision in Man and Machine", Levine Martin D., Published by McGraw-Hill, c1985.

- (19) "Machine Vision Systems - A Summary and a Forecast" - Second Edition
- Lake Geneva, WI : Tech Tran Consultants Inc., c1985
- (20) "Digital Image Processing", Pratt. William K., New York : Wiley, c1978,
"A Wiley Interscience Publication", c1978
- (21) DT-IRIS version 1.04, *Users Manual*
- (22) DT-2851 Frame Grabber, *Users Manual*
- (23) MSTEP-5 (MSTEP-METRABYTE), *Users Manual*
- (24) Qiyu Chen, "A multimode Index Detecting Sensor For Use In Plastic Concrete", M.S. Thesis, Electrical Engineering, NJIT, Directed by Dr. Farhad Ansari
- (25) Richard Plateau, Patrick Plante, Richard Gagne, and Michel Pigeon,
"Practical Considerations Pertaining to the Microscopical Determination of Air Void Characteristics of Hardened Concrete(ASTM C 457 Standard)", *Cement, Concrete and Aggregates*, Vol 12, No. 2, Summer 1990, pp. 3-11.
- (26) S. Chatterjee & H. Gudmundsson, "Charaterisation of Entrained Air Bubble Systems in Concrete by means of an Image Analysing Microscope", *Cement and Concrete Research*, Vol. 7, pp 423-428

Appendix A

Calculation of Percentage Error in the calculation of Paste Content:

Paste Content calculated by microscopic analysis = 0.2609 = 26.09 %

Paste Content calculated by mix design :

$$p = \frac{C + W}{C + S + A + W} = \frac{1 + 0.5}{1 + 2.1 + 3.4 + 0.5} = 0.248 = 24.8\% \quad (1)$$

Percentage Error =

$$\frac{26.9 - 24.8}{24.8} \times 100 = 5.1 \% \quad (2)$$

Appendix B

Results of Experiments

Final Results of Specimen cast on October 5

Total Length of Traverse : 2553.6 mm (100.5 inches)
Number of Air Bubbles intercepted : 975
Sum of Bubble Lengths : 52.571 mm

Air Void Content : 2.06 %

Specimen cast on October 5 - Concrete [1]

Results of Slice # 1 from top

TOTAL LENGTH TRAVERSED : 354.67 mm = 13.96 inches
NUMBER OF AIR BUBBLES : 59
TOTAL LENGTH OF AIR BUBBLES : .46233010E+01mm

AIR VOID CONTENT : 1.3035 %

Specimen cast on October 5 - Concrete [1]

Results of Slice # 2 from top

TOTAL LENGTH TRAVERSED : 354.67 mm = 13.96 inches
NUMBER OF AIR BUBBLES : 198
TOTAL LENGTH OF AIR BUBBLES : .11204550E+02mm
TOTAL LENGTH OF CHORD : .14296630E+03mm

AIR VOID CONTENT : 3.1591 %

Specimen cast on October 5 - Concrete [1]

Results of Slice # 3 from top

TOTAL LENGTH TRAVERSED : 354.67 mm = 13.96 inches
NUMBER OF AIR BUBBLES : 134
TOTAL LENGTH OF AIR BUBBLES : .62058120E+01mm
TOTAL LENGTH OF CHORD : .14796110E+03mm

AIR VOID CONTENT : 1.7497 %

Specimen cast on October 5 - Concrete [1]

Results of Slice # 4 from top

TOTAL LENGTH TRAVERSED : 354.67 mm = 13.96 inches

NUMBER OF AIR BUBBLES : 195

TOTAL LENGTH OF AIR BUBBLES : .11466580E+02mm

TOTAL LENGTH OF CHORD : .14270430E+03mm

AIR VOID CONTENT : 3.2330 %

Specimen cast on October 5 - Concrete [1]

Results of Slice # 5 from top

TOTAL LENGTH TRAVERSED : 354.67 mm = 13.96 inches

NUMBER OF AIR BUBBLES : 132

TOTAL LENGTH OF AIR BUBBLES : .44161760E+01mm

TOTAL LENGTH OF CHORD : .14975070E+03mm

AIR VOID CONTENT : 1.2452 %

Specimen cast on October 5 - Concrete [1]

Results of Slice # 6 from top

TOTAL LENGTH TRAVERSED : 354.67 mm = 13.96 inches

NUMBER OF AIR BUBBLES : 62

TOTAL LENGTH OF AIR BUBBLES : .21638000E+01mm

TOTAL LENGTH OF CHORD : .15200310E+03mm

AIR VOID CONTENT : .6101 %

Specimen cast on October 5 - Concrete [1]

Results of Slice # 7 from top

TOTAL LENGTH TRAVERSED : 354.67 mm = 13.96 inches

NUMBER OF AIR BUBBLES : 76

TOTAL LENGTH OF AIR BUBBLES : .53878150E+01mm

TOTAL LENGTH OF CHORD : .14877910E+03mm

AIR VOID CONTENT : 1.5191 %

Specimen cast on October 5 - Concrete [1]

Results of Slice # 8 from top

TOTAL LENGTH TRAVERSED : 354.67 mm = 13.96 inches

NUMBER OF AIR BUBBLES : 119

TOTAL LENGTH OF AIR BUBBLES : .71028530E+01mm

TOTAL LENGTH OF CHORD : .14706400E+03mm

AIR VOID CONTENT : 2.0027 %

Specimen cast on October 16 - Concrete [2]

Total Length of Traverse : 2553.6 mm (100.5 inches)
Number of Air Bubbles intercepted : 1832
Sum Of Bubble Lengths : 109.68 mm

Air Void Content : 4.29 %

Specimen cast on October 16 - Concrete [2]

Result of Slice # 1 from top

TOTAL LENGTH TRAVERSED : 319.203 mm = 12.57 inches
NUMBER OF AIR BUBBLES : 84
TOTAL LENGTH OF AIR BUBBLES : .156213740E+02mm
TOTAL LENGTH OF CHORD : .339048630E+03mm

AIR VOID CONTENT : 4.4041 %

Specimen Cast on October 16 - Concrete [2]

Result of Slice # 2 from top

TOTAL LENGTH TRAVERSED : 319.20 mm = 12.57 inches
NUMBER OF AIR BUBBLES : 113
TOTAL LENGTH OF AIR BUBBLES : .46778660E+01mm
TOTAL LENGTH OF CHORD : .14948900E+03mm

AIR VOID CONTENT : 1.4655 %

Specimen cast on October 16 - Concrete [2]

Result of Slice # 3 from top

TOTAL LENGTH TRAVERSED : 319.20 mm = 12.57 inches
NUMBER OF AIR BUBBLES : 310
TOTAL LENGTH OF AIR BUBBLES : .14611540E+02mm
TOTAL LENGTH OF CHORD : .13956330E+03mm

AIR VOID CONTENT : 4.5775 %

Specimen cast on October 16 - Concrete [2]

Results of Slice # 4 from top

TOTAL LENGTH TRAVERSED : 319.20 mm = 12.57 inches
NUMBER OF AIR BUBBLES : 534
TOTAL LENGTH OF AIR BUBBLES : .17254780E+02mm
TOTAL LENGTH OF CHORD : .13693000E+03mm

AIR VOID CONTENT : 5.4056 %

Specimen cast on October 16 - Concrete [2]

Results of Slice # 5 from top

TOTAL LENGTH TRAVERSED : 319.20 mm = 12.57 inches
NUMBER OF AIR BUBBLES : 132
TOTAL LENGTH OF AIR BUBBLES : .13265150E+02mm
TOTAL LENGTH OF CHORD : .30531790E+03mm

AIR VOID CONTENT : 4.1557 %

Specimen cast on October 16 - Concrete [1]

Results of Slice # 6 from top

TOTAL LENGTH TRAVERSED : 319.203 mm = 12.57 inches
NUMBER OF AIR BUBBLES : 172
TOTAL LENGTH OF AIR BUBBLES : .213002150E+02mm
TOTAL LENGTH OF CHORD : .333371100E+03mm

AIR VOID CONTENT : 6.0056 %

Specimen cast on October 16 - Concrete [2]

Results of Slice # 7 from top

TOTAL LENGTH TRAVERSED : 319.20 mm = 12.57 inches
NUMBER OF AIR BUBBLES : 304
TOTAL LENGTH OF AIR BUBBLES : .10827830E+02mm
TOTAL LENGTH OF CHORD : .14334300E+03mm

AIR VOID CONTENT : 3.3922 %

Specimen cast on October 16 - Concrete [2]

Results of Slice # 8 from top

TOTAL LENGTH TRAVERSED : 319.20 mm = 12.57 inches

NUMBER OF AIR BUBBLES : 183

TOTAL LENGTH OF AIR BUBBLES : .12120620E+02mm

TOTAL LENGTH OF CHORD : .23338310E+03mm

AIR VOID CONTENT : 3.7972 %

Specimen cast on October 19 - Concrete [3]

TOTAL LENGTH TRAVERSED : 2634.68 mm = 103.73 inches
NUMBER OF AIR BUBBLES : 815
TOTAL LENGTH OF AIR BUBBLES : .11264410E+03mm
TOTAL LENGTH OF CHORD : .25169780E+04mm

AIR VOID CONTENT : 4.2754%
SPECIFIC SURFACE : 762.4963 sq mm/cu mm
MEAN CHORD LENGTH : 0.13821360mm
Number of bubbles per cm : 3.0993/cm
Number of bubbles per inch : 7.8722/inch
Spacing Factor (with traverse) : .0055mm
Spacing Factor (by mix ratio) : .0046mm

Specimen cast on October 19 - Concrete [3]

Results of Slice # 1 from top

TOTAL LENGTH TRAVERSED : 526.94 mm = 20.75 inches
NUMBER OF AIR BUBBLES : 194
TOTAL LENGTH OF AIR BUBBLES : .19907710E+02mm
TOTAL LENGTH OF CHORD : .50600080E+03mm

AIR VOID CONTENT : 3.7780 %
MEAN CHORD LENGTH : 0.1026 mm
Number of bubbles per cm : 3.6889/cm
Number of bubbles per inch : 9.3697/inch

Specimen cast on October 19 - Concrete [3]

Results of Slice # 2 from top

TOTAL LENGTH TRAVERSED : 526.94 mm = 20.75 inches
NUMBER OF AIR BUBBLES : 153
TOTAL LENGTH OF AIR BUBBLES : .28983860E+02mm
TOTAL LENGTH OF CHORD : .49697450E+03mm

AIR VOID CONTENT : 5.5004 %
MEAN CHORD LENGTH : 0.18943700mm
Number of bubbles per cm : 2.9090/cm
Number of bubbles per inch : 7.3888/inch

Specimen cast on October 19 - Concrete [3]

Results of Slice # 3 from top

TOTAL LENGTH TRAVERSED : 526.94 mm = 20.75 inches
NUMBER OF AIR BUBBLES : 162
TOTAL LENGTH OF AIR BUBBLES : .15908210E+02mm
TOTAL LENGTH OF CHORD : .51001020E+03mm

AIR VOID CONTENT : 3.0190 %
MEAN CHORD LENGTH : 0.09819 mm
Number of bubbles per cm : 3.0803/cm
Number of bubbles per inch : 7.8240/inch

Specimen cast on October 19 - Concrete [3]

Results of Slice # 4 from top

TOTAL LENGTH TRAVERSED : 526.94 mm = 20.75 inches
NUMBER OF AIR BUBBLES : 135
TOTAL LENGTH OF AIR BUBBLES : .22441050E+02mm
TOTAL LENGTH OF CHORD : .50348740E+03mm

AIR VOID CONTENT : 4.2588%
MEAN CHORD LENGTH : 0.1662 mm
Number of bubbles per cm : 2.5669/cm
Number of bubbles per inch : 6.5199/inch

Specimen cast on October 19 - Concrete [3]

Results of Slice # 5 from top

TOTAL LENGTH TRAVERSED : 526.94 mm = 20.75 inches
NUMBER OF AIR BUBBLES : 171
TOTAL LENGTH OF AIR BUBBLES : .25403270E+02mm
TOTAL LENGTH OF CHORD : .50050520E+03mm

AIR VOID CONTENT : 4.8209 %
MEAN CHORD LENGTH : 0.1485 mm
Number of bubbles per cm : 3.2515/cm
Number of bubbles per inch : 8.2589/inch

Specimen cast on October 22 - Concrete [4]

TOTAL LENGTH TRAVERSED : 2634.68 mm = 103.73 inches
NUMBER OF AIR BUBBLES : 1068
TOTAL LENGTH OF AIR BUBBLES : .13030770E+03mm
TOTAL LENGTH OF CHORD : .24992150E+04mm

AIR VOID CONTENT : 4.9459 %
SPECIFIC SURFACE : 863.7533 sq mm/cu mm
MEAN CHORD LENGTH : 0.1220 mm
Number of bubbles per cm : 4.0616/cm
Number of bubbles per inch : 10.3164/inch
Spacing Factor : .0037mm

Specimen cast on October 22 - Concrete [4]

Results of Slice # 1 from top

TOTAL LENGTH TRAVERSED : 526.94 mm = 20.75 inches
NUMBER OF AIR BUBBLES : 267
TOTAL LENGTH OF AIR BUBBLES : .29382820E+02mm
TOTAL LENGTH OF CHORD : .49651570E+03mm

AIR VOID CONTENT : 5.5762 %
MEAN CHORD LENGTH : 0.11004800mm
Number of bubbles per cm : 5.0770/cm
Number of bubbles per inch : 12.8956/inch

Specimen cast on October 22 - Concrete [22]

Results of Slice # 2 from top

TOTAL LENGTH TRAVERSED : 526.94 mm = 20.75 inches
NUMBER OF AIR BUBBLES : 222
TOTAL LENGTH OF AIR BUBBLES : .26550250E+02mm
TOTAL LENGTH OF CHORD : .49934820E+03mm

AIR VOID CONTENT : 5.0386 %
MEAN CHORD LENGTH : 0.11959570mm
Number of bubbles per cm : 4.2213/cm
Number of bubbles per inch : 10.7222/inch

Specimen cast on October 22 - Concrete [4]

Results of Slice # 3 from top

TOTAL LENGTH TRAVERSED : 526.94 mm = 20.75 inches
NUMBER OF AIR BUBBLES : 187
TOTAL LENGTH OF AIR BUBBLES : .21932390E+02mm
TOTAL LENGTH OF CHORD : .50398610E+03mm

AIR VOID CONTENT : 4.1622%
MEAN CHORD LENGTH : 0.11728550mm
Number of bubbles per cm : 3.5557/cm
Number of bubbles per inch : 9.0314/inch

Specimen cast on October 22 - Concrete [4]

Results of Slice # 4 from top

TOTAL LENGTH TRAVERSED : 526.94 mm = 20.75 inches
NUMBER OF AIR BUBBLES : 193
TOTAL LENGTH OF AIR BUBBLES : .25901960E+02mm
TOTAL LENGTH OF CHORD : .50000650E+03mm

AIR VOID CONTENT : 4.9156 %
MEAN CHORD LENGTH : 0.13420700mm
Number of bubbles per cm : 3.6698/cm
Number of bubbles per inch : 9.3214/inch

Specimen cast on October 22 - Concrete [4]

Results of Slice # 5 from top

TOTAL LENGTH TRAVERSED : 526.94 mm = 20.75 inches
NUMBER OF AIR BUBBLES : 199
TOTAL LENGTH OF AIR BUBBLES : .26540280E+02mm
TOTAL LENGTH OF CHORD : .49935820E+03mm

AIR VOID CONTENT : 5.0367 %
MEAN CHORD LENGTH : 0.13336830mm
Number of bubbles per cm : 3.7840/cm
Number of bubbles per inch : 9.6114/inch

Specimen Cast on March 12 - Mortar [1]

TOTAL LENGTH TRAVERSED : 2634.68 mm:103.73 in
NUMBER OF AIR BUBBLES : 224
TOTAL LENGTH OF AIR BUBBLES : .58386630E+02mm
TOTAL LENGTH OF CHORD : .25711360E+04mm

AIR VOID CONTENT : 2.2161%
SPECIFIC SURFACE : 404.31810000sq mm/cu mm
MEAN CHORD LENGTH : 0.26065460mm
Number of bubbles per cm : 0.8519/cm
Number of bubbles per inch : 2.1637/inch
Spacing Factor(without sand) : .0197 mm

Specimen cast on March 12 - Mortar [1]

Results of Slice # 1 from top

TOTAL LENGTH TRAVERSED : 526.94 mm = 20.75 in
NUMBER OF AIR BUBBLES : 49
TOTAL LENGTH OF AIR BUBBLES : .14531830E+02mm
TOTAL LENGTH OF CHORD : .51138660E+03mm

AIR VOID CONTENT : 2.7578%
MEAN CHORD LENGTH : 0.29656790 mm
Number of bubbles per cm : 0.9317/cm
Number of bubbles per inch : 2.3665/inch

Specimen cast on March 12 - Mortar [1]

Results of Slice # 2 from top

TOTAL LENGTH TRAVERSED : 526.94 mm = 20.75 in
NUMBER OF AIR BUBBLES : 39
TOTAL LENGTH OF AIR BUBBLES : .79690660E+01mm
TOTAL LENGTH OF CHORD : .51792940E+03mm

AIR VOID CONTENT : 1.5123%
MEAN CHORD LENGTH : 0.20433500 mm
Number of bubbles per cm : 0.7416/cm
Number of bubbles per inch : 1.8836/inch

Specimen cast on March 12 - Mortar [1]

Results of Slice # 3 from top

TOTAL LENGTH TRAVERSED : 526.94 mm = 20.75 in
NUMBER OF AIR BUBBLES : 45
TOTAL LENGTH OF AIR BUBBLES : .96745850E+01mm
TOTAL LENGTH OF CHORD : .51622390E+03mm

AIR VOID CONTENT : 1.8360%
MEAN CHORD LENGTH : 0.21499080 mm
Number of bubbles per cm : 0.8557/cm
Number of bubbles per inch : 2.1734/inch

Specimen cast on March 12 - Mortar [1]

Results of Slice # 4 from top

TOTAL LENGTH TRAVERSED : 526.94 mm = 20.75 in
NUMBER OF AIR BUBBLES : 45
TOTAL LENGTH OF AIR BUBBLES : .13484580E+02mm
TOTAL LENGTH OF CHORD : .51241390E+03mm

AIR VOID CONTENT : 2.5591%
MEAN CHORD LENGTH : 0.29965730mm
Number of bubbles per cm : 0.8557/cm
Number of bubbles per inch : 2.1734/inch

Specimen cast on March 12 - Mortar [1]

Results of Slice # 5 from top

TOTAL LENGTH TRAVERSED : 526.94 mm = 20.75 in
NUMBER OF AIR BUBBLES : 46
TOTAL LENGTH OF AIR BUBBLES : .12726570E+02mm
TOTAL LENGTH OF CHORD : .51318190E+03mm

AIR VOID CONTENT : 2.4152%
MEAN CHORD LENGTH : 0.27666460mm
Number of bubbles per cm : 0.8747/cm
Number of bubbles per inch : 2.2217/inch

Specimen cast on March 14 - Mortar [2]

TOTAL LENGTH TRAVERSED : 2634.68 mm = 103.73 inches
NUMBER OF AIR BUBBLES : 677
TOTAL LENGTH OF AIR BUBBLES : .91080740E+02mm
TOTAL LENGTH OF CHORD : .25384720E+04mm

AIR VOID CONTENT : 3.4570%
SPECIFIC SURFACE : 783.3406 sq mm/cu mm
MEAN CHORD LENGTH : 0.13453580mm
Number of bubbles per cm : 2.5746/cm
Number of bubbles per inch : 6.5394/inch
Spacing Factor : .0081mm

Specimen cast on March 14 - Mortar [2]

Results of Slice # 1 from top

TOTAL LENGTH TRAVERSED : 526.94 mm = 20.75 inches
NUMBER OF AIR BUBBLES : 114
TOTAL LENGTH OF AIR BUBBLES : .20007440E+02mm
TOTAL LENGTH OF CHORD : .50589110E+03mm

AIR VOID CONTENT : 3.7969%
MEAN CHORD LENGTH : .17550390mm
Number of bubbles per cm : 2.1677/cm
Number of bubbles per inch : 5.5060/inch

Specimen cast on March 14 - Mortar [2]

Results of Slice # 2 from top

TOTAL LENGTH TRAVERSED : 526.94 mm = 20.75 inches
NUMBER OF AIR BUBBLES : 77
TOTAL LENGTH OF AIR BUBBLES : .15269890E+02mm
TOTAL LENGTH OF CHORD : .51062860E+03mm

AIR VOID CONTENT : 2.8979%
MEAN CHORD LENGTH : .19831020mm
Number of bubbles per cm : 1.4642/cm
Number of bubbles per inch : 3.7190/inch

Specimen cast on March 14 - Mortar [2]

Results of Slice # 3 from top

TOTAL LENGTH TRAVERSED : 526.94 mm = 20.75 inches

NUMBER OF AIR BUBBLES : 228

TOTAL LENGTH OF AIR BUBBLES : .19508750E+02mm

TOTAL LENGTH OF CHORD : .50640970E+03mm

AIR VOID CONTENT : 3.7023%

MEAN CHORD LENGTH : 0.08556470mm

Number of bubbles per cm : 4.3353/cm

Number of bubbles per inch : 11.0116/inch

Specimen cast on March 14 - Mortar [2]

Results of Slice # 4 from top

TOTAL LENGTH TRAVERSED : 526.94 mm = 20.75 in

NUMBER OF AIR BUBBLES : 133

TOTAL LENGTH OF AIR BUBBLES : .18810590E+02mm

TOTAL LENGTH OF CHORD : .50710780E+03mm

AIR VOID CONTENT : 3.5698%

MEAN CHORD LENGTH : 0.14143300mm

Number of bubbles per cm : 2.5289/cm

Number of bubbles per inch : 6.4234/inch

Specimen cast on March 14 - Mortar [2]

Results of Slice 5 from top

TOTAL LENGTH TRAVERSED : 526.94 mm = 20.75 inches

NUMBER OF AIR BUBBLES : 125

TOTAL LENGTH OF AIR BUBBLES : .17484070E+02mm

TOTAL LENGTH OF CHORD : .50843440E+03mm

AIR VOID CONTENT : 3.3181%

MEAN CHORD LENGTH : 0.13987260mm

Number of bubbles per cm : 2.3768/cm

Number of bubbles per inch : 6.0371/inch

Specimen cast on MARCH 15 - Mortar [3]

TOTAL LENGTH TRAVERSED : 2634.68 mm = 103.73 inches
NUMBER OF AIR BUBBLES : 661
TOTAL LENGTH OF AIR BUBBLES : .12370510E+03mm
TOTAL LENGTH OF CHORD : .25058370E+04mm

AIR VOID CONTENT : 4.6953%
SPECIFIC SURFACE : 563.1221 sq mm/cu mm
MEAN CHORD LENGTH : 0.18714830mm
Number of bubbles per cm : 2.5137/cm
Number of bubbles per inch : 6.3849/inch
Spacing Factor : 0.0093mm

Specimen cast on MARCH 15 - Mortar [3]

Results of Slice # 1 from top

TOTAL LENGTH TRAVERSED : 526.94 mm = 20.75 in
NUMBER OF AIR BUBBLES : 142
TOTAL LENGTH OF AIR BUBBLES : .25233720E+02mm
TOTAL LENGTH OF CHORD : .50068470E+03mm

AIR VOID CONTENT : 4.7888%
MEAN CHORD LENGTH : 0.17770220mm
Number of bubbles per cm : 2.7000/cm
Number of bubbles per inch : 6.8581/inch

Specimen cast on MARCH 15 - Mortar [3]

Results of Slice # 2 from top

TOTAL LENGTH TRAVERSED : 526.94 mm = 20.75 in
NUMBER OF AIR BUBBLES : 185
TOTAL LENGTH OF AIR BUBBLES : .36214870E+02mm
TOTAL LENGTH OF CHORD : .48969360E+03mm

AIR VOID CONTENT : 6.8727%
MEAN CHORD LENGTH : 0.19575600mm
Number of bubbles per cm : 3.5177/cm
Number of bubbles per inch : 8.9350/inch

Specimen cast on MARCH 15 - Mortar [3]

Results of Slice # 3 from top

TOTAL LENGTH TRAVERSED : 526.94 mm = 20.75 in
NUMBER OF AIR BUBBLES : 138
TOTAL LENGTH OF AIR BUBBLES : .23069400E+02mm
TOTAL LENGTH OF CHORD : .50283910E+03mm

AIR VOID CONTENT : 4.3780%
MEAN CHORD LENGTH : 0.16716950mm
Number of bubbles per cm : 2.6240/cm
Number of bubbles per inch : 6.6650/inch

Specimen cast on MARCH 15 - Mortar [3]

Results of Slice # 4 from top

TOTAL LENGTH TRAVERSED : 526.94 mm = 20.75 in
NUMBER OF AIR BUBBLES : 100
TOTAL LENGTH OF AIR BUBBLES : .15529210E+02mm
TOTAL LENGTH OF CHORD : .51036930E+03mm

AIR VOID CONTENT : 2.9471%
MEAN CHORD LENGTH : 0.15529210mm
Number of bubbles per cm : 1.9015/cm
Number of bubbles per inch : 4.8298/inch

Specimen cast on MARCH 15 - Mortar [3]

Results of Slice # 5 from top

TOTAL LENGTH TRAVERSED : 526.94 mm = 20.75 in
NUMBER OF AIR BUBBLES : 96
TOTAL LENGTH OF AIR BUBBLES : .23657850E+02mm
TOTAL LENGTH OF CHORD : .50225060E+03mm

AIR VOID CONTENT : 4.4897%
MEAN CHORD LENGTH : 0.24643600mm
Number of bubbles per cm : 1.8254/cm
Number of bubbles per inch : 4.6365/inch

Specimen cast on MARCH 19 - [4]

TOTAL LENGTH TRAVERSED : 2634.68 mm = 103.73 inches
NUMBER OF AIR BUBBLES : 774
TOTAL LENGTH OF AIR BUBBLES : .14433090E+03mm
TOTAL LENGTH OF CHORD : .24852310E+04mm

AIR VOID CONTENT : 5.4781%
SPECIFIC SURFACE : 565.1586 sq mm/cu mm
MEAN CHORD LENGTH : 0.18647400mm
Number of bubbles per cm : 2.9435/cm
Number of bubbles per inch : 7.4764/inch
Spacing Factor : .0096mm

Specimen cast on MARCH 19 - Mortar [4]

Results of Slice # 1 from top

TOTAL LENGTH TRAVERSED : 526.94 mm = 20.75 inches
NUMBER OF AIR BUBBLES : 187
TOTAL LENGTH OF AIR BUBBLES : .28405380E+02mm
TOTAL LENGTH OF CHORD : .49750310E+03mm

AIR VOID CONTENT : 5.3907%
MEAN CHORD LENGTH : .15190040mm
Number of bubbles per cm : 3.5558/cm
Number of bubbles per inch : 9.0316/inch

Specimen cast on MARCH 19 - Mortar [4]

Results of Slice # 2 from top

TOTAL LENGTH TRAVERSED : 526.94 mm = 20.75 in
NUMBER OF AIR BUBBLES : 180
TOTAL LENGTH OF AIR BUBBLES : .26809580E+02mm
TOTAL LENGTH OF CHORD : .49910890E+03mm

AIR VOID CONTENT : 5.0878%
MEAN CHORD LENGTH : 0.14894210mm
Number of bubbles per cm : 3.4226/cm
Number of bubbles per inch : 8.6934/inch

Specimen cast on MARCH 19 - Mortar [4]

Results of Slice # 3 from top

TOTAL LENGTH TRAVERSED : 526.94 mm = 20.75 inches
NUMBER OF AIR BUBBLES : 130
TOTAL LENGTH OF AIR BUBBLES : .25183840E+02mm
TOTAL LENGTH OF CHORD : .50071470E+03mm

AIR VOID CONTENT : 4.7793%
MEAN CHORD LENGTH : 0.19372190mm
Number of bubbles per cm : 2.4720/cm
Number of bubbles per inch : 6.2788/inch

Specimen cast on MARCH 19 - Mortar [4]

Results of Slice # 4 from top

TOTAL LENGTH TRAVERSED : 526.94 mm = 20.75 inches
NUMBER OF AIR BUBBLES : 116
TOTAL LENGTH OF AIR BUBBLES : .30799090E+02mm
TOTAL LENGTH OF CHORD : .49510940E+03mm

AIR VOID CONTENT : 5.8449%
MEAN CHORD LENGTH : 0.26550940mm
Number of bubbles per cm : 2.2057/cm
Number of bubbles per inch : 5.6025/inch

Specimen cast on MARCH 19 - Mortar [4]

Results of Slice # 5 from top

TOTAL LENGTH TRAVERSED : 526.94 mm = 20.75 inches
NUMBER OF AIR BUBBLES : 161
TOTAL LENGTH OF AIR BUBBLES : .33132970E+02mm
TOTAL LENGTH OF CHORD : .49279540E+03mm

AIR VOID CONTENT : 6.2878%
MEAN CHORD LENGTH : 0.20579480mm
Number of bubbles per cm : 3.0613/cm
Number of bubbles per inch : 7.7756/inch

Specimen cast on MARCH 20 - [5]

TOTAL LENGTH TRAVERSED : 2634.68 mm = 103.73 inches
NUMBER OF AIR BUBBLES : 566
TOTAL LENGTH OF AIR BUBBLES : .13361900E+03mm
TOTAL LENGTH OF CHORD : .24959430E+04mm

AIR VOID CONTENT : 5.0715%
SPECIFIC SURFACE : 446.4129 sq mm/cu mm
MEAN CHORD LENGTH : 0.23607600mm
Number of bubbles per cm : 2.1524/cm
Number of bubbles per inch : 5.4672/inch
Spacing Factor : .0127mm

Specimen cast on MARCH 20 - [5]

Results of Slice #1 from top

TOTAL LENGTH TRAVERSED : 526.94 mm = 20.75 inches
NUMBER OF AIR BUBBLES : 105
TOTAL LENGTH OF AIR BUBBLES : .30599620E+02mm
TOTAL LENGTH OF CHORD : .49531880E+03mm

AIR VOID CONTENT : 5.8071%
MEAN CHORD LENGTH : 0.29142490mm
Number of bubbles per cm : 1.9965/cm
Number of bubbles per inch : 5.0711/inch

Specimen cast on MARCH 20 - [5]

Results of Slice # 2 from top

TOTAL LENGTH TRAVERSED : 526.94 mm = 20.75 inches
NUMBER OF AIR BUBBLES : 114
TOTAL LENGTH OF AIR BUBBLES : .30858940E+02mm
TOTAL LENGTH OF CHORD : .49506950E+03mm

AIR VOID CONTENT : 5.8563%
MEAN CHORD LENGTH : 0.27069240mm
Number of bubbles per cm : 2.1676/cm
Number of bubbles per inch : 5.5057/inch

Specimen cast on MARCH 20 - [5]

Results of Slice # 3 from top

TOTAL LENGTH TRAVERSED : 526.94 mm = 20.75 inches
NUMBER OF AIR BUBBLES : 78
TOTAL LENGTH OF AIR BUBBLES : .24286200E+02mm
TOTAL LENGTH OF CHORD : .50162230E+03mm

AIR VOID CONTENT : 4.6089%
MEAN CHORD LENGTH : 0.31136160mm
Number of bubbles per cm : 1.4831/cm
Number of bubbles per inch : 3.7672/inch

Specimen cast on MARCH 20 - [5]

Results of Slice # 4 from top

TOTAL LENGTH TRAVERSED : 526.94 mm = 20.75 inches
NUMBER OF AIR BUBBLES : 109
TOTAL LENGTH OF AIR BUBBLES : .21972280E+02mm
TOTAL LENGTH OF CHORD : .50393620E+03mm

AIR VOID CONTENT : 4.1698%
MEAN CHORD LENGTH : 0.20158060mm
Number of bubbles per cm : 2.0726/cm
Number of bubbles per inch : 5.2644/inch

Specimen cast on MARCH 20 -[5]

Results of Slice #5 from top

TOTAL LENGTH TRAVERSED : 526.94 mm = 20.75 inches
NUMBER OF AIR BUBBLES : 160
TOTAL LENGTH OF AIR BUBBLES : .25901960E+02mm
TOTAL LENGTH OF CHORD : .49999660E+03mm

AIR VOID CONTENT : 4.9156%
MEAN CHORD LENGTH : 0.16188720mm
Number of bubbles per cm : 3.0424/cm
Number of bubbles per inch : 7.7277/inch

Total Length of Traverse : 2553.6 mm (100.5 inches)
Number of Air Bubbles intercepted : 1832
Sum Of Bubble Lengths : 109.68 mm

Air Void Content : 4.29 %

Specimen cast on October 16 - Concrete [2]

Result of Slice # 1 from top

TOTAL LENGTH TRAVERSED : 319.203 mm = 12.57 inches
NUMBER OF AIR BUBBLES : 84
TOTAL LENGTH OF AIR BUBBLES : .156213740E+02mm
TOTAL LENGTH OF CHORD : .339048630E+03mm

AIR VOID CONTENT : 4.4041 %

Specimen Cast on October 16 - Concrete [2]

Result of Slice # 2 from top

TOTAL LENGTH TRAVERSED : 319.20 mm = 12.57 inches
NUMBER OF AIR BUBBLES : 113
TOTAL LENGTH OF AIR BUBBLES : .46778660E+01mm
TOTAL LENGTH OF CHORD : .14948900E+03mm

AIR VOID CONTENT : 1.4655 %

Specimen cast on October 16 - Concrete [2]

Result of Slice # 3 from top

TOTAL LENGTH TRAVERSED : 319.20 mm = 12.57 inches
NUMBER OF AIR BUBBLES : 310
TOTAL LENGTH OF AIR BUBBLES : .14611540E+02mm
TOTAL LENGTH OF CHORD : .13956330E+03mm

AIR VOID CONTENT : 4.5775 %

Final Results of Specimen cast on October 5

Total Length of Traverse : 2553.6 mm (100.5 inches)
Number of Air Bubbles intercepted : 975
Sum of Bubble Lengths : 52.571 mm

Air Void Content : 2.06 %

Specimen cast on October 5 - Concrete [1]

Results of Slice # 1 from top

TOTAL LENGTH TRAVERSED : 354.67 mm = 13.96 inches
NUMBER OF AIR BUBBLES : 59
TOTAL LENGTH OF AIR BUBBLES : .46233010E+01mm

AIR VOID CONTENT : 1.3035 %

Specimen cast on October 5 - Concrete [1]

Results of Slice # 2 from top

TOTAL LENGTH TRAVERSED : 354.67 mm = 13.96 inches
NUMBER OF AIR BUBBLES : 198
TOTAL LENGTH OF AIR BUBBLES : .11204550E+02mm
TOTAL LENGTH OF CHORD : .14296630E+03mm

AIR VOID CONTENT : 3.1591 %

Specimen cast on October 5 - Concrete [1]

Results of Slice # 3 from top

TOTAL LENGTH TRAVERSED : 354.67 mm = 13.96 inches
NUMBER OF AIR BUBBLES : 134
TOTAL LENGTH OF AIR BUBBLES : .62058120E+01mm
TOTAL LENGTH OF CHORD : .14796110E+03mm

Specimen cast on October 16 - Concrete [2]

Appendix C

Program Listings

cd\iris1.04

```
display.exe
main1.exe
cd\mstep-5
basica mtr2
cd\bin
FL /c c:\iris1.04\combin.for
cd\iris1.04
display.exe
main2.exe
cd\mstep-5
basica mtr2
cd\bin
FL /c c:\iris1.04\combin.for
cd\iris1.04
display.exe
main3.exe
cd\mstep-5
basica mtr2
cd\bin
FL /c c:\iris1.04\combin.for
cd\iris1.04
display.exe
main4.exe
cd\mstep-5
basica mtr2
cd\bin
FL /c c:\iris1.04\combin.for
cd\iris1.04
display.exe
main5.exe
cd\mstep-5
basica mtr2
cd\bin
FL /c c:\iris1.04\combin.for
cd\iris1.04
display.exe
main6.exe
cd\mstep-5
basica mtr2
cd\bin
FL /c c:\iris1.04\combin.for
cd\iris1.04
display.exe
main7.exe
cd\mstep-5
basica mtr2
cd\bin
FL /c c:\iris1.04\combin.for
cd\iris1.04
display.exe
main8.exe
cd\mstep-5
basica mtr2
cd\bin
FL /c c:\iris1.04\combin.for
cd\iris1.04
display.exe
main9.exe
cd\mstep-5
```

```
basica mtr2
cd\bin
FL /c c:\iris1.04\combin.for
cd\iris1.04
display.exe
main10.exe
cd\mstep-5
basica mtr2
cd\bin
FL /c c:\iris1.04\combin.for
cd\iris1.04
display.exe
main11.exe
cd\mstep-5
basica mtr2
cd\bin
FL /c c:\iris1.04\combin.for
cd\iris1.04
display.exe
main12.exe
cd\mstep-5
basica mtr2
cd\bin
FL /c c:\iris1.04\combin.for
cd\iris1.04
display.exe
main13.exe
compact.exe
cd\
xtree
```

PROGRAM MAIN1

```

C-----
C This program captures an image from a concrete section and stores
C the image in the directory 'images' and stores the data in 2 files
C :b1.dat and bb1.dat. This program uses the software DT-Iris version
C 4.0 and calls subroutines from the library 'c:\iris1.04\isforlib.lib'
C This program assumes the user is providing a video input signal to
C the appropriate input line on the DT2851 and there is an appropriate
C display. This program is meant for lower magnification.
C-----
$include:'c:\IRIS1.04\ISDEFS.FOR'
$include:'c:\IRIS1.04\ISERRS.FOR'
C
      INTEGER*2 STATUS
C
      INTEGER*2 NCH1,LCHORD1,LNUMBER1,LSUM1,K,A,Y0,X0,CX0,CX
      INTEGER*2 IP(511)
      INTEGER*2 LB(20),LC(20)
      REAL SUM1,CHORD1
      REAL RB1(20),RC1(20)
      LSUM1 = 0
      LNUMBER1 = 0
      LCHORD1 = 0
      NCH1=0

C
C open a channel to the device driver
C
      STATUS = ISINIT()
C
C select input look-up table 0 ( monochrome translation )
C
      STATUS = ISINTS(0)
C
C select output look-up table 0 ( monochrome translation )
C
      STATUS = ISOUTS(0)
C
C select sync source ( for real-time pass-thru sync must be externally
C supplied by source ; 1 = external sync )
C
      STATUS = ISSYNC(1)
C
C select frame buffer 0 to use for video input
C
      STATUS = ISINFR(0)
C
C select frame buffer 0 to use for video output
C
      STATUS = ISOTFR(0)
C
C set board in real-time acquisition and display mode ( pass-thru )
C
      STATUS = ISPASS()
C
C allocate memory for frame buffer 2
C
      STATUS = ISALOC(2)
C
C clear buffer 2

```

```

C      STATUS = ISFCLR(2)
C
C acquire one frame to buffer 2
C
C      STATUS = ISACQ(2,1)
C
C save image in a file:filename to buffer 2
C
C      STATUS = ISSAVE(2,0,1,0,'C:\IM\CC1.IMG')
C
C enable display circuitry
C
C      STATUS = ISDISP(1)
C
C get pixels
C
C      STATUS = ISGETP(2,255,0,511,IP)
C
C      OPEN (7, FILE = 'C:\IM-DATA\BB1.DAT',STATUS='NEW')
C      DO 100 I=1,511
C      WRITE (7,50)I,IP(I)
50      FORMAT(2I12.4)
100     CONTINUE
C
C      DO 200 I=1,508
C      IF ( IP(I) .GE. 245 ) THEN
C      LSUM1=LSUM1+1
C
C      IF (IP(I-1) .LT. 245) THEN
C      LNUMBER1=LNUMBER1+1
C      K=K+1
C      ELSE
C      LNUMBER1=LNUMBER1
C      ENDIF
C      LB(K)=LB(K)+1
C      ENDIF
200     CONTINUE
C
C      Y=0
C      DO 250 K1=1,20
C      IF (LB(K1) .EQ. 0) THEN
C      Y=Y+1
C      ENDIF
250     CONTINUE
C      Y0=20-Y
C
C      J=0
C      IF (IP(1) .LT. 245) THEN
C      NCH1=1
C      J=1
C      LC(1)=CX0+1
C      ENDIF
C
C      DO 300 I=2,508
C      IF (IP(I) .LT. 245) THEN
C      LCHORD1=LCHORD1+1
C
C      IF (IP(I-1) .GE. 245) THEN
C      NCH1=NCH1+1
C      J=J+1

```

```

ELSE
NCH1=NCH1
ENDIF
LC(J)=LC(J)+1
ENDIF
300 CONTINUE
SUM1=LSUM1*0.0099738
CHORD1=LCHORD1*0.0099738
C
X=0
DO 310 J1=1,20
IF (LC(J1) .EQ. 0) THEN
X=X+1
ENDIF
310 CONTINUE
X0=19-X
CX=LC(X0+1)
C
WRITE (7,*) ' TOTAL LENGTH TRAVERSED : 5.0667 mm '
WRITE (7,*) ' NUMBER OF AIR BUBBLES : ',LNUMBER1
WRITE (7,*) '      NUMBER      ', '      PIXELS      ', '      MILLIMETERS'
DO 350 K=1,Y0
RB1(K)=LB(K)*0.0099738
WRITE (7,330)K,LB(K),RB1(K)
330 FORMAT(2I12.4,1E15.8)
OPEN (1, FILE = 'C:\IM-DATA\GP1.DAT',STATUS = 'NEW')
WRITE(1,340)LB(K),RB1(K)
340 FORMAT(1I12.4,1E15.8)
350 CONTINUE
C
WRITE (7,*) ' ----- '
WRITE (7,*) ' NUMBER OF CHORDS INTERCEPTED : ',NCH1
WRITE (7,*) ' CHORD NUMBER ', '      PIXELS      ', '      MILLIMETERS'
DO 375 A=1,X0
RC1(A)=LC(A)*0.0099738
WRITE (7,390)A,LC(A),RC1(A)
390 FORMAT(2I12.4,1E15.8,'mm')
375 CONTINUE
WRITE (7,*) ' ----- '
WRITE (7,*) ' TOTAL AIR BUBBLE LENGTH (&L in Pixels) :',LSUM1
WRITE (7,400) SUM1
400 FORMAT(' TOTAL AIR BUBBLE LENGTH in millimeters :',1E15.8,'mm')
WRITE (7,*) ' TOTAL CHORD LENGTH (Pixels) : ',LCHORD1
WRITE (7,410)CHORD1
410 FORMAT('TOTAL CHORD LENGTH IN millimeters :',1E15.8,'mm')
OPEN (8, FILE = 'C:\IM-DATA\B1.DAT', STATUS = 'NEW')
WRITE (8,*)CX
WRITE (8,*)LNUMBER1
WRITE (8,425)SUM1
WRITE (8,425)CHORD1
WRITE (8,*)NCH1
425 FORMAT(1E15.8)
CLOSE (1)
CLOSE (7)
CLOSE (8)
C
C close channel to driver
C
STATUS = ISEND()
C

```

STOP
END

PROGRAM COMBIN1

C This program combines the data of files RUN1.DAT through
C RUN10.DAT and gives the cumulative result.

```

C
    REAL AVC,MCL,F1,F2
    SUM = 0
    LNUMBER = 0
    CHORD = 0

C
    OPEN (1, FILE = 'C:\RESULTS\RUN2.DAT', STATUS='OLD')
    READ (1,*) LN2
    READ (1,100) S2
    READ (1,100) CD2
    READ (1,*) NCH2
    OPEN (2, FILE = 'C:\RESULTS\RUN3.DAT', STATUS = 'OLD')
    READ (2,*) LN3
    READ (2,100) S3
    READ (2,100) CD3
    READ (2,*) NCH3
    OPEN (3, FILE = 'C:\RESULTS\RUN4.DAT', STATUS = 'OLD')
    READ (3,*) LN4
    READ (3,100) S4
    READ (3,100) CD4
    READ (3,*) NCH4
    OPEN (4, FILE = 'C:\RESULTS\RUN5.DAT', STATUS = 'OLD')
    READ (4,*) LN5
    READ (4,100) S5
    READ (4,100) CD5
    READ (4,*) NCH5
    OPEN (5, FILE = 'C:\RESULTS\RUN6.DAT', STATUS='OLD')
    READ (5,*) LN6
    READ (5,100) S6
    READ (5,100) CD6
    READ (5,*) NCH6
    OPEN (6, FILE = 'C:\RESULTS\RUN7.DAT', STATUS = 'OLD')
    READ (6,*) LN7
    READ (6,100) S7
    READ (6,100) CD7
    READ (6,*) NCH7
    OPEN (7, FILE = 'C:\RESULTS\RUN8.DAT', STATUS = 'OLD')
    READ (7,*) LN8
    READ (7,100) S8
    READ (7,100) CD8
    READ (7,*) NCH8
    OPEN (8, FILE = 'C:\RESULTS\RUN9 .DAT', STATUS = 'OLD')
    READ (8,*) LN9
    READ (8,100) S9
    READ (8,100) CD9
    READ (8,*) NCH9
100  FORMAT(1E15.8)
C
    LNUMBER = LN2+LN3+LN4+LN5+LN6+LN7+LN8+LN9
    SUM = S2+S3+S4+S5+S6+S7+S8+S9
    NCH = NCH2+NCH3+NCH4+NCH5+NCH6+NCH7+NCH8+NCH9
    CHORD = CD2+CD3+CD4+CD5+CD6+CD7+CD8+CD9
    TL=SUM+CHORD
    MCL=SUM/LNUMBER
    AVC=(SUM/526.9368)*100
    F1=(LNUMBER*10/TL)
    F2=(LNUMBER*25.4/TL)

```

C

```
OPEN (10, FILE = 'C:\RESULTS\RESULT1.DAT', STATUS = 'NEW')
WRITE (10,*) '          SUMMATION OF RUN2 TO RUN9 ', '(526.94 mm)'
WRITE (10,*) '          -----'
WRITE (10,*) ' TOTAL LENGTH TRAVERSED : 526.94 mm', '= 20.75 in'
WRITE (10,*) 'NUMBER OF AIR BUBBLES : ', LNUMBER
WRITE (10,200)SUM
200  FORMAT(' TOTAL LENGTH OF AIR BUBBLES : ',1E15.8,'mm')
WRITE (10,250)CHORD
250  FORMAT(' TOTAL LENGTH OF CHORD : ',1E15.8,'mm')
WRITE (10,300)AVC
300  FORMAT(' AIR VOID CONTENT : ',1F7.4,'%')
WRITE (10,400)MCL
400  FORMAT(' MEAN CHORD LENGTH : ',1F15.8,'mm')
WRITE (10,450)F1
450  FORMAT(' Number of bubbles per cm : ',1F7.4,'/cm')
WRITE (10,475)F2
475  FORMAT(' Number of bubbles per inch : ',1F7.4,'/cm')
```

C

```
OPEN (11, FILE = 'C:\RESULTS\XSLICE1.DAT', STATUS = 'NEW')
WRITE (11,410)SUM
WRITE (11,410)CHORD
WRITE (11,*)LNUMBER
WRITE (11,*)NCH
410  FORMAT(1E15.8)
DO 425 I=1,11
CLOSE (I)
425  CONTINUE
```

C

```
STOP
END
```


PROGRAM COMPACT

C This program combines the data of files MAIN1.FOR through
C MAIN8.FOR and gives the cumulative result.

C
C LN1, LN2, LN3..= Number of bubbles
C S1, S2, S3... = Air Bubble Length
C CD1, CD2, CD3..= Chord Length
C LC1, LC2, LC3..= Number of chords
C ACL = Mean Chord Length
C

REAL AVC, ACL, SUM, CHORD
SUM = 0
LNUMBER = 0
CHORD = 0

C
OPEN (1, FILE = 'C:\IM-DATA\B1.DAT', STATUS='OLD')
READ (1,*) X1
READ (1,*) LN1
READ (1,100) S1
READ (1,100) CD1
READ (1,*) LC1
CLOSE (1)
OPEN (2, FILE = 'C:\IM-DATA\B2.DAT', STATUS = 'OLD')
READ (2,*) X2
READ (2,*) LN2
READ (2,100) S2
READ (2,100) CD2
READ (2,*) LC2
CLOSE (2)
OPEN (3, FILE = 'C:\IM-DATA\B3.DAT', STATUS = 'OLD')
READ (3,*) X3
READ (3,*) LN3
READ (3,100) S3
READ (3,100) CD3
READ (3,*) LC3
CLOSE (3)
OPEN (4, FILE = 'C:\IM-DATA\B4.DAT', STATUS = 'OLD')
READ (4,*) X4
READ (4,*) LN4
READ (4,100) S4
READ (4,100) CD4
READ (4,*) LC4
CLOSE (4)
OPEN (5, FILE = 'C:\IM-DATA\B5.DAT', STATUS = 'OLD')
READ (5,*) X5
READ (5,*) LN5
READ (5,100) S5
READ (5,100) CD5
READ (5,*) LC5
CLOSE (5)
OPEN (6, FILE = 'C:\IM-DATA\B6.DAT', STATUS = 'OLD')
READ (6,*) X6
READ (6,*) LN6
READ (6,100) S6
READ (6,100) CD6
READ (6,*) LC6
CLOSE (6)
OPEN (7, FILE = 'C:\IM-DATA\B7.DAT', STATUS = 'OLD')
READ (7,*) X7
READ (7,*) LN7

```

READ (7,100) S7
READ (7,100) CD7
READ (7,*) LC7
CLOSE (7)
OPEN (8, FILE = 'C:\IM-DATA\B8.DAT', STATUS='OLD')
READ (8,*) X8
READ (8,*) LN8
READ (8,100) S8
READ (8,100) CD8
READ (8,*) LC8
CLOSE (8)
OPEN (9, FILE = 'C:\IM-DATA\B9.DAT', STATUS = 'OLD')
READ (9,*) X9
READ (9,*) LN9
READ (9,100) S9
READ (9,100) CD9
READ (9,*) LC9
CLOSE (9)
OPEN (10, FILE = 'C:\IM-DATA\B10.DAT', STATUS = 'OLD')
READ (10,*) X10
READ (10,*) LN10
READ (10,100) S10
READ (10,100) CD10
READ (10,*) LC10
CLOSE (10)
OPEN (11, FILE = 'C:\IM-DATA\B11.DAT', STATUS = 'OLD')
READ (11,*) X11
READ (11,*) LN11
READ (11,100) S11
READ (11,100) CD11
READ (11,*) LC11
CLOSE (11)
OPEN (12, FILE = 'C:\IM-DATA\B12.DAT', STATUS = 'OLD')
READ (12,*) X12
READ (12,*) LN12
READ (12,100) S12
READ (12,100) CD12
READ (12,*) LC12
CLOSE (12)
OPEN (13, FILE = 'C:\IM-DATA\B13.DAT', STATUS = 'OLD')
READ (13,*) X13
READ (13,*) LN13
READ (13,100) S13
READ (13,100) CD13
READ (13,*) LC13
CLOSE (13)

C
100
C
FORMAT(1E15.8)

LNUMBER=LN1+LN2+LN3+LN4+LN5+LN6+LN7+LN8+LN9+LN10+LN11+LN12+LN13
NCH=LC1+LC2+LC3+LC4+LC5+LC6+LC7+LC8+LC9+LC10+LC11+LC12+LC13
SUM = S1+S2+S3+S4+S5+S6+S7+S8+S9+S10+S11+S12+S13
CHORD=CD1+CD2+CD3+CD4+CD5+CD6+CD7+CD8+CD9+CD10+CD11+CD12+CD13
CAVG=(CHORD/NCH)
ACL=(SUM/LNUMBER)
AVC=(SUM/0.65867)

C
OPEN (14, FILE = 'C:\RESULTS\BBBB.DAT',STATUS = 'NEW')
WRITE (14,*) '          SUMMATION OF BB1 TO BB13 '
WRITE (14,*) '          -----'

```

```

        WRITE (14,*) ' TOTAL LENGTH TRAVERSED : 65.867 mm '
        WRITE (14,*) 'NUMBER OF AIR BUBBLES : ',LNUMBER
        WRITE (14,200)SUM
200    FORMAT(' TOTAL LENGTH OF AIR BUBBLES : ',1E15.8,'mm')
        WRITE (14,250)CHORD
250    FORMAT(' TOTAL LENGTH OF CHORD : ',1E15.8,'mm')
        WRITE (14,275)ACL
275    FORMAT ('Mean Chord Length : ',1E15.8)
        WRITE (14,300)AVC
300    FORMAT(' AIR VOID CONTENT : ',1F7.4,'%')
C
        OPEN (15, FILE = 'C:\RESULTS\RUN1.DAT', STATUS = 'NEW')
        WRITE (15,*)LNUMBER
        WRITE (15,350)SUM
        WRITE (15,350)CHORD
        WRITE (15,*)NCH
350    FORMAT(1E15.8)
C
        STOP
        END

```

PROGRAM FINAL

C This program combines the data of files of 5 slices gives the
C cummulative result.

C
C SFS = Spacing Factor with sand
C SF = Spacing factor without sand
C

REAL AVC,SA,MCL,F1,F2,SFS1,SFS2,SFS,SF1,SF2,SF,TL
SUM = 0
LNUMBER = 0
CHORD = 0

C
OPEN (1, FILE = 'C:\RESULTS\XSLICE2.DAT', STATUS='OLD')
READ (1,100) S2
READ (1,100) CD2
READ (1,*) LN2
READ (1,*) NCH2
OPEN (2, FILE = 'C:\RESULTS\XSLICE3.DAT', STATUS = 'OLD')
READ (2,100) S3
READ (2,100) CD3
READ (2,*) LN3
READ (2,*) NCH3
OPEN (3, FILE = 'C:\RESULTS\XSLICE4.DAT', STATUS = 'OLD')
READ (3,100) S4
READ (3,100) CD4
READ (3,*) LN4
READ (3,*) NCH4
OPEN (4, FILE = 'C:\RESULTS\XSLICE5.DAT', STATUS = 'OLD')
READ (4,100) S5
READ (4,100) CD5
READ (4,*) LN5
READ (4,*) NCH5
OPEN (5, FILE = 'C:\RESULTS\XSLICE6.DAT', STATUS='OLD')
READ (5,100) S6
READ (5,100) CD6
READ (5,*) LN6
READ (5,*) NCH6

100 FORMAT(1E15.8)

C
C OPEN(7,FILE = 'C:\RESULTS\POUT.DAT',STATUS='OLD')
C READ (7,*) p1
C WRITE (*,*) ' Enter paste content :'
C READ (*,*) p2
LNUMBER = LN2+LN3+LN4+LN5+LN6
SUM = S2+S3+S4+S5+S6
NCH = NCH2+NCH3+NCH4+NCH5+NCH6
CHORD = CD2+CD3+CD4+CD5+CD6
TL=SUM+CHORD
MCL=SUM/LNUMBER
AVC=(SUM/2634.684)*100
SA=(4*LNUMBER)/AVC
F1=(LNUMBER*10/TL)
F2=(LNUMBER*25.4/TL)

C
C SFS1 = (p1/(SA*AVC))
C SFS2 = (3/SA) * (1.4*(((p1/AVC)-1)**0.333)-1)
C IF (SFS1 .GT. SFS2) THEN
C SPS=SFS2
C ELSE

```

C      SFS=SFS1
C      ENDIF
C
      SF1 = (p2/(SA*AVC))
      SF2 = (3/SA) * (1.4*((p2/AVC)-1)**0.333)-1)
      IF (SF1 .GT. SF2) THEN
      SF=SF2
      ELSE
      SF=SF1
      ENDIF
C
      OPEN (6, FILE = 'C:\RESULTS\OUTPUT.DAT',STATUS = 'NEW')
      WRITE (6,*) '          SUMMATION OF 5 SLICES ', '(2634.684 mm)'
      WRITE (6,*) '          -----'
      WRITE (6,*) ' TOTAL LENGTH TRAVERSED : 2634.68 mm', ':103.73 in'
      WRITE (6,*) ' NUMBER OF AIR BUBBLES : ', LNUMBER
      WRITE (6,200)SUM
200    FORMAT(' TOTAL LENGTH OF AIR BUBBLES : ',1E15.8,'mm')
      WRITE (6,250)CHORD
250    FORMAT(' TOTAL LENGTH OF CHORD : ',1E15.8,'mm')
      WRITE (6,300)AVC
300    FORMAT(' AIR VOID CONTENT : ',1F7.4,'%')
      WRITE (6,350)SA
350    FORMAT(' SPECIFIC SURFACE : ',1F15.8,'sq mm/cu mm')
      WRITE (6,400)MCL
400    FORMAT(' MEAN CHORD LENGTH : ',1F15.8,'mm')
      WRITE (6,450)F1
450    FORMAT (' Number of bubbles per cm :',1F7.4,'/cm')
      WRITE (6,475)F2
475    FORMAT (' Number of bubbles per inch :',1F7.4,'/cm')
C      WRITE (6,500)SPS
C500    FORMAT (' Spacing Factor(with sand) :',1F15.4,'mm')
      WRITE (6,505)SF
505    FORMAT (' Spacing Factor(without sand) :',1F15.4,'mm')

      DO 510 I=1,7
      CLOSE (I)
510    CONTINUE
C
      STOP
      END

```

cd\iris1.04

```
display.exe
pcl.exe
cd\mstep-5
basica mtr2
cd\
waitup.exe
cd\bin
FL /c c:\waitup.for
cd\iris1.04
display.exe
pc2.exe
cd\mstep-5
basica mtr2
cd\
waitup.exe
cd\bin
FL /c c:\waitup.for
cd\iris1.04
display.exe
pc3.exe
cd\mstep-5
basica mtr2
cd\
waitup.exe
cd\bin
FL /c c:\waitup.for
cd\iris1.04
display.exe
pc4.exe
cd\mstep-5
basica mtr2
cd\
waitup.exe
cd\bin
FL /c c:\waitup.for
cd\iris1.04
display.exe
pc5.exe
cd\mstep-5
basica mtr2
cd\
waitup.exe
cd\bin
FL /c c:\waitup.for
cd\iris1.04
display.exe
pc6.exe
cd\mstep-5
basica mtr2
cd\
waitup.exe
cd\bin
FL /c c:\waitup.for
cd\iris1.04
display.exe
pc7.exe
cd\mstep-5
basica mtr2
cd\
```

```
waitup.exe
cd\bin
FL /c c:\waitup.for
cd\iris1.04
display.exe
pc8.exe
cd\mstep-5
basica mtr2
cd\
waitup.exe
cd\bin
FL /c c:\waitup.for
cd\iris1.04
display.exe
pc9.exe
cd\mstep-5
basica mtr2
cd\
waitup.exe
cd\bin
FL /c c:\waitup.for
cd\iris1.04
display.exe
pc10.exe
cd\mstep-5
basica mtr2
cd\
waitup.exe
cd\bin
FL /c c:\waitup.for
cd\iris1.04
display.exe
pc11.exe
cd\mstep-5
basica mtr2
cd\
waitup.exe
cd\bin
FL /c c:\waitup.for
cd\iris1.04
display.exe
pc12.exe
cd\mstep-5
basica mtr2
cd\
waitup.exe
cd\bin
FL /c c:\waitup.for
cd\iris1.04
display.exe
pc13.exe
pat.exe
cd\
xtree
```

PROGRAM PASTE CONTENT

```

C-----
C This program captures an image from a concrete
C section and stores the data in file :pcl.dat
C This program uses the software DT-Iris version 4.0
C and calls subroutines from the library
C 'c:\iris1.04\isforlib.lib'. This program assumes the
C user is providing a video input signal to the
C appropriate input line on the DT2851 and there is an
C appropriate display. This program is meant for lower
C magnification
C-----
$include:'c:\IRIS1.04\ISDEFS.FOR'
$include:'c:\IRIS1.04\ISERRS.FOR'
C
      INTEGER*2 STATUS
C
      INTEGER*2 IP(511)
      REAL Tlength1,Tpaste1,Tagg1
      Tpaste1 = 0
      Tagg1 = 0
C
C open a channel to the device driver
C
      STATUS = ISINIT()
C
C select input look-up table 0 ( monochrome
C translation)
C
      STATUS = ISINTS(0)
C
C select output look-up table 0 ( monochrome
C translation )
C
      STATUS = ISOUTS(0)
C
C select sync source ( for real-time pass-thru sync           must be
C supplied by source ; 1 = external sync )
C
      STATUS = ISSYNC(1)
C
C select frame buffer 0 to use for video input
C
      STATUS = ISINFR(0)
C
C select frame buffer 0 to use for video output
C
      STATUS = ISOTFR(0)
C
C set board in real-time acquisition and display mode (       pass-thr
C
      STATUS = ISPASS()
C
C allocate memory for frame buffer 2
C
      STATUS = ISALOC(2)
C
C clear buffer 2
C
      STATUS = ISFCLR(2)
C

```



```

C acquire one frame to buffer 2
C
      STATUS = ISACQ(2,1)
C
C save image in a file:filename to buffer 2
C
      STATUS = ISSAVE(2,0,1,0,'C:\IM\CC1.IMG')
C
C enable display circuitry
C
      STATUS = ISDISP(1)
C
C get pixels
C
      STATUS = ISGETP(2,255,0,511,IP)
C
C      DO 100 I=1,511
C      WRITE (7,50) I,IP(I)
C50      FORMAT(2I12.4)
C100      CONTINUE
C
      DO 100 I=1,508
      Tlength1=Tlength1+1
      IF ( IP(I) .LT. 215 ) THEN
      Tagg1=Tagg1+1
      ENDIF
100      CONTINUE
C
      Tpaste1=Tlength1-Tagg1
      Tpaste1=Tpaste1*0.0099738
      Tagg1=Tagg1*0.0099738
      Tlength1=Tlength1*0.0099738
      OPEN (1, FILE = 'C:\IM-DATA\PC1.DAT',STATUS = 'NEW')
      WRITE (1,150) Tpaste1
      WRITE (1,150) Tagg1
      WRITE (1,150) Tlength1
150      FORMAT(1E15.8)
      CLOSE (1)
C
C close channel to driver
C
      STATUS = ISEND()
C
      STOP
      END

```

```

PROGRAM PUNE
C This program combines the data of files PC1.DAT,PC2.DAT,PC3.DAT..
C upto PC14.DAT and gives the cummulative result .
C
C
C          S1,S2,S3... = Air Bubble Length
C          CD1,CD2,CD3..= Chord Length
C
REAL PT,AT,TL,PC
C
OPEN (1, FILE = 'C:\RESULTS\PASTE1.DAT', STATUS = 'OLD')
READ (1,100) P1
READ (1,100) A1
OPEN (2, FILE = 'C:\RESULTS\PASTE2.DAT', STATUS = 'OLD')
READ (2,100) P2
READ (2,100) A2
OPEN (3, FILE = 'C:\RESULTS\PASTE3.DAT', STATUS = 'OLD')
READ (3,100) P3
READ (3,100) A3
OPEN (4, FILE = 'C:\RESULTS\PASTE4.DAT', STATUS = 'OLD')
READ (4,100) P4
READ (4,100) A4
OPEN (5, FILE = 'C:\RESULTS\PASTE5.DAT', STATUS = 'OLD')
READ (5,100) P5
READ (5,100) A5
OPEN (6, FILE = 'C:\RESULTS\PASTE6.DAT', STATUS = 'OLD')
READ (6,100) P6
READ (6,100) A6
OPEN (7, FILE = 'C:\RESULTS\PASTE7.DAT', STATUS = 'OLD')
READ (7,100) P7
READ (7,100) A7
OPEN (8, FILE = 'C:\RESULTS\PASTE8.DAT', STATUS = 'OLD')
READ (8,100) P8
READ (8,100) A8
100  FORMAT(1E15.8)
C
PT=P1+P2+P3+P4+P5+P6+P7+P8
AT=A1+A2+A3+A4+A5+A6+A7+A8
TL=AT+PT
C
PC=(PT*100)/TL
C
OPEN (9, FILE = 'C:\RESULTS\PSLICE.DAT',STATUS = 'NEW')
WRITE (9,200)PT
WRITE (9,200)AT
200  FORMAT(1E15.8)
DO 400 I=1,9
CLOSE (I)
400  CONTINUE
C
STOP
END

```

PROGRAM PFINAL

C This program combines the data of files PC1.DAT,PC2.DAT,PC3.DAT..
C upto PC14.DAT and gives the cummulative result .

C
C S1,S2,S3... = Air Bubble Length
C CD1,CD2,CD3..= Chord Length
C

REAL PT,AT,TL,PC

C
OPEN (1, FILE = 'C:\RESULTS\PSLICE1.DAT', STATUS = 'OLD')
READ (1,100) P1
READ (1,100) A1
OPEN (2, FILE = 'C:\RESULTS\PSLICE2.DAT', STATUS = 'OLD')
READ (2,100) P2
READ (2,100) A2
OPEN (3, FILE = 'C:\RESULTS\PSLICE3.DAT', STATUS = 'OLD')
READ (3,100) P3
READ (3,100) A3
OPEN (4, FILE = 'C:\RESULTS\PSLICE4.DAT', STATUS = 'OLD')
READ (4,100) P4
READ (4,100) A4
OPEN (5, FILE = 'C:\RESULTS\PSLICE5.DAT', STATUS = 'OLD')
READ (5,100) P5
READ (5,100) A5

100 FORMAT(1E15.8)

C
PT=P1+P2+P3+P4+P5
AT=A1+A2+A3+A4+A5
TL=AT+PT

C
PC=(PT*100)/TL

C
OPEN (6, FILE = 'C:\RESULTS\POUT.DAT',STATUS = 'NEW')
WRITE (6,200) PC
WRITE (6,200) PT
WRITE (6,200) AT
200 FORMAT(1E15.8)
DO 400 I=1,6
CLOSE (I)
400 CONTINUE

C
STOP
END

PROGRAM DISPLAY

```
C
C This program is a simple example implementing calls from the FORTRAN
C library in DT-IRIS (ISFORLIB) to place a DT2851 Frame Grabber in a
C real-time display mode. This program assumes the user is providing a
C video input signal to the appropriate input line on the DT2851 and
C there is an appropriate display monitor attached to the video output
C lines from the DT2851. Upon successful execution of this program the
C input signal will be continually digitized and displayed in real-time
C at the output display monitor.
C
$INCLUDE:'C:\IRIS1.04\ISDEFS.FOR'
$INCLUDE:'C:\IRIS1.04\ISERRS.FOR'
C
      INTEGER*2 STATUS
C
C open a channel to the device driver
C
      STATUS = ISINIT()
C
C select input look-up table 0 ( monochrome translation )
C
      STATUS = ISINTS(0)
C
C select output look-up table 0 ( monochrome translation )
C
      STATUS = ISOUTS(0)
C
C select sync source ( for real-time pass-thru sync must be externally
C supplied by source ; 1 = external sync )
C
      STATUS = ISSYNC(1)
C
C enable display circuitry (1 = turn display on)
C
      STATUS = ISDISP(1)
C
C select frame buffer 0 to use for video input
C
      STATUS = ISINFR(0)
C
C select frame buffer 0 to use for video output
C
      STATUS = ISOTFR(0)
C
C set board in real-time acquisition and display mode ( pass-thru )
C
      STATUS = ISPASS()
C
C close channel to driver
C
      STATUS = ISEND()
C
C terminate program
C
      STOP 'PROGRAM TERMINATED'
      END
```